UNITED NATIONS EDUCATIONAL, SCIENTIFIC AND CULTURAL ORGANIZATION
INTERNATIONAL CENTRE FOR THEORETICAL PHYSICS
I.C.T.P., P.O. BOX 586, 34100 TRIESTE, ITALY, CABLE: CENTRATOM TRIESTE

SMR/388 - 44

SPRING COLLEGE IN MATERIALS SCIENCE
ON
'CERAMICS AND COMPOSITE MATERIALS'
(17 April - 26 May 1989)

STRENGTHENING MECHANISMS AND STRONG MICROSTRUCTURES

M.H. LEWIS
Department of Physics
Centre for Advanced Materials Technology
University of Warwick
Coventry CV4 7AL
U.K.

These are preliminary lecture notes, intended only for distribution to participants.

Strengthening Mechanisms and High Strength Ceramic Microstructures

Lecture 1. Principles of Microstructural Design for High Strength

-Ceramic Applications and Target Properties

-The origin of strength; fracture mechanics (processing flaws, failure statistics, fracture-toughness).

Lecture 2. Silicon-based Ceramics; Microstructural Evolution

-Crystallography and Phase Relations (Si_3N_4, Sialons, SiC)

-Material sources, Processing, Fabrication and Applications.

-Microstructures; ideal and real systems.

Lecture 3. Silicon-based ceramics; Mechanical Behaviour

-Hardness, Strength (MOR), Fracture Toughness

-High Temperature Creep and Stress-Rupture

-The Influence of Environment (corrosion and oxidation)

Lecture 4. Oxide and Silicate Ceramics

-Zirconia toughening

-Silicate glass-ceramics; crystallisation and mechanical behaviour, potential as matrices in CMCs.

-Oxynitride glass-ceramics

Lecture 5. Dispersion Strengthening

-Principles

-Phase Combinations and Processing

-Attainable Strength and Toughness

-Comparison with Fibre-Reinforcement

References

1. M.H. Lewis, 'Ceramics, Applications and Limitations' in 'Materials at their Limits' (Inst. of Metals, London 1986) - contains many References.

2. M.H. Lewis, 'Developments in Ceramics' in 'Welding and Allied Developments for the Process Industries' (The Welding Inst. 1988) - copied for circulation at ICTP; many references listed.

3. A. Kelly & N. Macmillan, 'Strong Solids' (Oxford Univ.Press 1987).

4. R.W. Davidge, 'Mechanical Behaviour of Ceramics', (Cambridge U.P. 1980).

5. F.F. Lange 'Powder processing science and technology for increased reliability, J.Amer.Ceram.Soc. 72 1989, 3.

6. R.J. Brook, W.H. Tuan and L.A. Xue, 'Critical Issues and Future Directions in Sintering Science' in Ceramic Transactions 1 (Amer.Ceram.Soc. 1988) 811.

7. A.G. Evans, 'New opportunities in the Processing of High Reliability Structural Ceramics', in Ceramic Transactions 1 (Amer.Ceram.Soc. 1988) 989.

8. M.H. Lewis, G. Leng-Ward and C. Jasper, 'Sintering-Additive Chemistry in Controlling Microstructure and Properties of Nitride Ceramics' in Ceramic Transations 1 (Amer.Ceram.Soc. 1988) 1019.

9. M.H. Lewis et al 'The Development of Single Phase Sialon Ceramics' J.Mat.Sci. 12 (1977) 61.

10. M.H. Lewis et al 'The Microstructure of Sintered Sialon Ceramics', J.Mat.Sci. 15 (1980) 103.

11. B.S.B. Karunaratne and M.H. Lewis, 'Grain Boundary de-segragation and intergranular cohesion in Sialon ceramics', J.Mat.Sci. 15 (1980) 1781.

12. B.S.B. Karunaratne and M.H. Lewis, 'High Temperature Fracture and Diffusional Deformation Mechanisms in Sialon Ceramics', J.Mat.Sci. 15 (1980) 449.

13. M.H. Lewis et al 'Microstructural design of High-Temperature Ceramics' in Engineering with Ceramics 2, ed. Freer et al (Brit.Ceram.Proc. 39 1987).

14. F.F. Lange 'High Temperature deformation and Failure Phenomena in Polyphase Si_3N_4 Materials' in 'Progress in Nitrogen Ceramics' ed. Riley (Martinus Nijoff 1983) 467.

15. R. Stevens, 'An Introduction to Zirconia' (Magnesium Elektron Public. No.113).

16. J.P. Northover and G.W. Groves, 'High Temperature Properties of LAS Glass Ceramics', J.Mat.Sci. 16 (1981) 1874.

17. Z.Strnad, 'Glass-Ceramic Materials' (Elsevier 1986).

18. P.W. McMillan, 'Glass-Ceramics' (Academic Press, London 1979).

19. M.H. Lewis (ed.) 'Glasses and Glass Ceramics' (Chapman and Hall 1988), - Chapters on 'Oxynitride Glasses and Glass Ceramics' (Leng-Ward & Lewis), 'Fibre-reinforced Glasses and Glass-Ceramics' by Prewo.

20. R.W. Davidge 'Fibre Reinforced Ceramics' in Proc. 6th CIMTEC Conf. on High Tech Ceramics (Elsevier 1986).

21. L.J. Schioler and J.J. Stiglich, 'Ceramic Matrix Composites: a review', Amer.Ceram.Soc.Bull 65 (1986) 289.

22. M.S. Newkirk et al, 'Preparation of Lanxide Ceramic Matrix Composites', Ceram.Eng.Sci.Proc. 8 (1987) 879.

23. P.F. Becher et al. 'Toughening Behaviour in Whisker-Reinforced Ceramic Matrix Composites', J.Amer.Ceram.Soc. 71 (1988) 1050.

Ceramic Phase Selection based on Intrinsic Properties

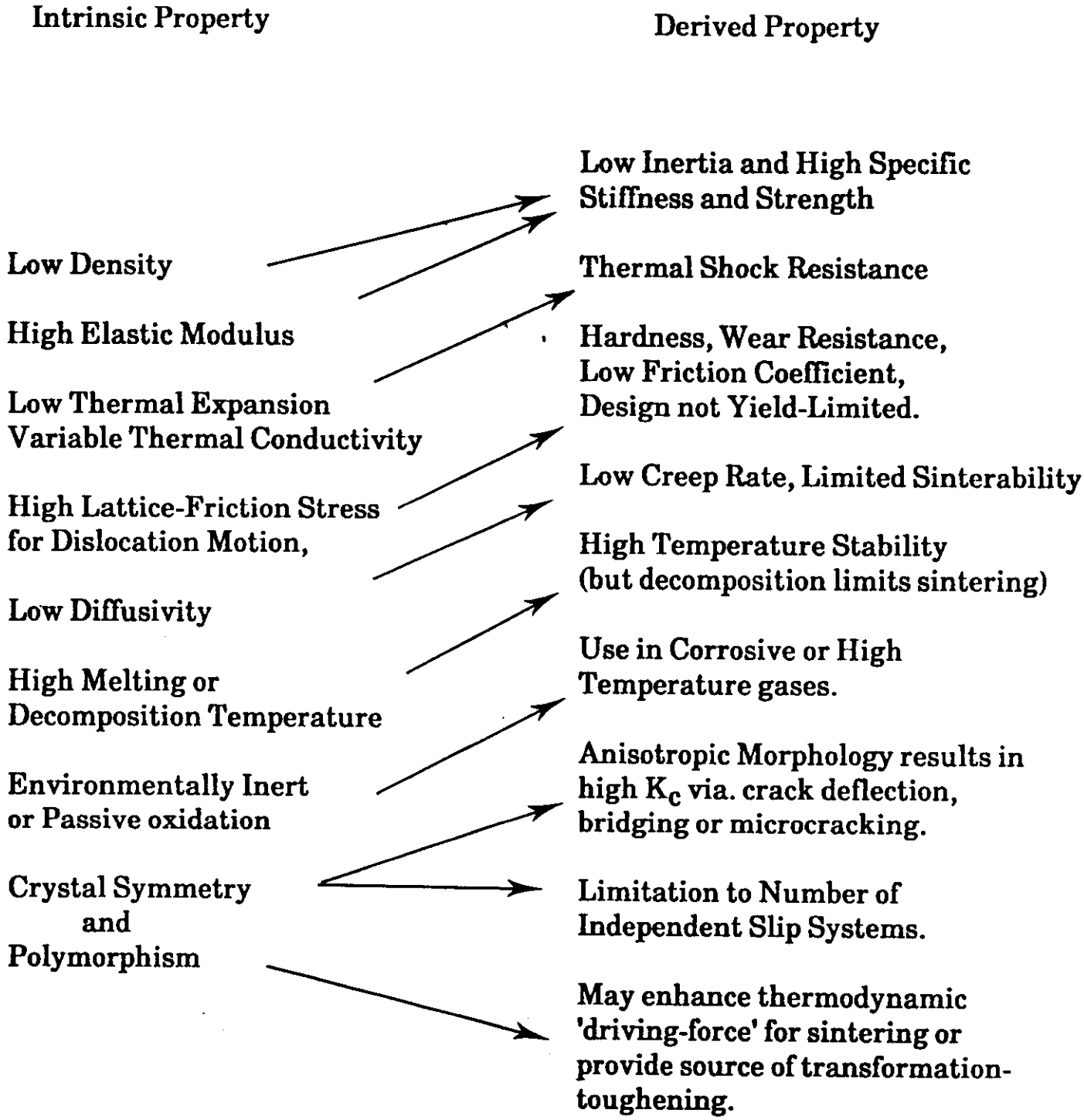

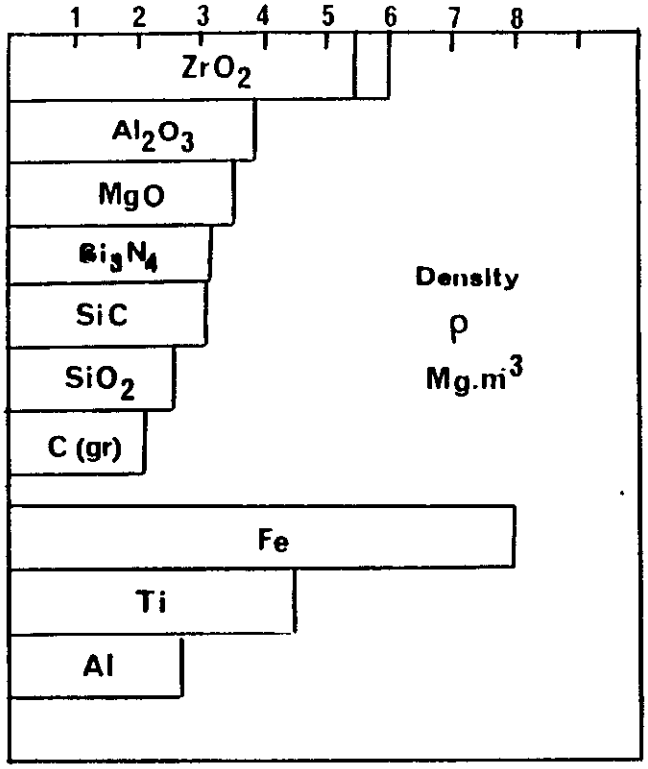
1 2 3 4 5 6 7 8
ZrO_2
Al_2O_3
MgO
Si_3N_4
SiC
SiO_2
C (gr)
Fe
Ti
Al
Density
ρ
$Mg.m^3$

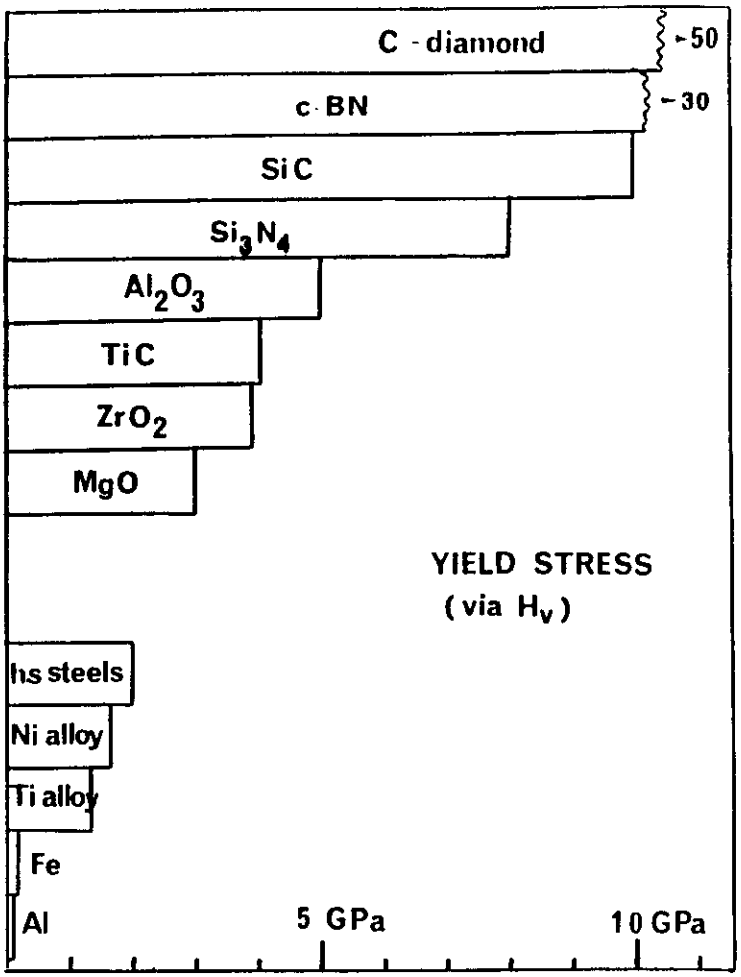
C - diamond
~50
c-BN
~30
SiC
Si_3N_4
Al_2O_3
TiC
ZrO_2
MgO
YIELD STRESS
(via H_v)
hs steels
Ni alloy
Ti alloy
Fe
Al
5 GPa
10 GPa

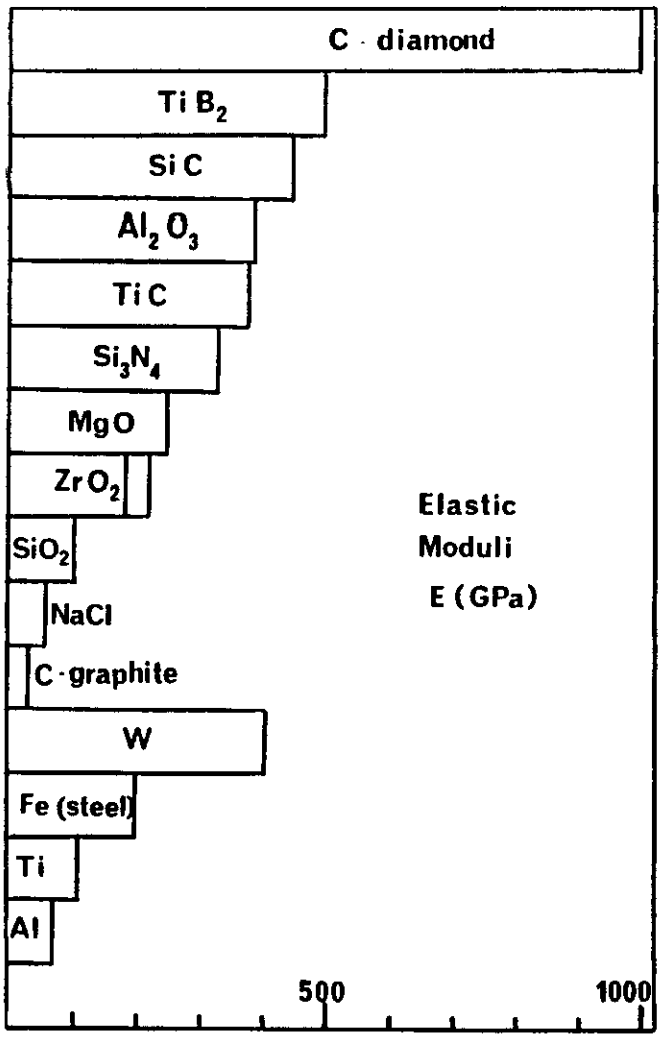
C - diamond
TiB_2
SiC
Al_2O_3
TiC
Si_3N_4
MgO
ZrO_2
SiO_2
NaCl
C-graphite
W
Fe (steel)
Ti
Al
Elastic
Moduli
E (GPa)
500
1000

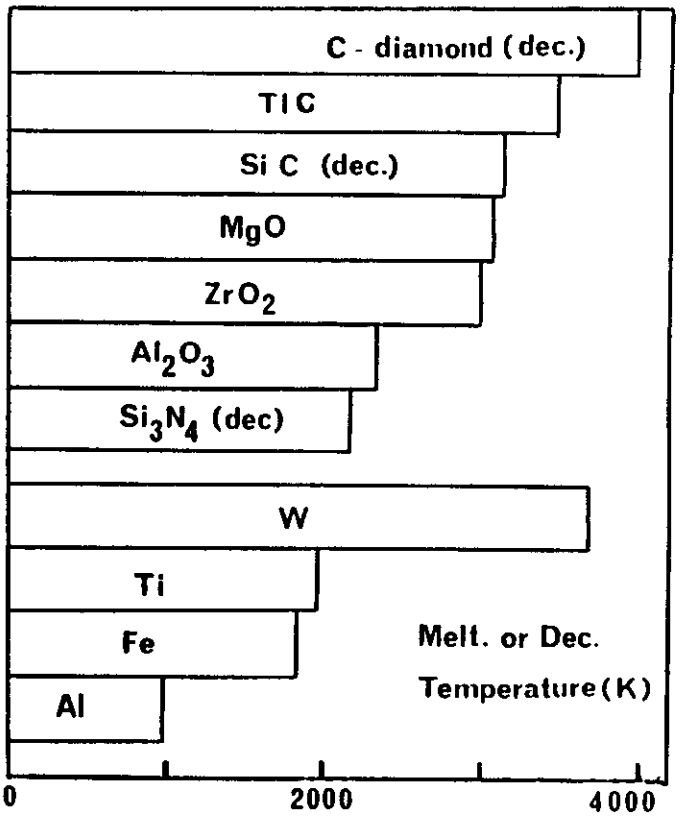
C - diamond (dec.)
TiC
SiC (dec.)
MgO
ZrO_2
Al_2O_3
Si_3N_4 (dec)
W
Ti
Fe
Al
Melt. or Dec.
Temperature (K)
0
2000
4000

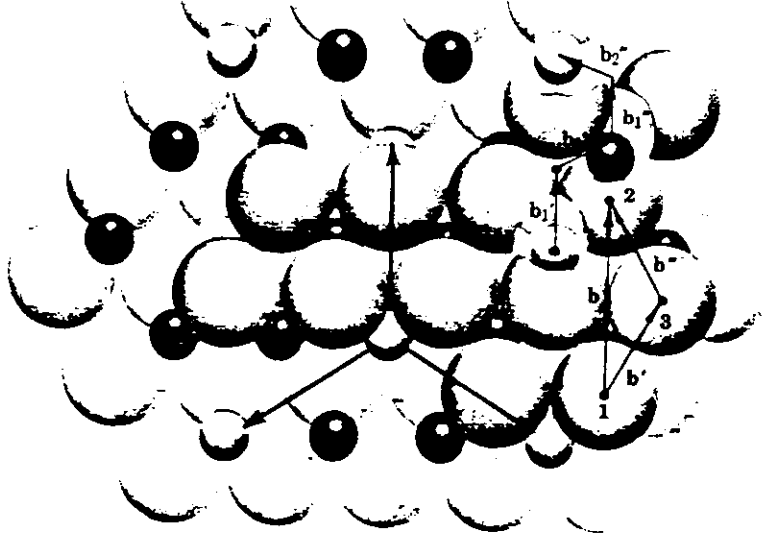

Fig. 14.28. Structure of Al_2O_3 showing two layers of large oxygen ions with hexagonal array of Al^{3+} and vacant octahedral interstices. Slip directions and Burgers' vector **b** for basal plane slip are indicated.

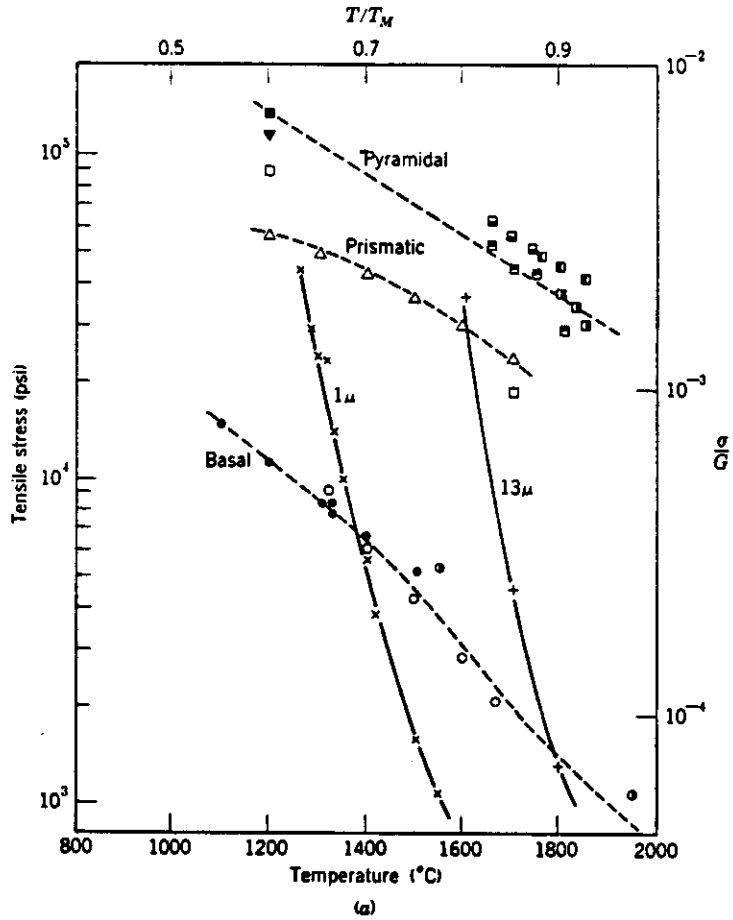

Fig. 14.40. (*a*) Tensile stress to activate various slip systems in single-crystal Al_2O_3 and flow stress for fine-grained alumina indicating diffusional creep rather than plastic flow.

from Kingery, 'Introduction to Ceramics'

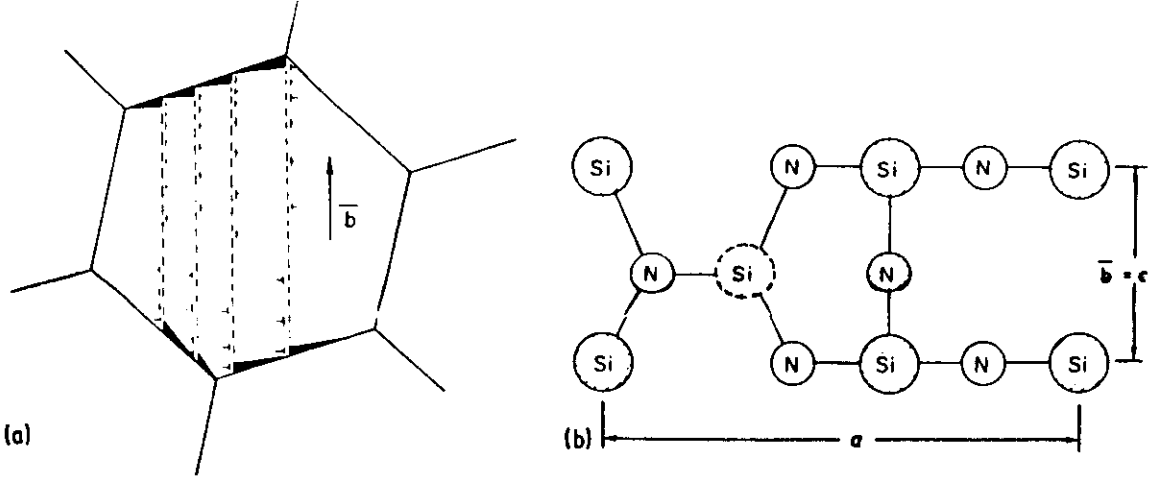

Figure 6 (a) Illustration of the nucleation of grain-boundary microcracks as a result of the operation of a singular dislocation Burgers vector $a[0001]$. (b) Projection of a unit cell of the β-Si_3N_4 crystal structure showing the relative sizes of lattice translation vectors in the a and c directions and hence the selection of an $a[0001]$ Burgers vector. (Open circles are atoms approximately within the diagram plane, shaded atoms lie above the diagram plane except for that in broken outline.)

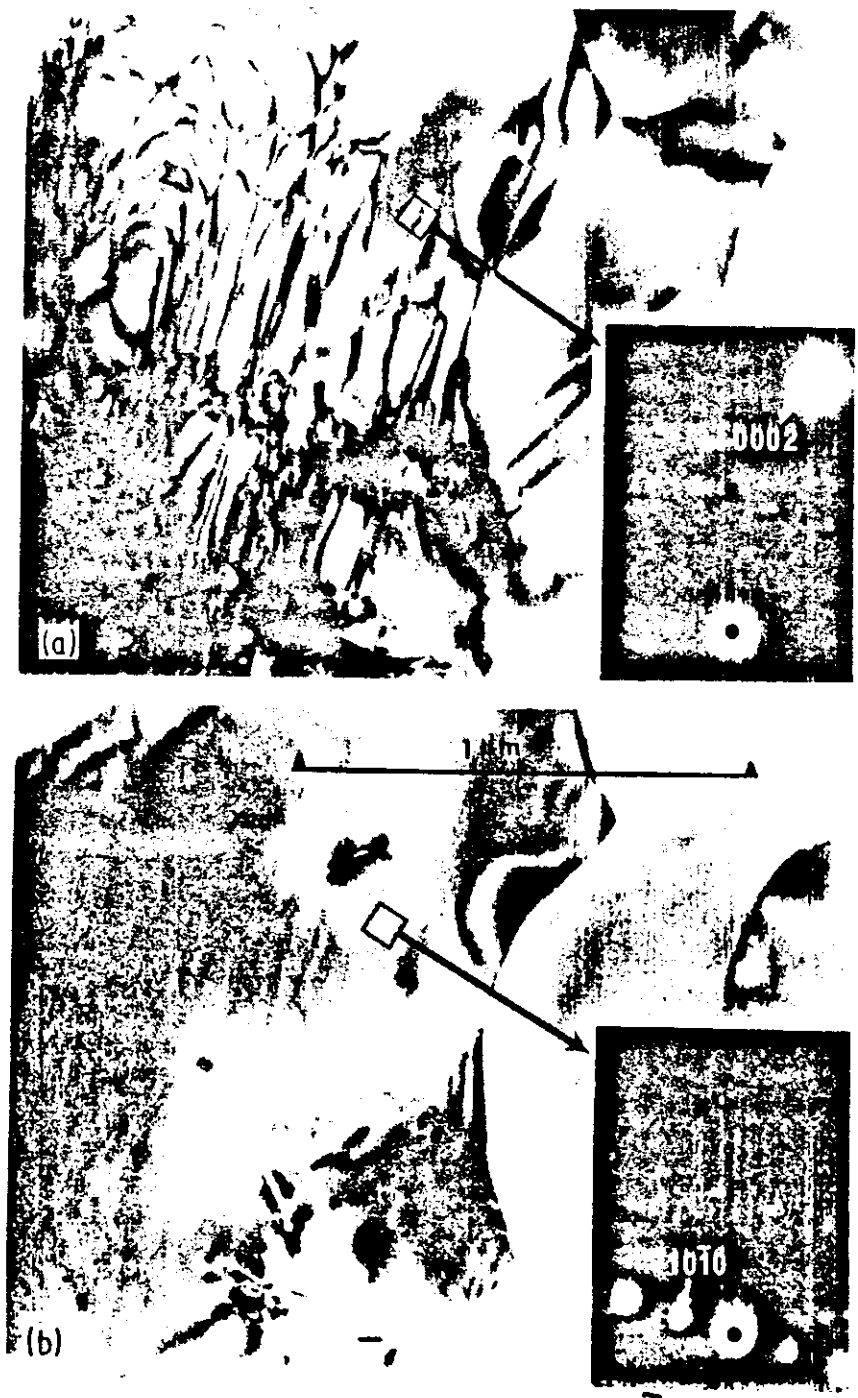

Figure 5 Burgers vector analysis in a β' grain near the periphery of the plastic zone. Dislocations, which are shown to have preferred $[0001]$ orientation and $a[0001]$ Burgers vector, are (a) imaged with 0002 reflections and (b) invisible with prism plane $10\bar{1}0$ reflections. The "stranger" dislocation segments which are imaged in both (a) and (b) must have Burgers vectors inclined to both a- and c-axes (e.g. $b = a + c$) and are observed in negligible density throughout the plastic zone.

I. Control of critical flaws.

Simple Fracture Mechanics Relation:-

$$\text{Fracture Stress } \sigma_f \approx \frac{1}{Y}\sqrt{\frac{EG_c}{c}} \approx \frac{1}{Y}\frac{K_c}{\sqrt{c}}$$

where Y = Geometrical constant
G_c = Critical energy release rate
K_c = Critical Stress Intensity (Fracture Toughness)
C = Critical Flaw size

Problems: - Values of C for typical monolithic ceramic (see Figure) (K_c-5 MPa.$m^{\frac{1}{2}}$) must be less than 100μm for $\sigma_f > 300$ MPa.
- Variability of σ_f due to statistical variation of C within a sample of material may lead to overlap of service stress and low-strength 'tail' of distribution.

Possible Solutions.

(i) 'Proof' test components (truncate sample distribution)

(ii) Use probabilistic approach; e.g. using Weibull statistics:

$$\text{Probability of failure } P_F = 1 - \exp\left[-V\left(\frac{\sigma}{\sigma_o}\right)^m\right]$$

where σ = (constant) stress in specimen
V = specimen volume
σ_o = scaling parameter
m = Weibull Modulus. (Measure of 'reliability' or distribution in σ_f)
m is obtained from the gradient of a $\ln \ln (P_F)$ against $\ln \sigma$ plot, for a material sample.

(iii) Reduce mean flaw size, distribution width or sensitivity via:-
- reduced sintering porosity
- removal of aggregates and impurity inclusions
- minimise surface machining damage
- introduce surface compressive stress (ion implant or (surface transformation)

(iv) Increase Fracture Toughness (K_c) via microstructural modification

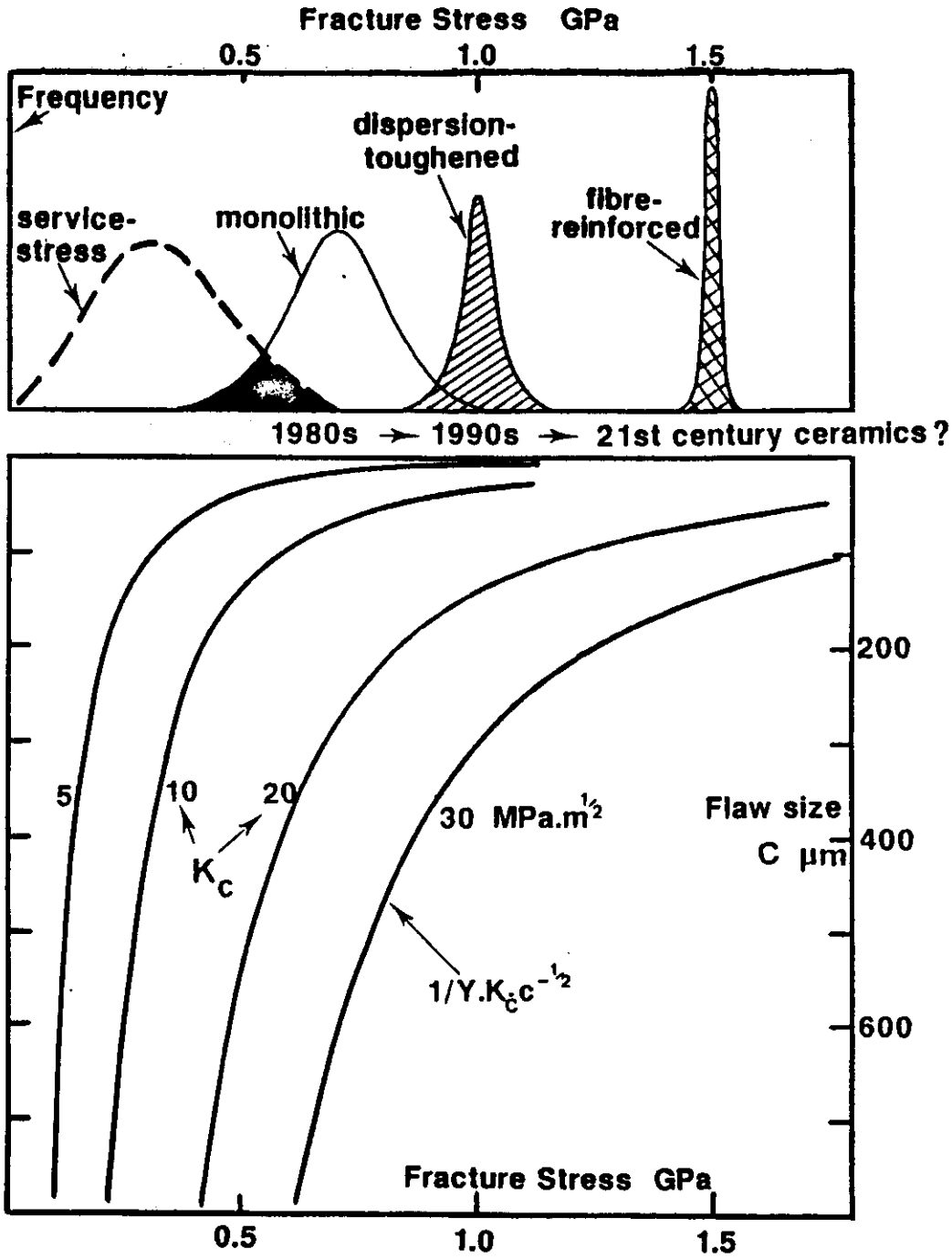
Fracture Stress GPa
0.5
1.0
1.5
Frequency
dispersion-
toughened
service-
stress
monolithic
fibre-
reinforced
1980s → 1990s → 21st century ceramics ?
200
5
10
20
30 MPa.m^½
Flaw size
C µm
400
K_C
1/Y.K_C c^-½
600
Fracture Stress GPa
0.5
1.0
1.5

from Ref 2.

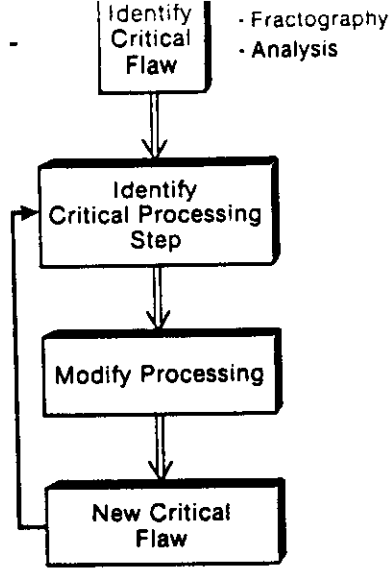

Fig. 4 The sequence involved in flaw size control by process iteration.

Ref.

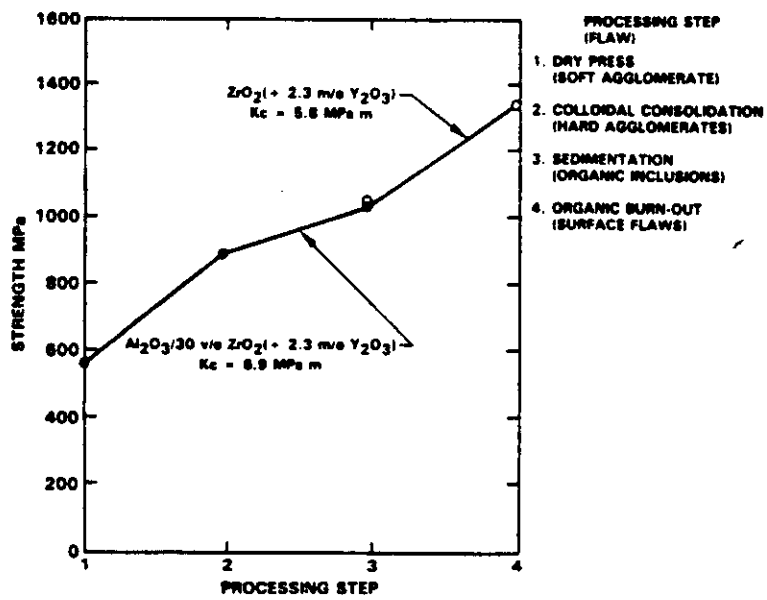

Fig. 5 A sequence of strength improvements obtained for Al_2O_3/ZrO_2 based on the schematic depicted in Fig. 4.

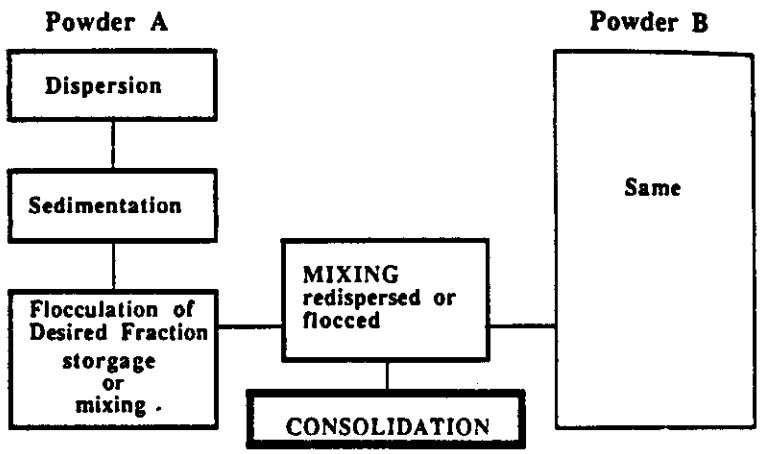

Ref

Figure 2. One scheme for colloidal treatment of powder prior to consolidation.

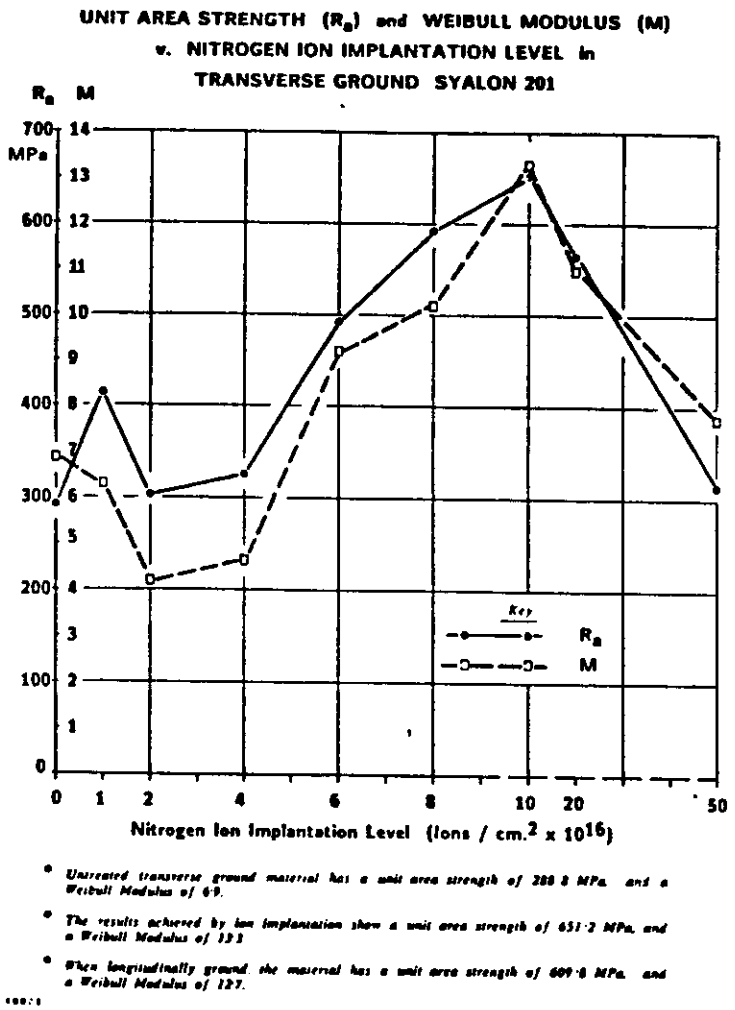

1. Unit area strength and Weibull Modulus against nitrogen ion implantation level in transverse ground syalon 201.

from G.E. Syers et al. Rolls Roy Leavesden, Ut

Crack Bridging

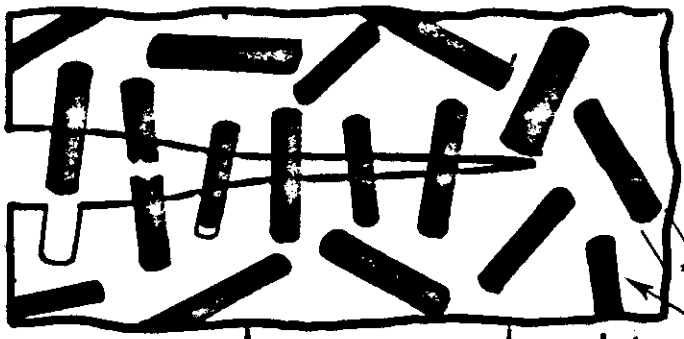

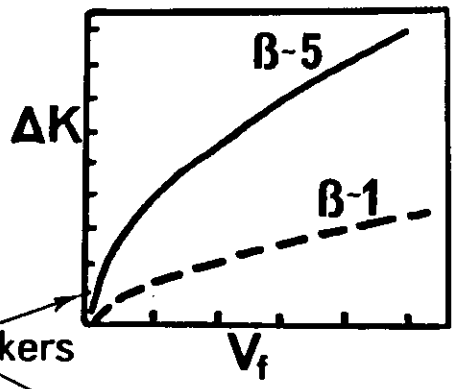

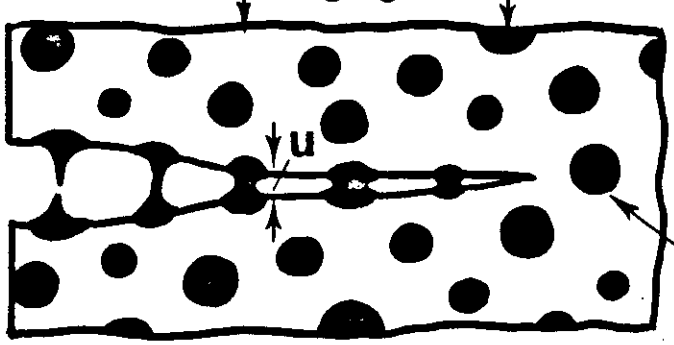

$$\Delta K \approx \sigma_f^w \left(V_f\, r\, \frac{E^c G^m}{E^w G^i} \right)^{1/2}$$

ß

general $\Delta G \approx V_f \int \sigma(u)\,du$

traction on crack surfaces

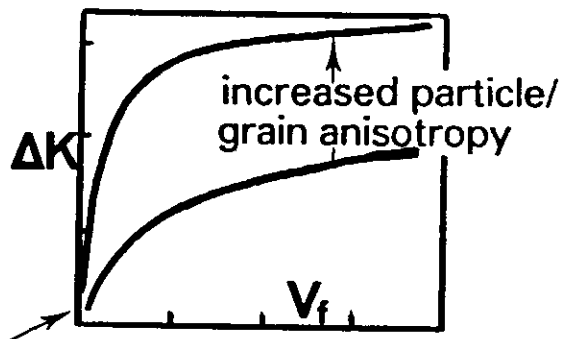

Process Zone Effects

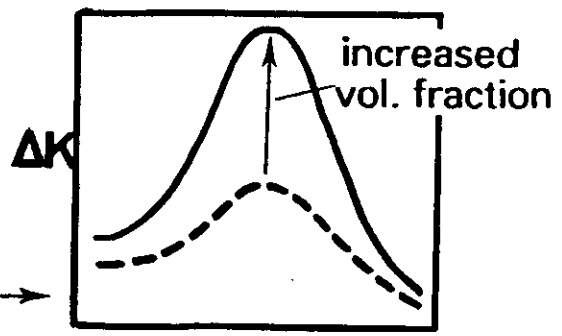

zone of transformation/
or
microcracking

local
σ-ε

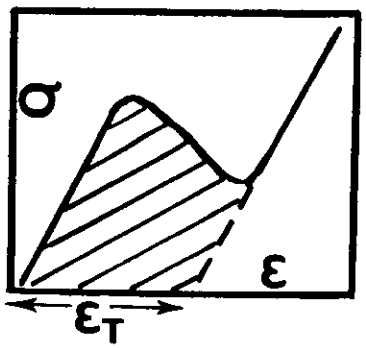

$$\Delta K \sim E\, V_f\, \varepsilon_T\, h^{1/2}$$

HIGH TEMPERATURE, TIME DEPENDENT DEFORMATION AND FRACTURE

$$\dot{\varepsilon} = \frac{a\Omega}{kT}\,\frac{\sigma D_b}{d^m}$$

m: 3 Grain Boundary Diffusion (D_b)
2 Lattice Diffusion (D_L)
1 Solution - Precipitation

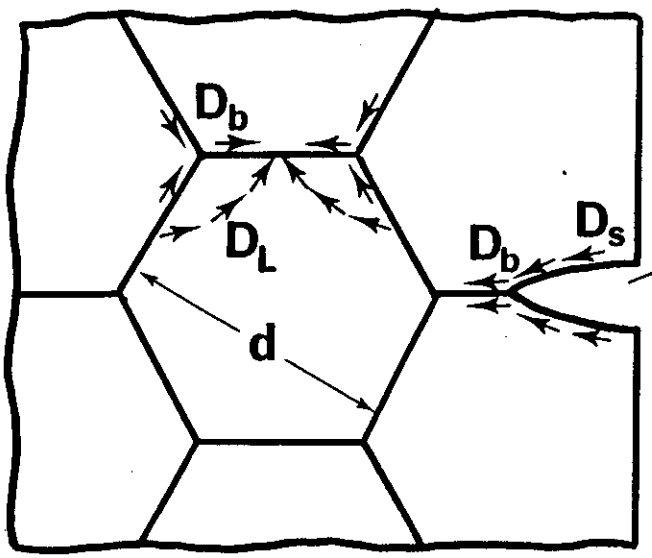

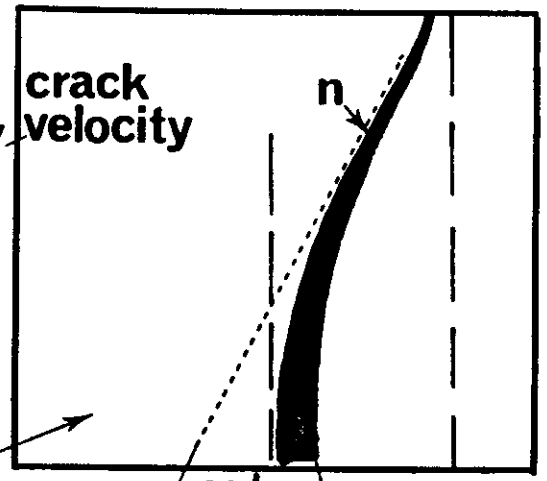

Diffusional Flaw Growth

Crack-Blunting Threshold

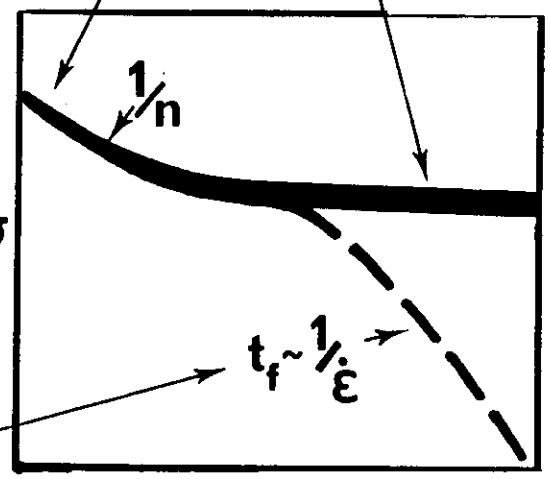

t_f – time to failure

σ

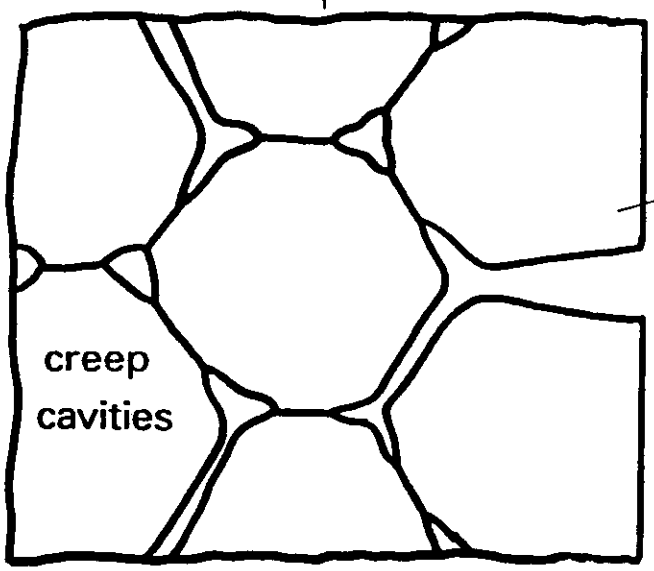

nucleation and coalescence of creep-cavitation

N.B. Creep rarely steady state; microstructural changes/ g.b. crystallisation or solute out-diffusion/cavitation

Alternative models; e.g. θ-protection (Wiltshire et al.)
- superposition of primary and tertiary.

$$\varepsilon = \theta_1 (1 - e^{\theta_2 t}) + \theta_3 (e^{\theta_4 t} - 1)$$

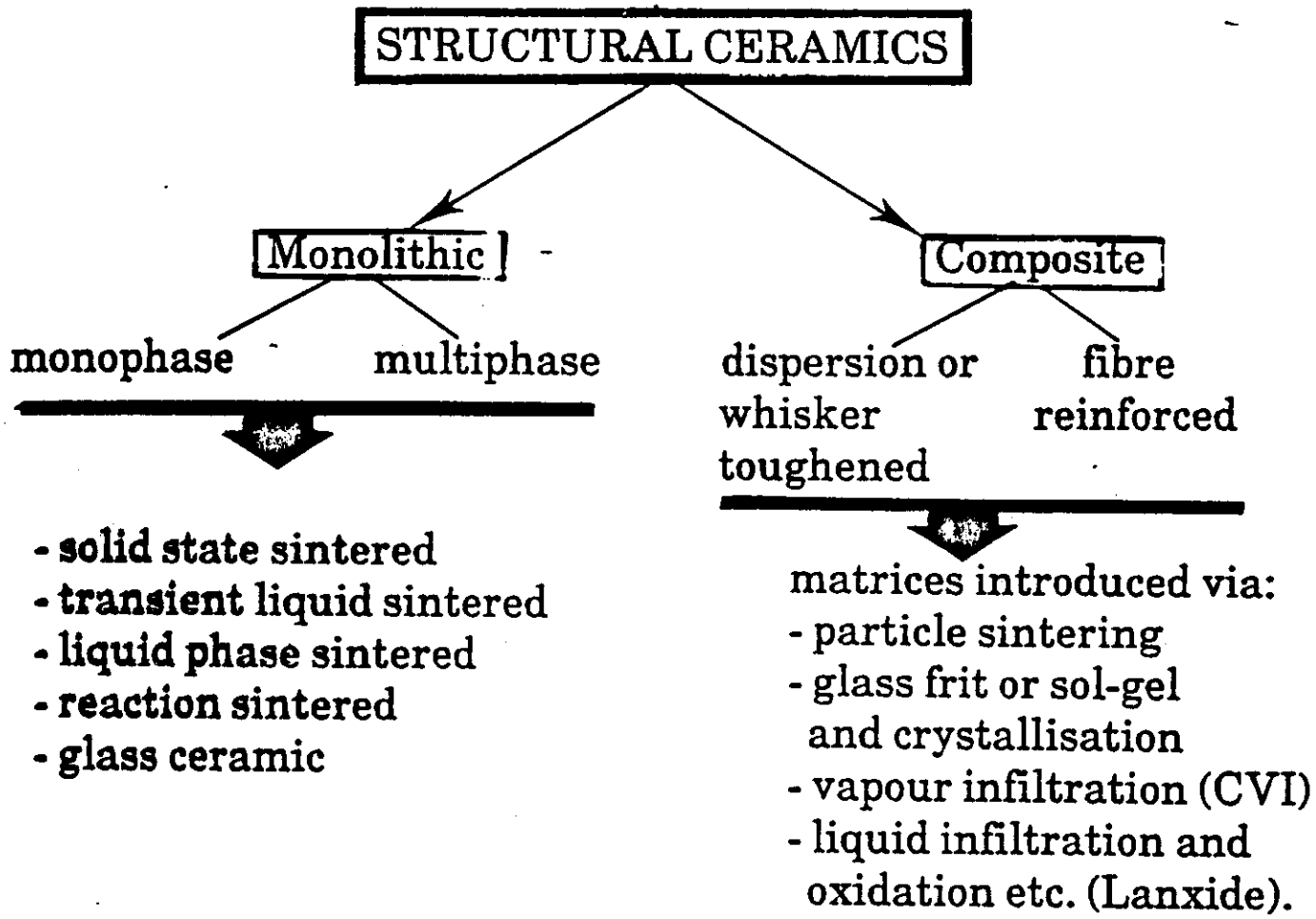
STRUCTURAL CERAMICS
Monolithic
Composite
monophase
multiphase
dispersion or whisker toughened
fibre reinforced
- solid state sintered
- transient liquid sintered
- liquid phase sintered
- reaction sintered
- glass ceramic
matrices introduced via:
- particle sintering
- glass frit or sol-gel and crystallisation
- vapour infiltration (CVI)
- liquid infiltration and oxidation etc. (Lanxide).

MONOLITHIC CERAMIC MICROSTRUCTURES

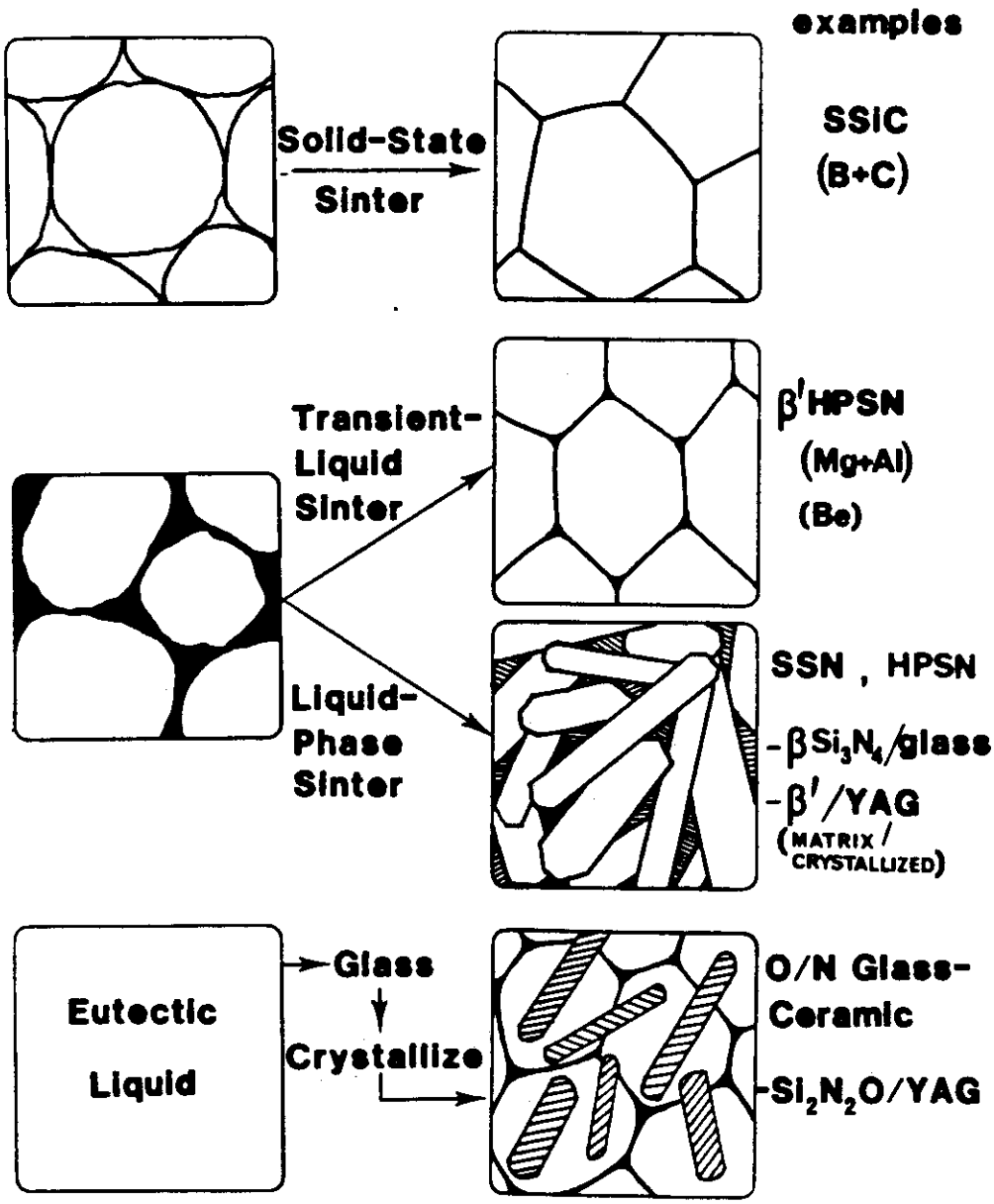

Ref. 2, 13.

Si_3N_4 - based ceramics

Major phase - normally β Si_3N_4 or substituted - derivatives β' ($Si_{3-x}Al_xO_xN_{4-x}$)

or ($Si_{3-x}Be_xO_{2x}N_{4-x}$)

HPSN e.g. 1% MgO additive — Norton NC132
8% Y_2O_3 " — " NCX34

HIPSN 100–200 MPa — 2–5% Y_2O_3 " — Battelle-USA or ASEA-sweden

} 2–5% mainly glassy intergranular residue.

SSN Contain β' known as 'Sialons'

e.g.
- 5% MgO + 9% Al_2O_3 — Kyocera SN205
- 6% Y_2O_3 + 2+% Al_2O_3 — GTE AY6/PY6
- 6% Y_2O_3 + Al_2O_3/AlN — Toshiba + Lucas-Cookson - Syalon 101/201
- $SiBeN_2$ — G.E.

} 5–10% glassy or crystalline 'matrix'.

1750–1850°C

SRBSN (post-sintered, 'reaction-bonded' with additives)

↓ related to RBSN in 1st step of processing

RBSN Nitriding of Si during sintering gives

- 60–90% α Si_3N_4
- 10–40% β Si_3N_4
- 5% Si
- 15–30% porosity.

NC350 - Norton
'Nitrasil' - AED

Developments in ceramics with new oxynitride phases. } α', Si_2N_2O

SiC - based ceramics

Major phase usually α SiC (hex. polytypes) } Normally 0-3% intergranular residuals
occasionally β SiC (cubic) }

HP SiC – 1% B_4C or Al/Al_2O_3 additives — Norton NC 203, Elektroschmelzwerk Co. FRG. } α Si
or
HIP SiC (smaller quantity ..)
200 MPa
1900 – 2000 °C

S SiC (B + C) or (Al + C) additives — Kyocera SC201, Carborundum, G.E. sintered } α SiC / β Si
0.5-1%
1950 – 2100 °C

Si SiC (Siliconized) — wide range of comp. + Sintering process. — eg. - Norton NC435, - Coors.
from SiC + graphite
reacts with Si in liquid or vapour state } ~ 10% free Si in pores.

Ref. 1

ZrO_2 – toughened ceramics.

PSZ ($8-10\%$ MgO)
- Sintered $1650-1850\,^\circ C$ + heat-treated $1100-1450\,^\circ C$

e.g. Feldmühle ZN-40

Coors (~ 35% tetragonal

TZP ($2-4\%$ Y_2O_3)
- Sintered $1350-1500$ with additives (Al_2O_3)

NGK Z-191 (fully tetragonal)

Property Comparison

	M.O.R. (MPa)	K_{IC} (MPa.$m^{1/2}$)
PSZ	600 – 800	6 – 8
TZP	1000 – 2500	7 – 12
ZT(Al_2O_3)	500 – 1300	5 – 8
CSZ (cubic)	180	2.5
SSN	400 – 800	5 – 7
SSiC	400 – 500	3 – 5

Ref. 1.

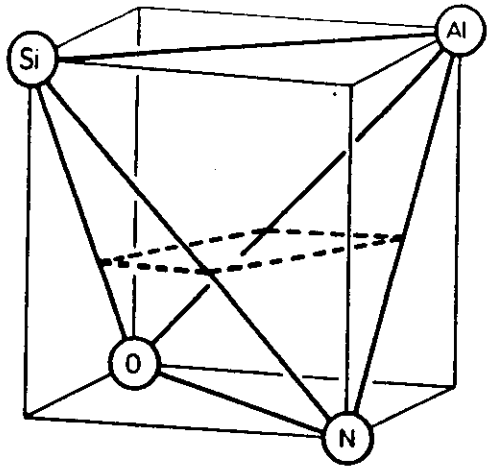

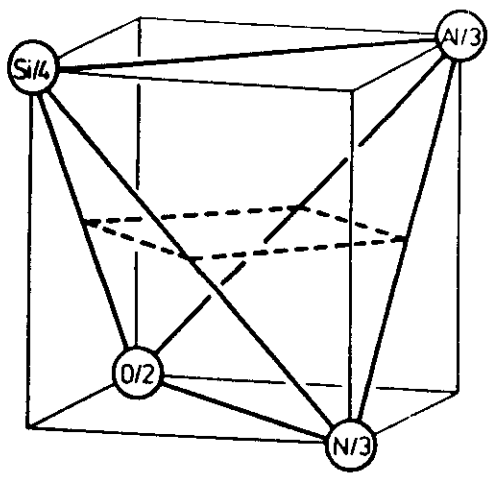

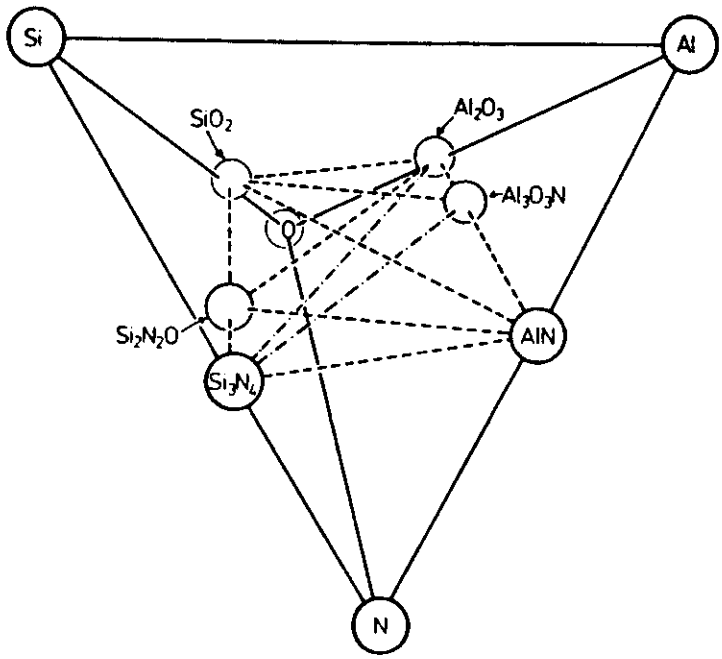

Representation of Sialon System

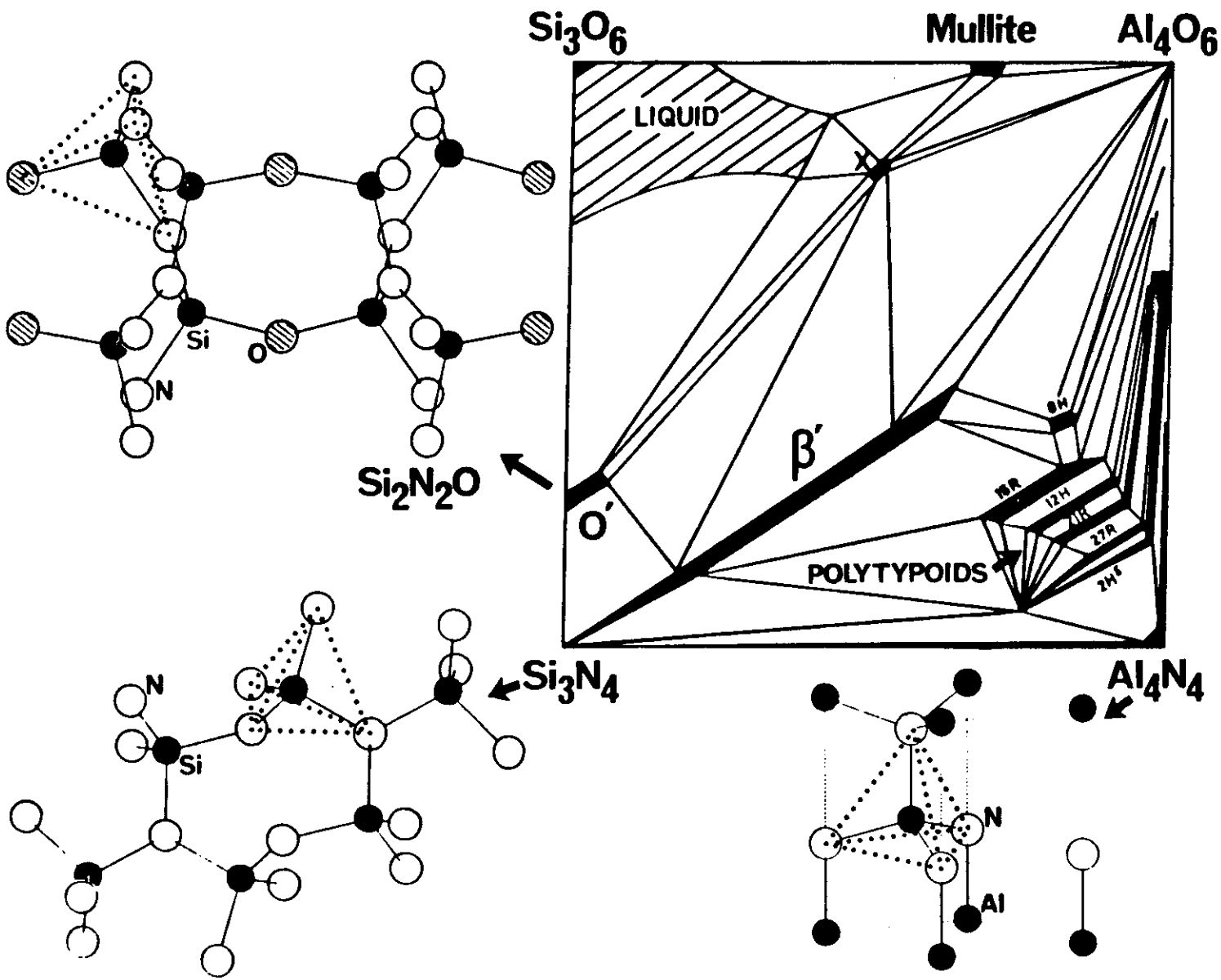
Si_3O_6
Mullite
Al_4O_6
LIQUID
X
Si
O
N
Si_2N_2O
O'
β'
8H
15R
12H
21R
27R
2H
POLYTYPOIDS
Si_3N_4
Al_4N_4
N
Si
N
Al

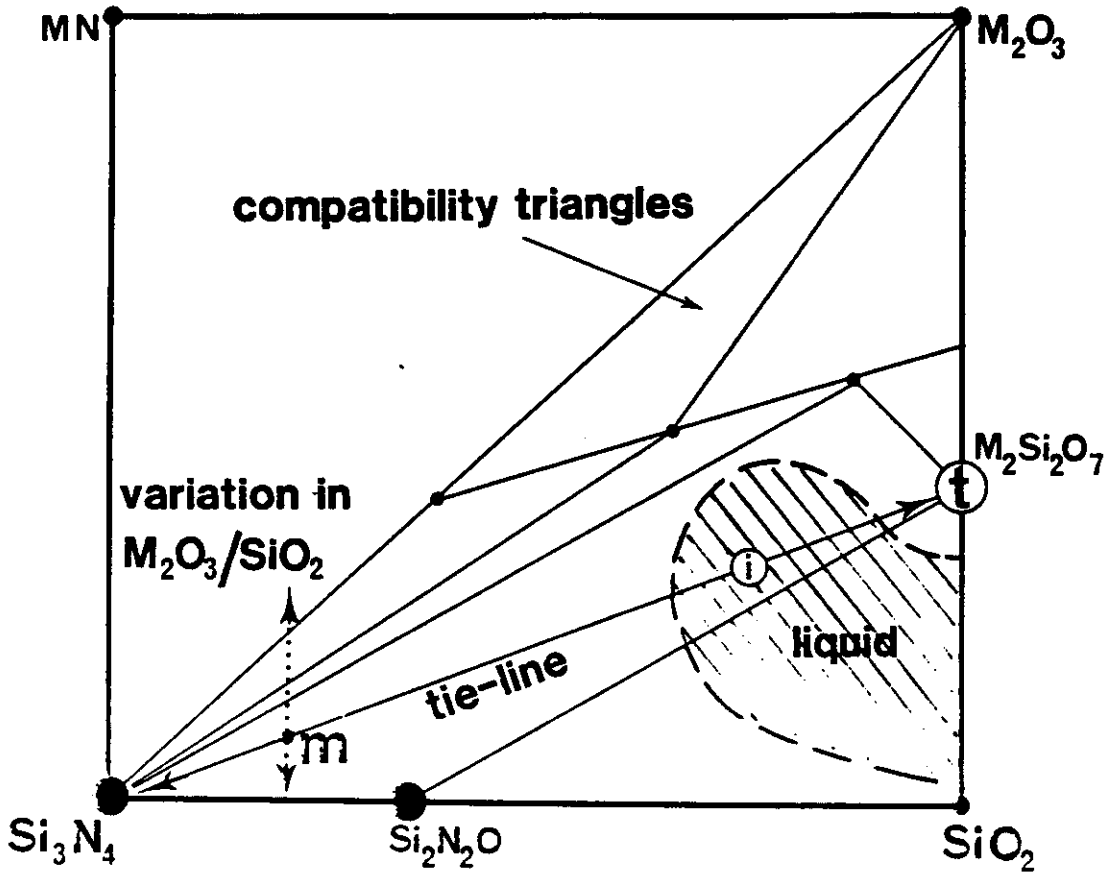
MN
M_2O_3
compatibility triangles
$M_2Si_2O_7$
t
variation in
M_2O_3/SiO_2
i
liquid
tie-line
m
Si_3N_4
Si_2N_2O
SiO_2

M = Y, Nd, La

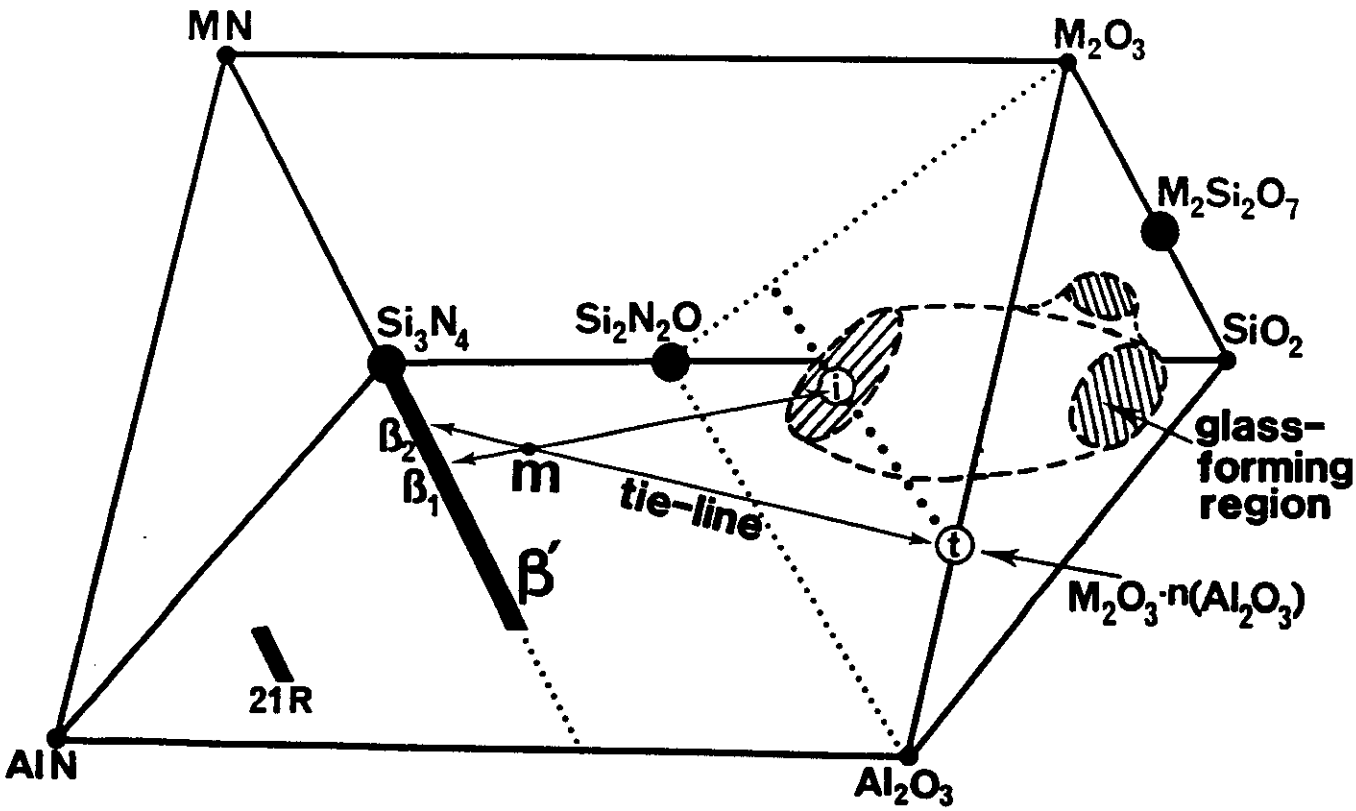
MN
M_2O_3
$M_2Si_2O_7$
Si_3N_4
Si_2N_2O
SiO_2
i
β_2
β_1
m
tie-line
glass-
forming
region
t
$M_2O_3 \cdot n(Al_2O_3)$
β'
21R
AlN
Al_2O_3

P.I.8

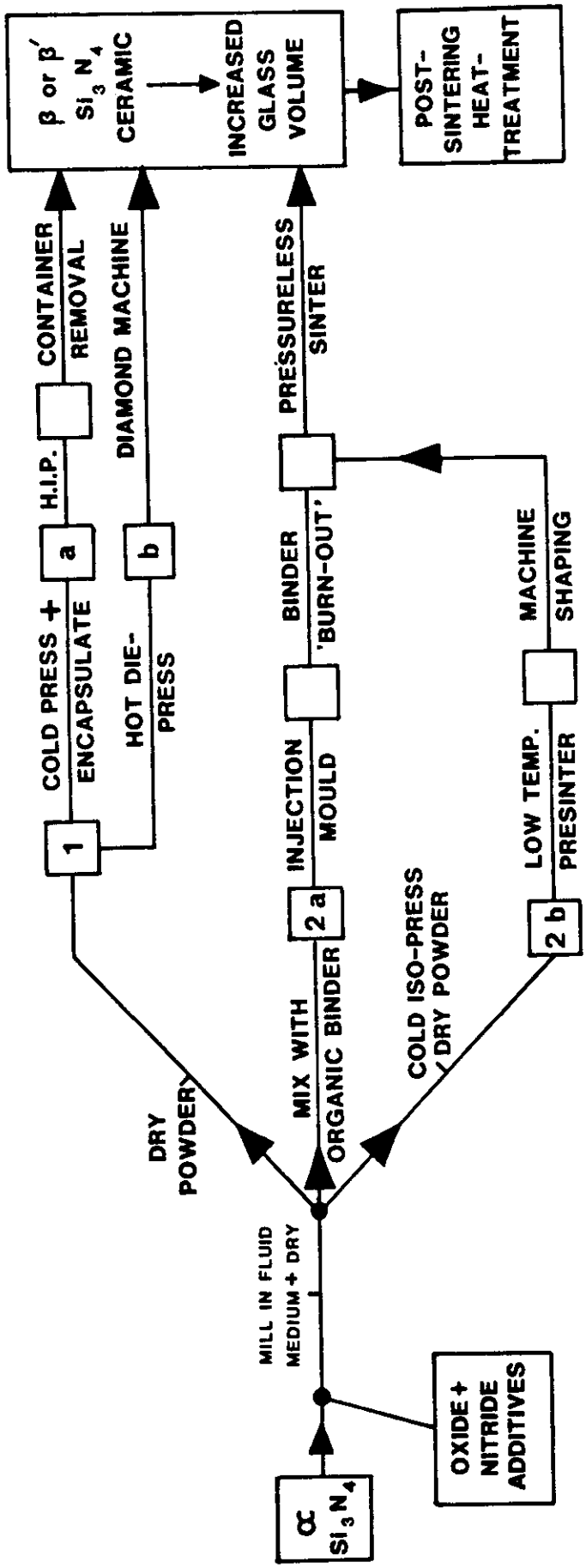

FABRICATION ROUTES FOR NITRIDE CERAMICS

Ref. 1

PROCESSING ROUTES FOR Si_3N_4 POWDERS

(a) $3Si + 2N_2 \rightarrow Si_3N_4$ (Direct nitriding)

(b) $3SiO_2 + 6C + 2N_2 \rightarrow Si_3N_4 + 6CO$ (Carbothermal Reduction)

(c) $3SiCl_4 + 16NH_3 \rightarrow Si_3N_4 + 12NH_4Cl$ (Vapour phase reaction)

(d) $SiCl_4 + 6NH_3 \rightarrow Si(NH)_2 + 4NH_4Cl$ (Vapour phase reaction +

$3Si(NH)_2 \rightarrow Si_3N_4 + 2NH_3$ imide decomposition)

TYPICAL POWDER CHARACTERISTICS

	(a)	(b)	(c)/(d)
oxygen(%) content	0.5-1.5	2-3	1-2
other main(%) impurities	Fe(0.5-0.2) Si(0.1-0.5)	C(1)	Cl(0.1)
Particle size(μm)	0.5-1	0.2-0.5	0.1-0.5
Surface(m^2g^{-1}) area	2.10	7-10	10-15
%βSi_3N_4	~5	1 (α-may be non-crystalline)	2-10

(i) $\alpha\text{-}Si_3N_4 + SiO_2 + MO \rightarrow \beta\text{-}Si_3N_4 + M\text{-}Si\text{-}O\text{-}N$

(ii) $\alpha\text{-}Si_3N_4 + \underbrace{SiO_2}_{\text{SURFACE}} + \underbrace{AlN + MO}_{\text{ADDITIVES}} \rightarrow \underbrace{\beta'\text{-}Si_{3-X}Al_XO_XN_{4-X}}_{\text{MAJOR PHASE}} + \underbrace{M\text{-}Si\text{-}Al\text{-}O\text{-}N}_{\text{GLASS RESIDUE}}$

Mg, Y, Sc, Ln

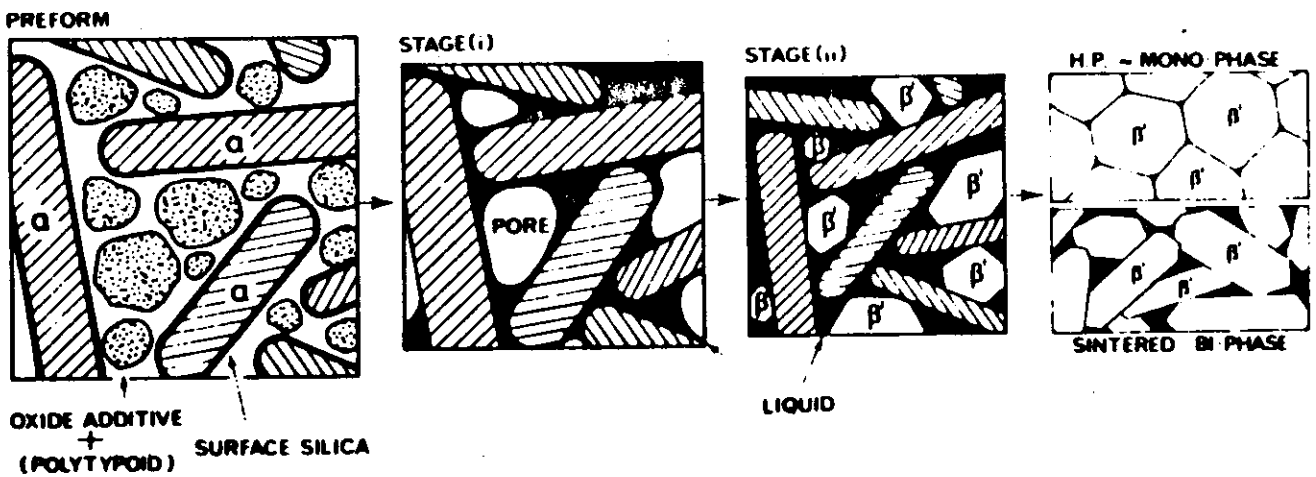

The liquid-phase sintering process for nitride ceramics illustrating the dissolution of αSi_3N_4 and reprecipitation as βSi_3N_4 or the substituted β'-sialon phase

Ref. 1

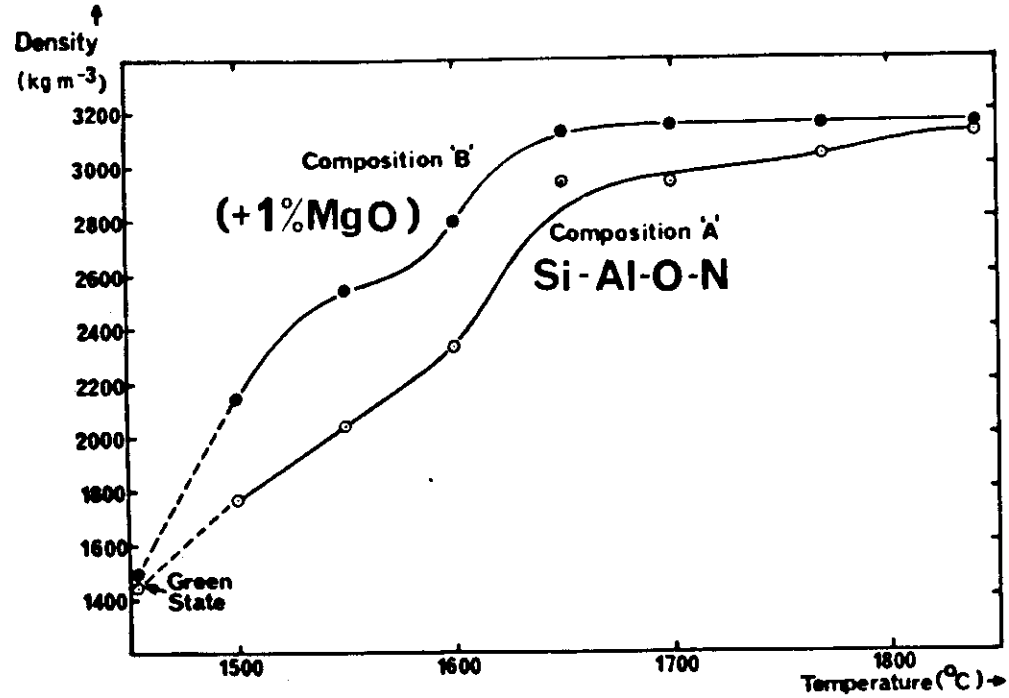
Density
(kg m⁻³)
3200
3000
2800
2600
2400
2200
2000
1800
1600
1400
Composition 'B'
(+1%MgO)
Composition 'A'
Si-Al-O-N
Green State
1500
1600
1700
1800
Temperature (°C)

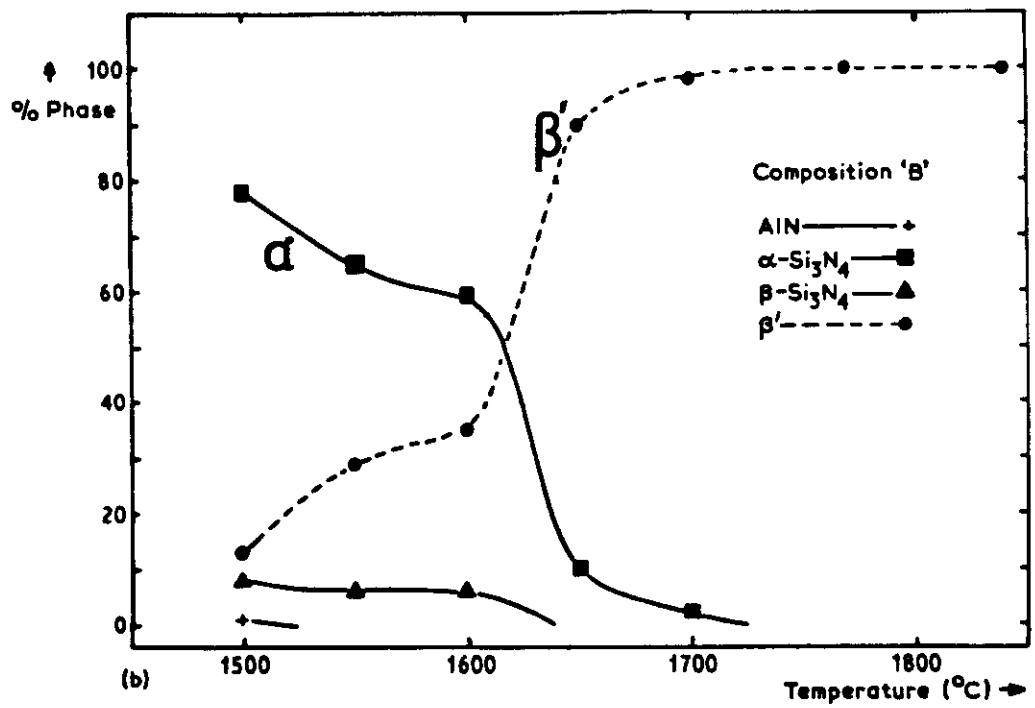
% Phase
100
80
60
40
20
0
α
β'
Composition 'B'
AlN
α-Si3N4
β-Si3N4
β'
(b)
1500
1600
1700
1800
Temperature (°C)

Ref. 9.

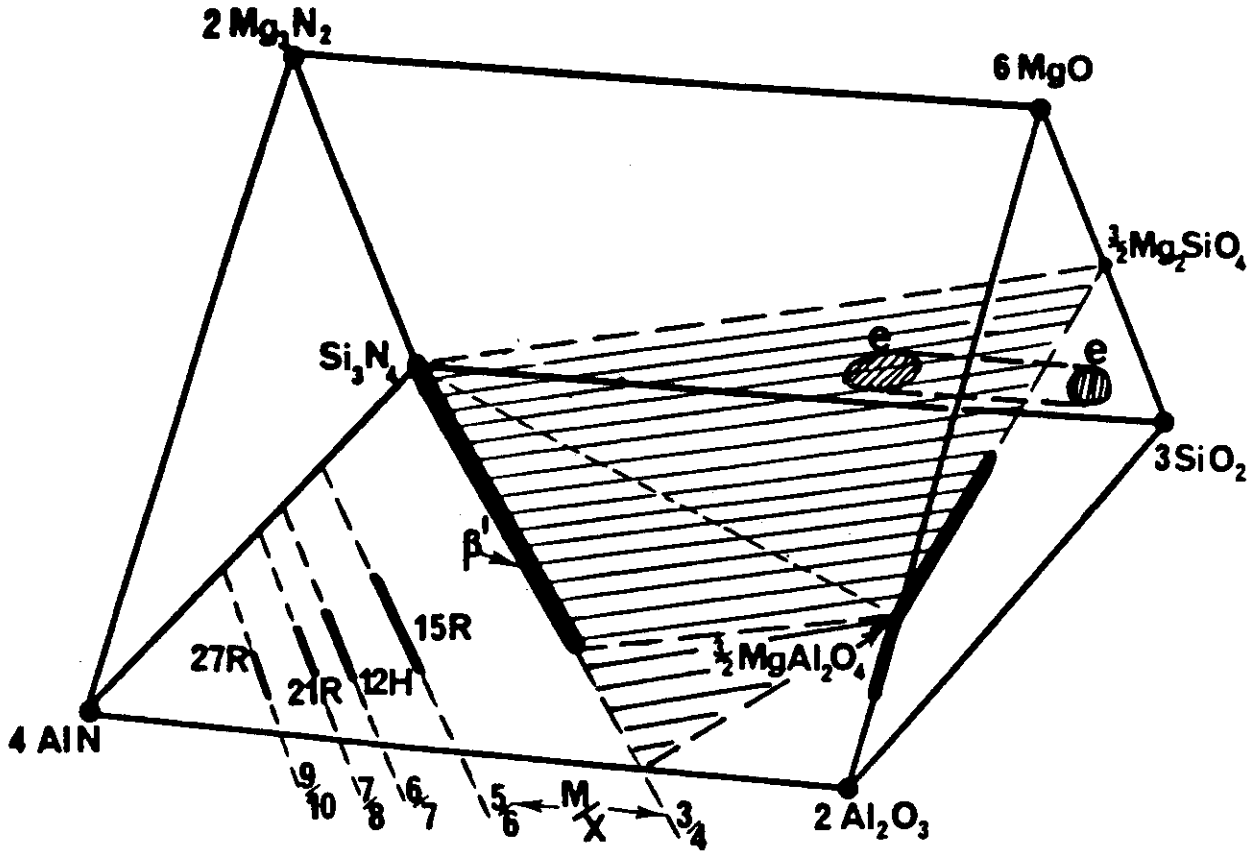
2 Mg3N2
6 MgO
3/2 Mg2SiO4
Si3N4
e
e
3SiO2
β'
15R
27R
21R
12H
1/2 MgAl2O4
4 AlN
9/10
7/8
6/7
5/6
M/X
3/4
2 Al2O3

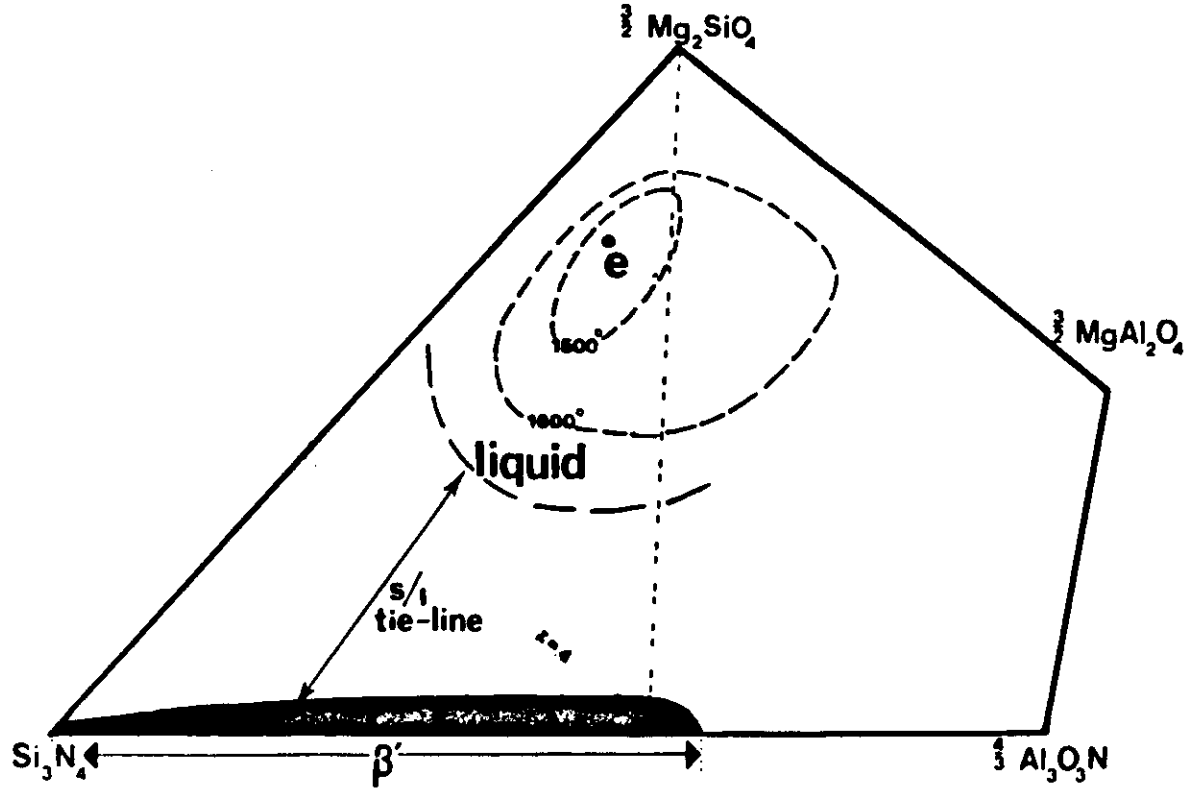
3/2 Mg2SiO4
e
1800°
1900°
liquid
3/2 MgAl2O4
s/l
tie-line
Si3N4
β'
4/3 Al3O3N

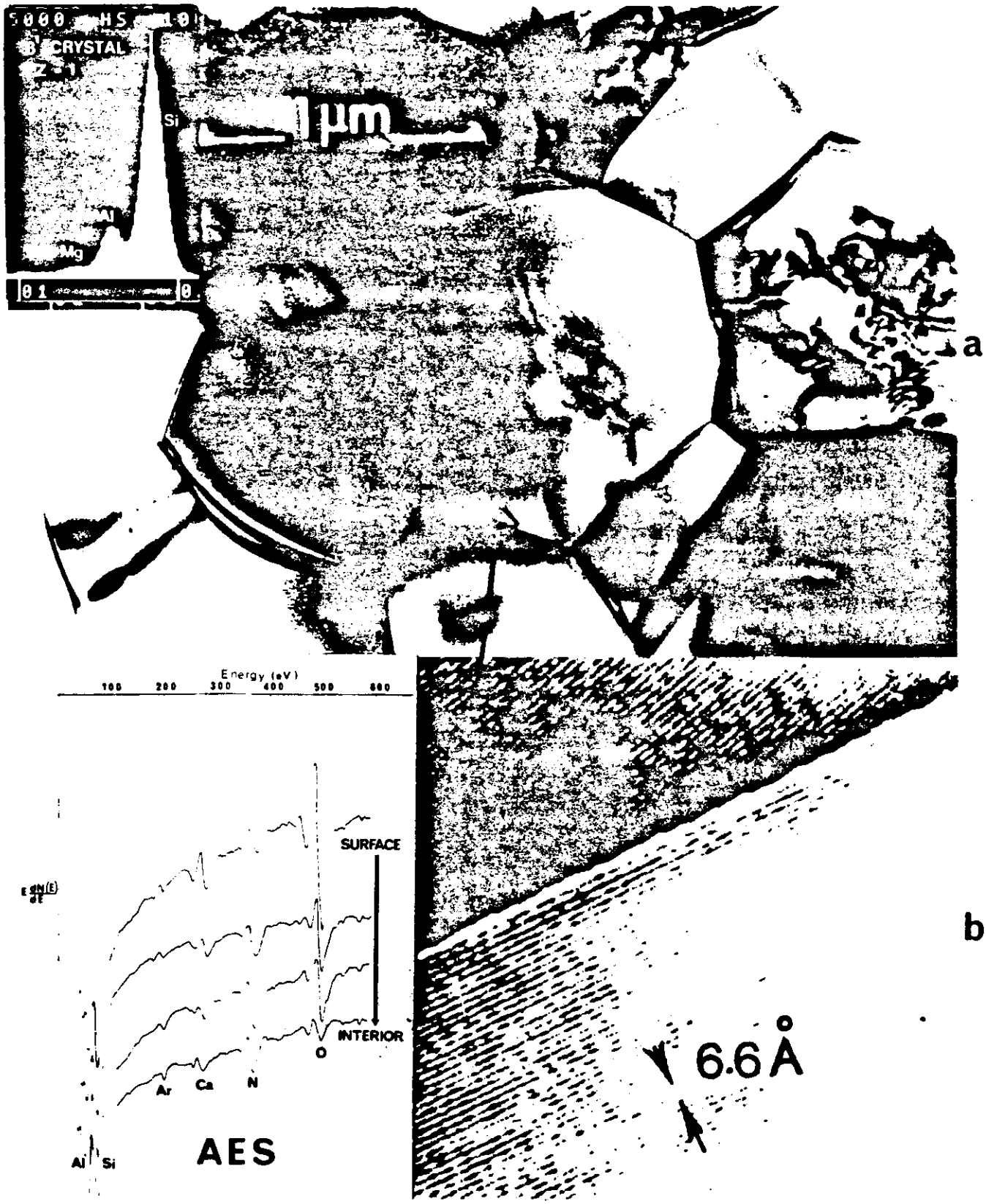
1µm
Si
a
Energy (eV)
100
200
300
400
500
600
SURFACE
INTERIOR
O
Ar
Ca
N
Al
Si
AES
b
6.6 Å

Ref. 9

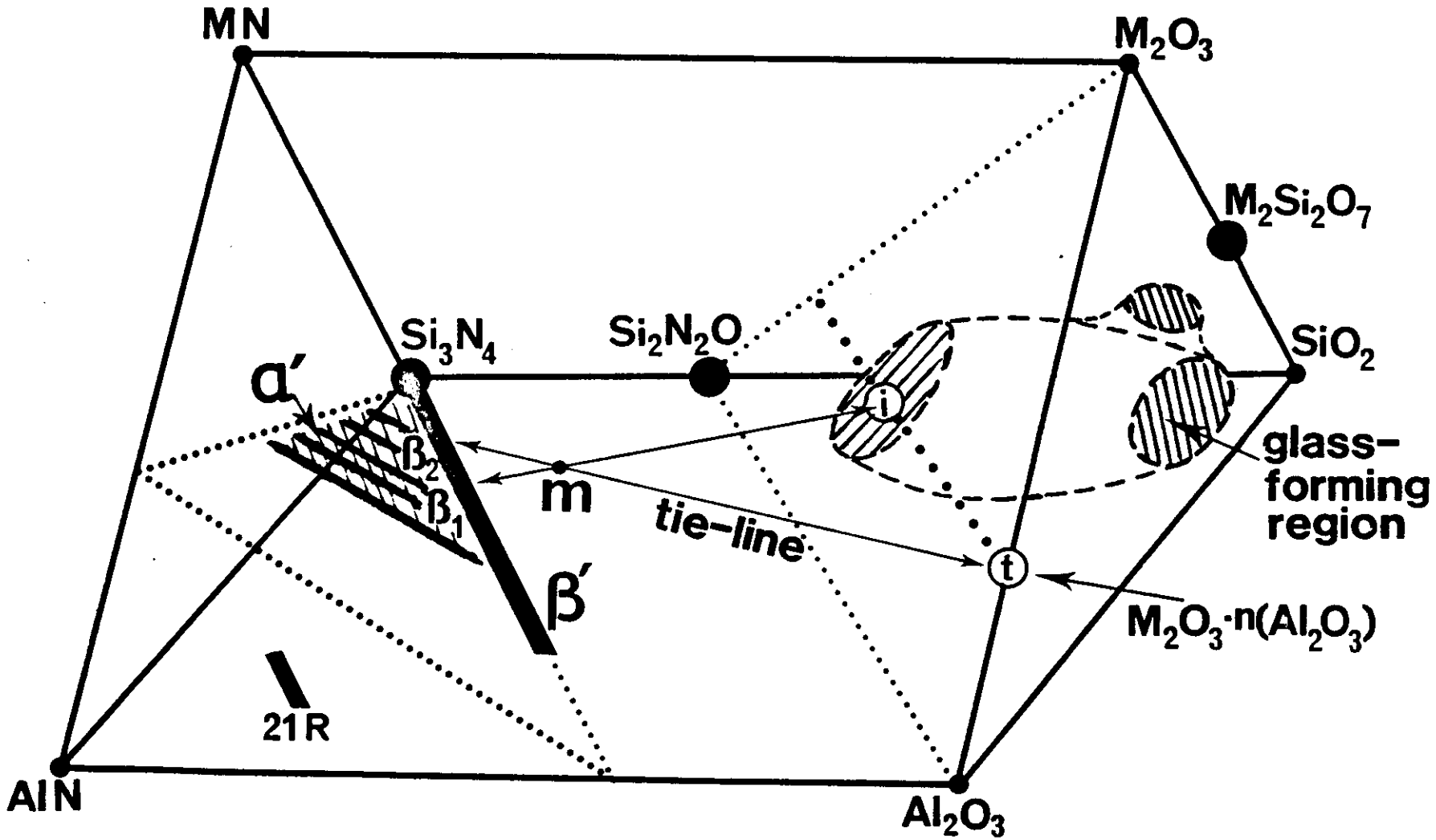
MN
M_2O_3
$M_2Si_2O_7$
Si_3N_4
Si_2N_2O
SiO_2
α′
$β_2$
$β_1$
m
tie-line
i
t
glass-forming region
β′
M_2O_3·n(Al_2O_3)
21R
AlN
Al_2O_3

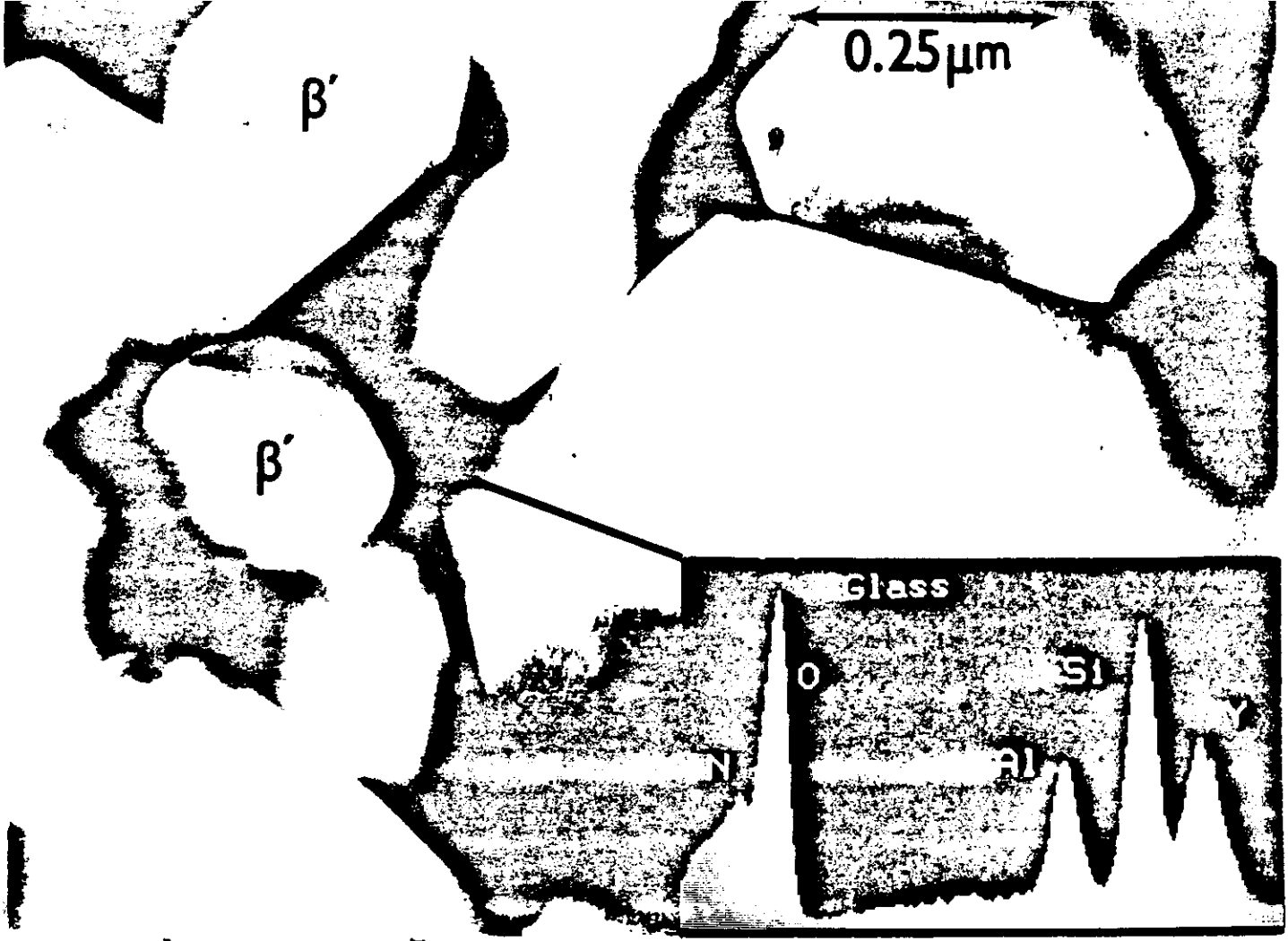

EDAX

EELS

glass

β′

398 eV

N

532 eV

O

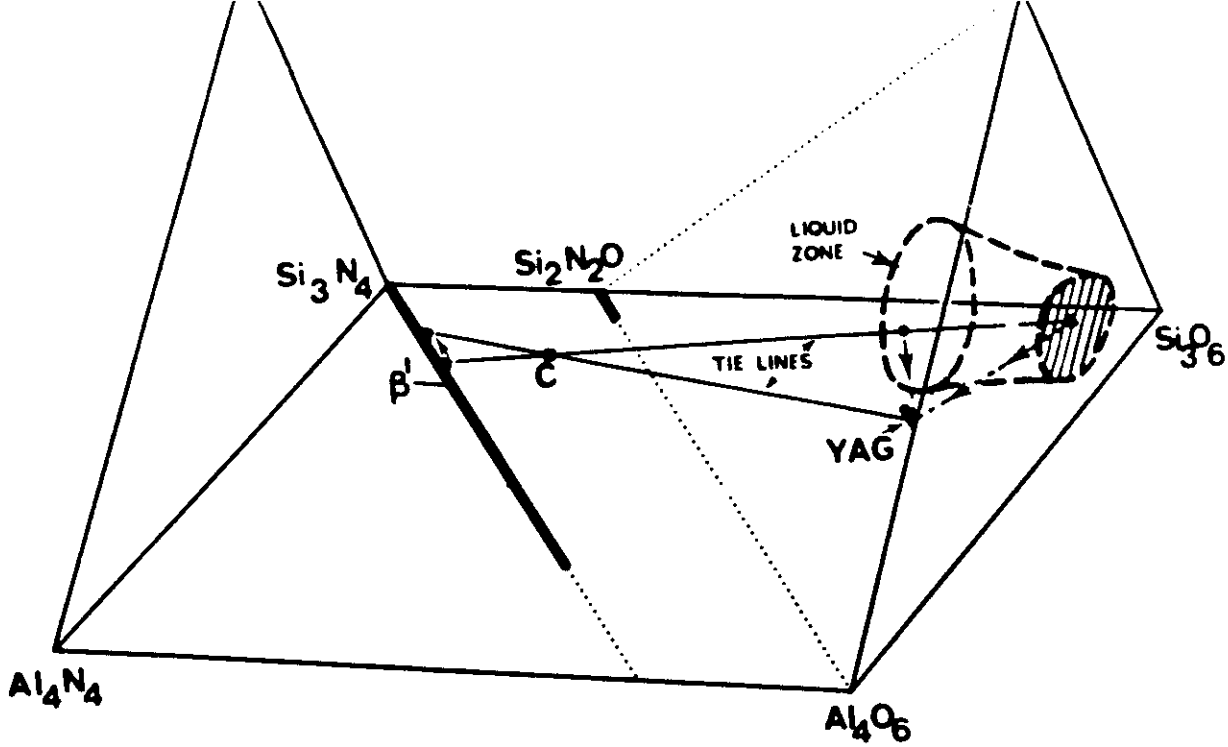

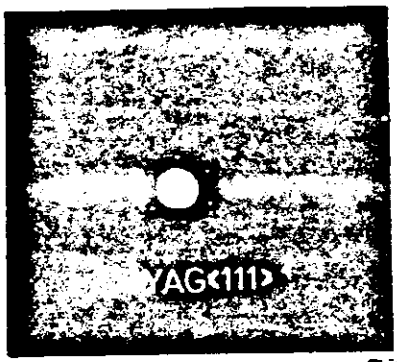

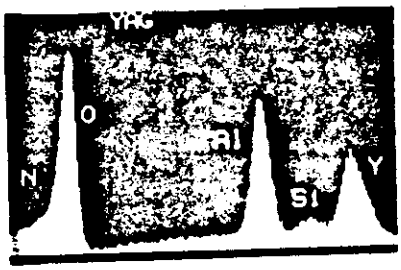

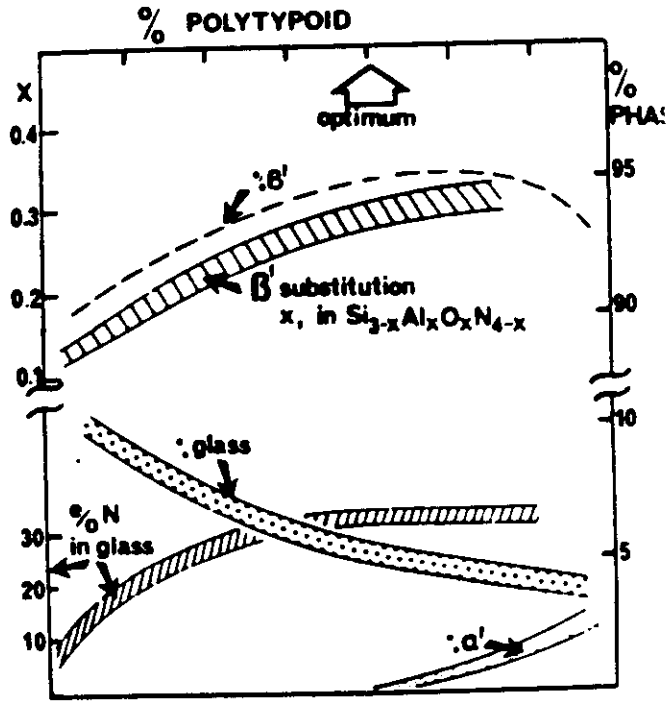

Fig. 6. A summary of constitutional changes with varying N/O ratio in β′ Syalon ceramics

Ref 10

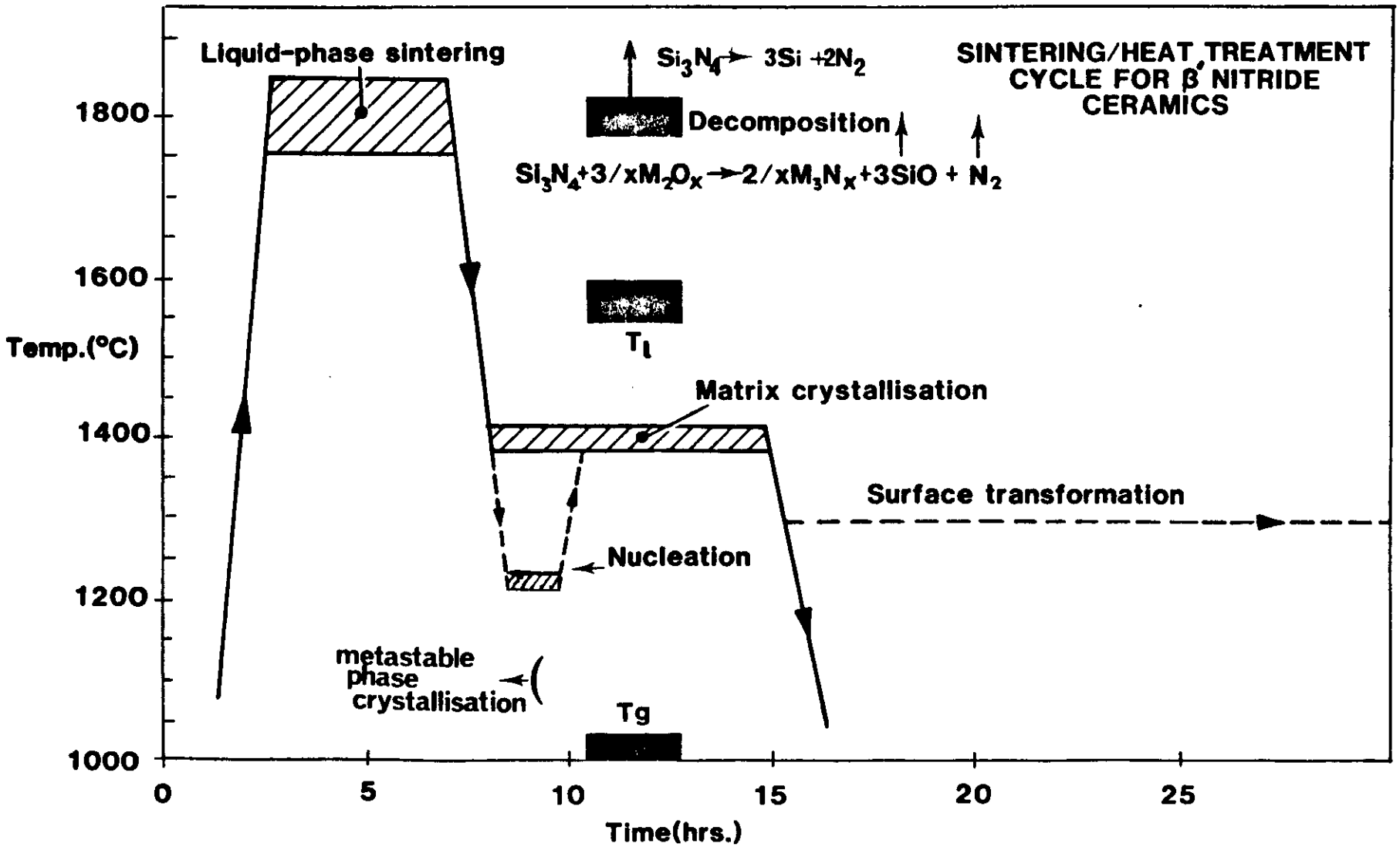
SINTERING/HEAT TREATMENT CYCLE FOR β' NITRIDE CERAMICS
Liquid-phase sintering
$Si_3N_4 \rightarrow 3Si + 2N_2$
Decomposition
$Si_3N_4 + 3/xM_2O_x \rightarrow 2/xM_3N_x + 3SiO + N_2$
T_l
Matrix crystallisation
Surface transformation
Nucleation
metastable phase crystallisation
Tg
Temp.(°C)
1800
1600
1400
1200
1000
0
5
10
15
20
25
Time(hrs.)

HIP-Si_3N_4

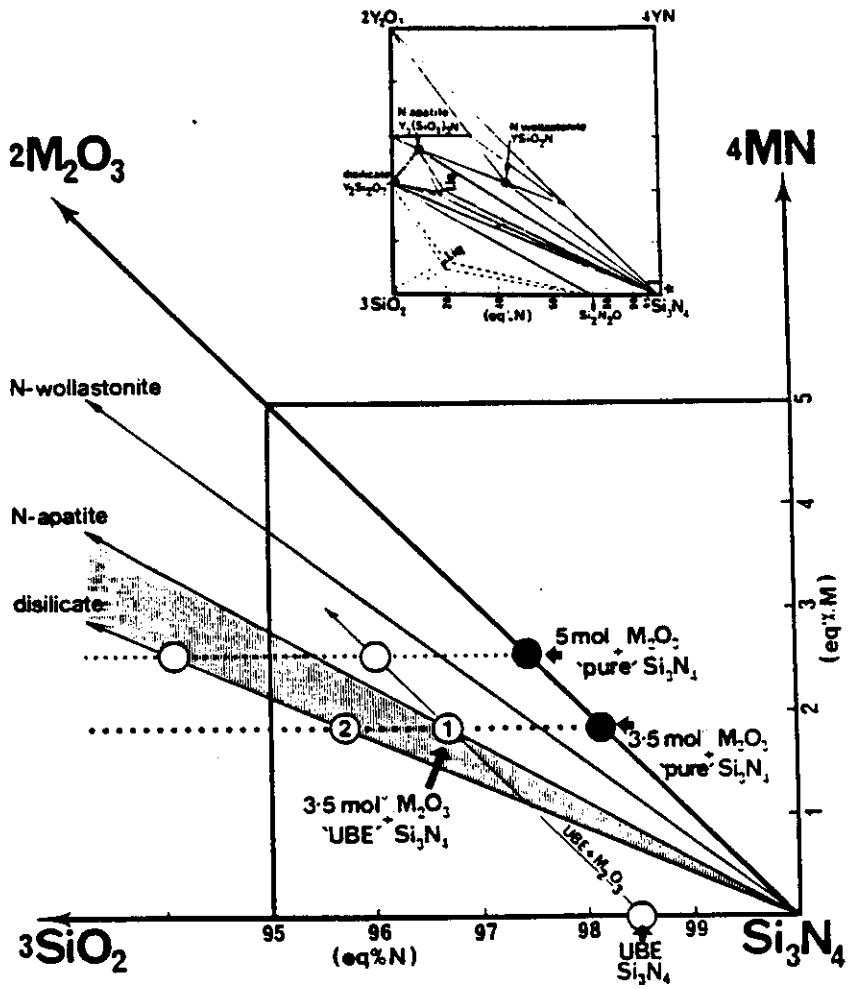

Ref. 8

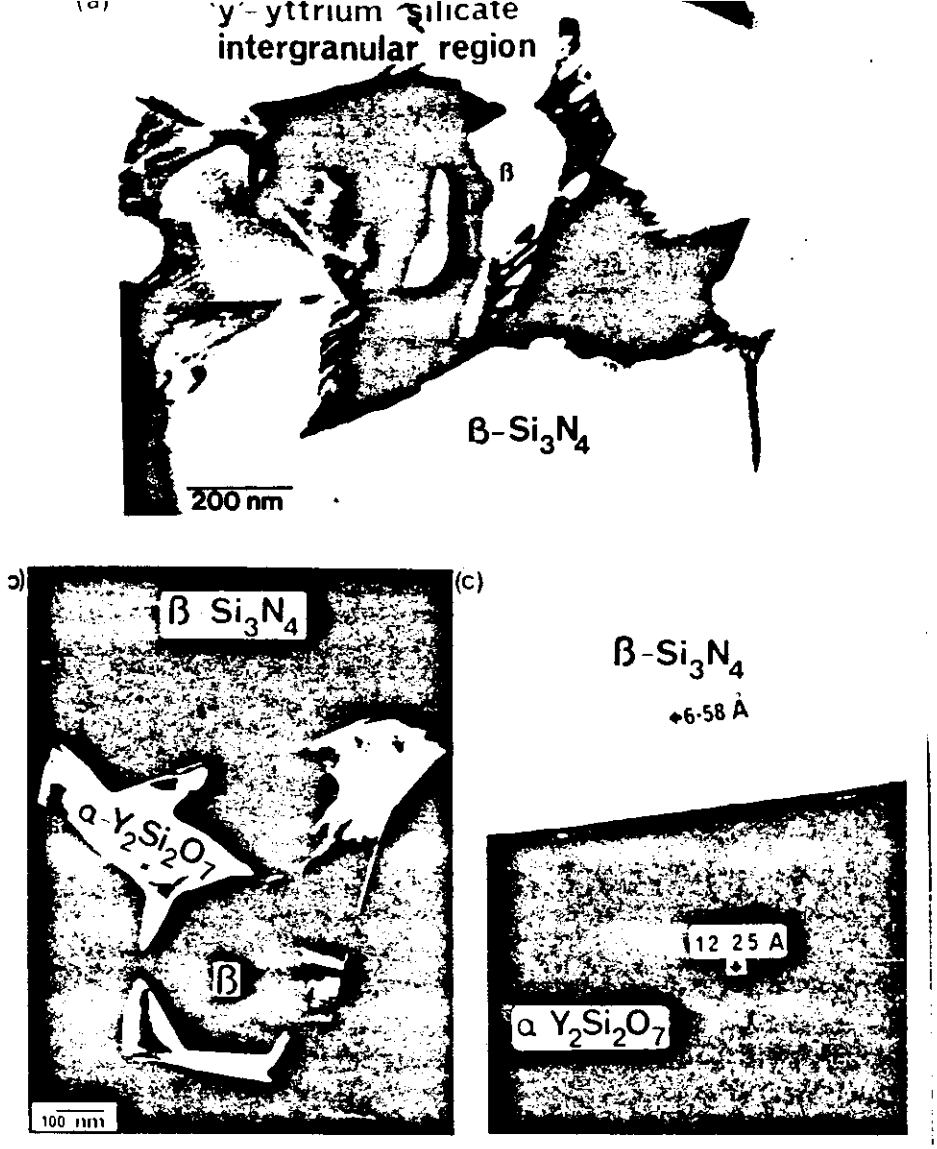

Figure 5. TEM micrographs of ceramic B showing in (a) the material as received with the intergranular region crystallized into the 'y'- yttrium silicate phase (dark mottled contrast). After annealing at 1280 °C, (b) shows an α-$Y_2Si_2O_7$ intergranular region in dark field contrast, and (c) a Si_3N_4-α-$Y_2Si_2O_7$ interface showing thin amorphous boundary layer.

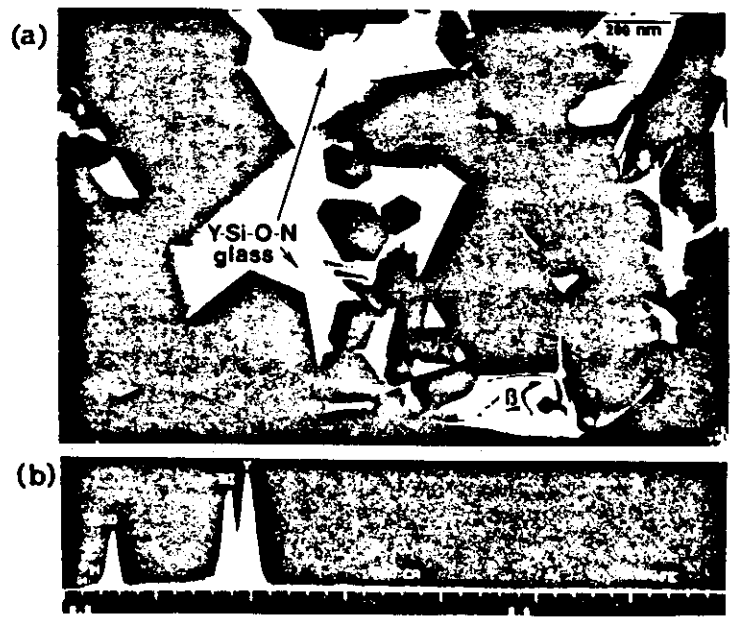

Figure 6. TEM micrograph of ceramic '3' after reannealing for 20 minutes at 1650°C followed by rapid quenching. A TEM EDX analysis of the residual intergranular glass is shown in (b).

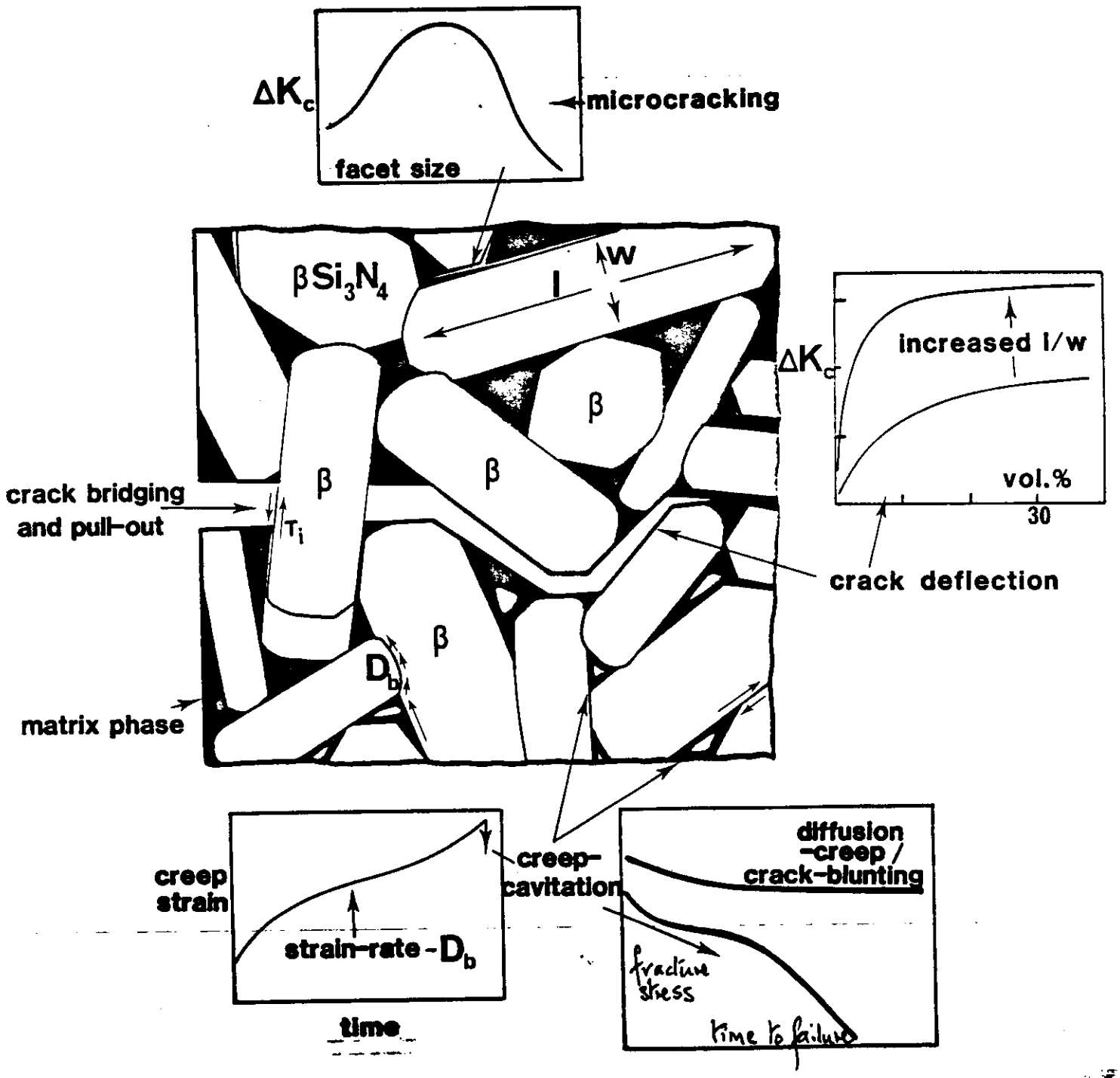
ΔKc
microcracking
facet size
βSi3N4
l
w
β
β
β
β
crack bridging
and pull-out
Ti
Db
matrix phase
ΔKc
increased l/w
vol.%
30
crack deflection
creep
strain
strain-rate - Db
time
creep-
cavitation
diffusion
-creep /
crack-blunting
fracture
stress
time to failure

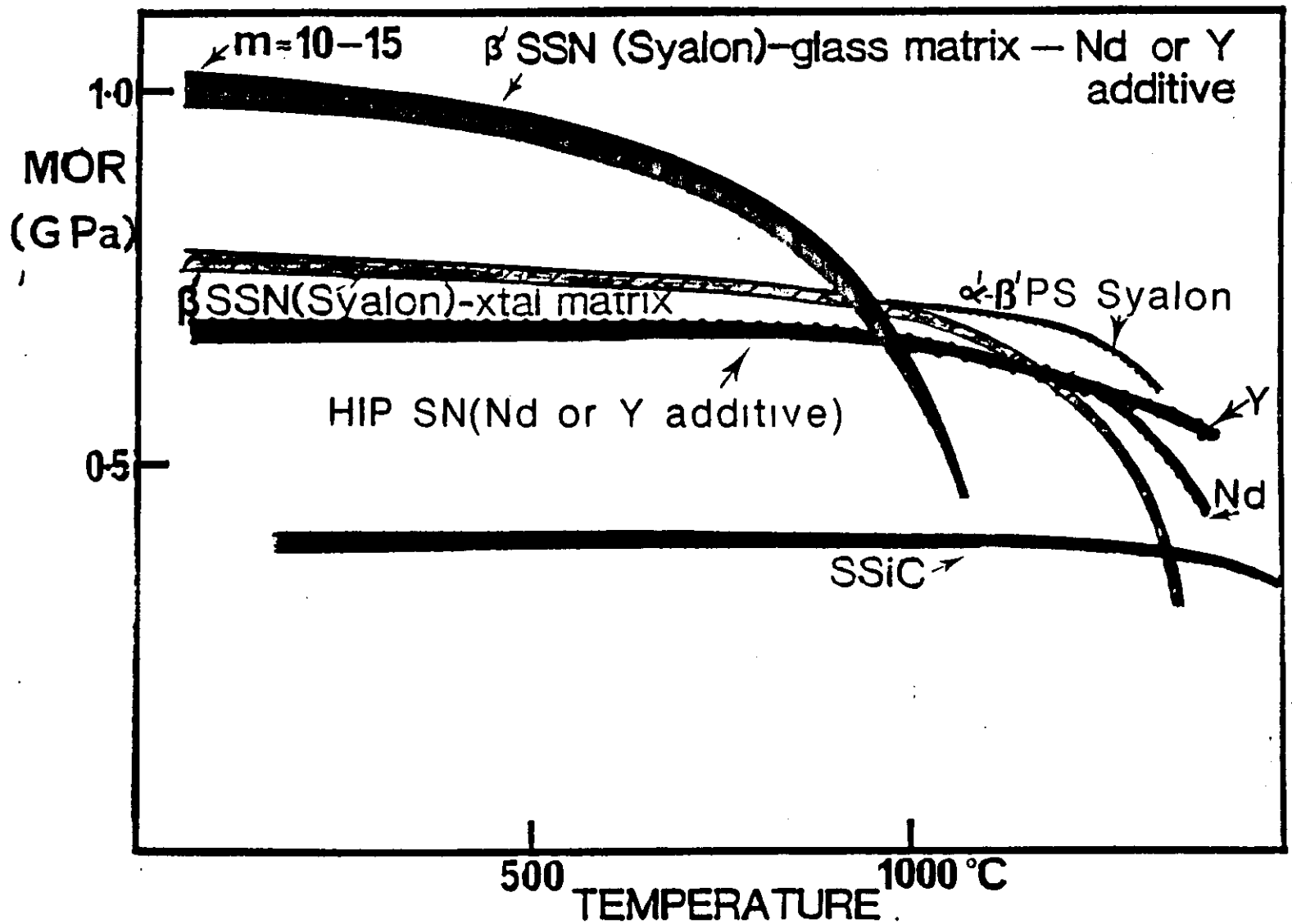
m=10–15
β' SSN (Syalon)–glass matrix — Nd or Y additive
1·0
MOR
(GPa)
β SSN(Syalon)-xtal matrix
α-β' PS Syalon
HIP SN(Nd or Y additive)
Y
0·5
Nd
SSiC
500
1000 °C
TEMPERATURE

Ref. 1, 2.

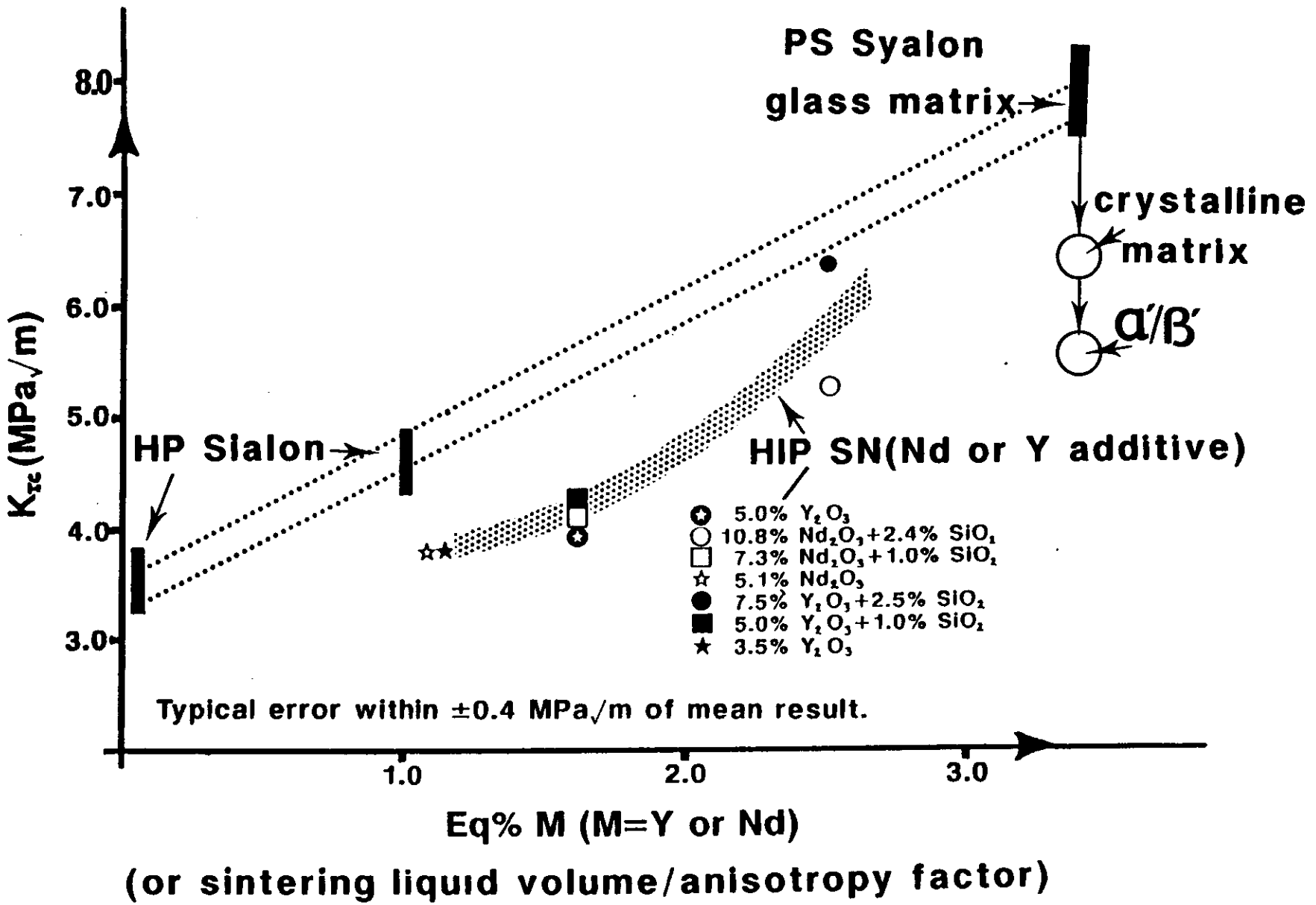
PS Syalon
glass matrix
crystalline
matrix
α′/β′
HP Sialon
HIP SN(Nd or Y additive)
5.0% Y2O3
10.8% Nd2O3+2.4% SiO2
7.3% Nd2O3+1.0% SiO2
5.1% Nd2O3
7.5% Y2O3+2.5% SiO2
5.0% Y2O3+1.0% SiO2
3.5% Y2O3
Typical error within ±0.4 MPa√m of mean result.
Kic (MPa√m)
8.0
7.0
6.0
5.0
4.0
3.0
1.0
2.0
3.0
Eq% M (M=Y or Nd)
(or sintering liquid volume/anisotropy factor)

STRESS RUPTURE MODES

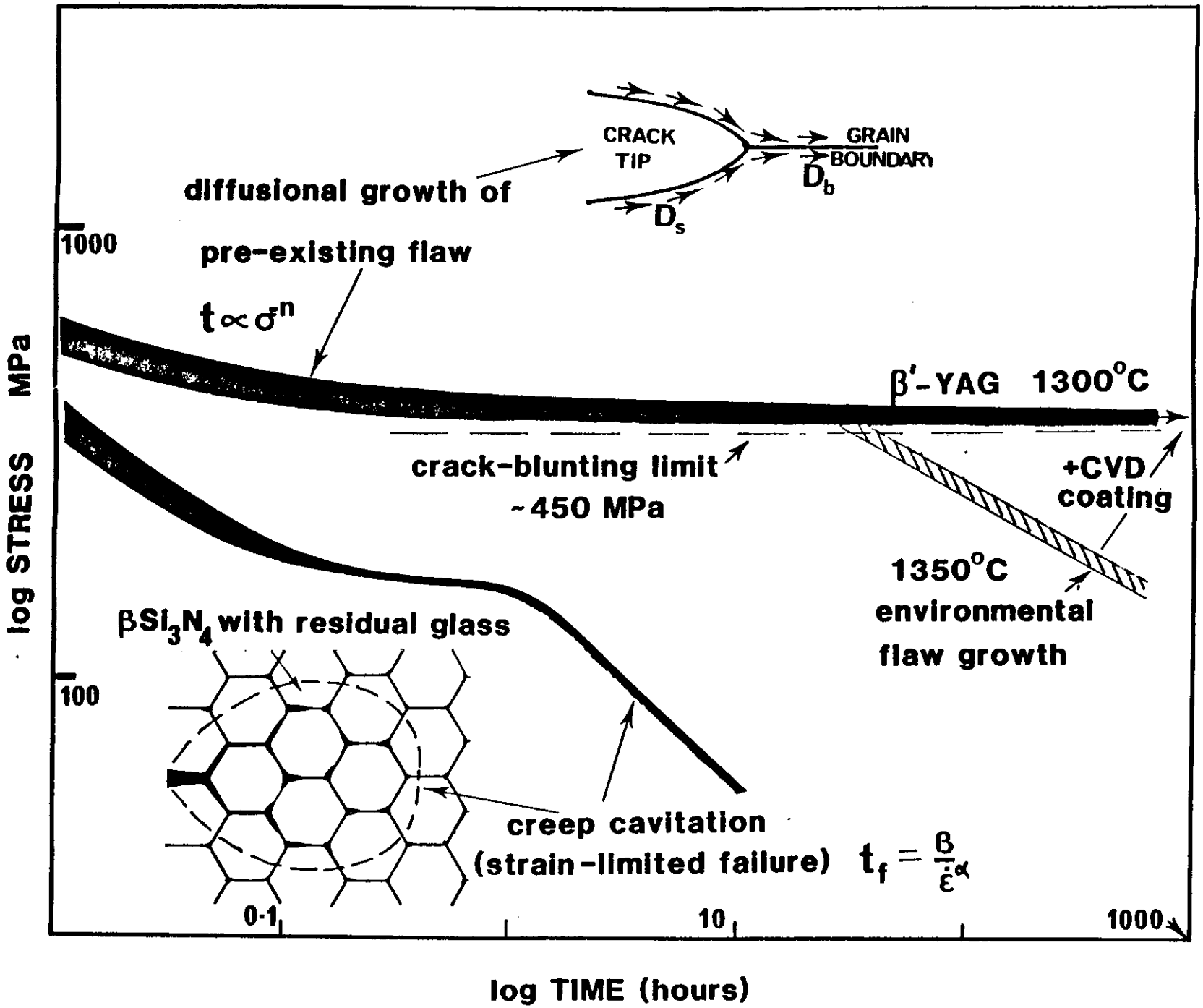

Ref. 2

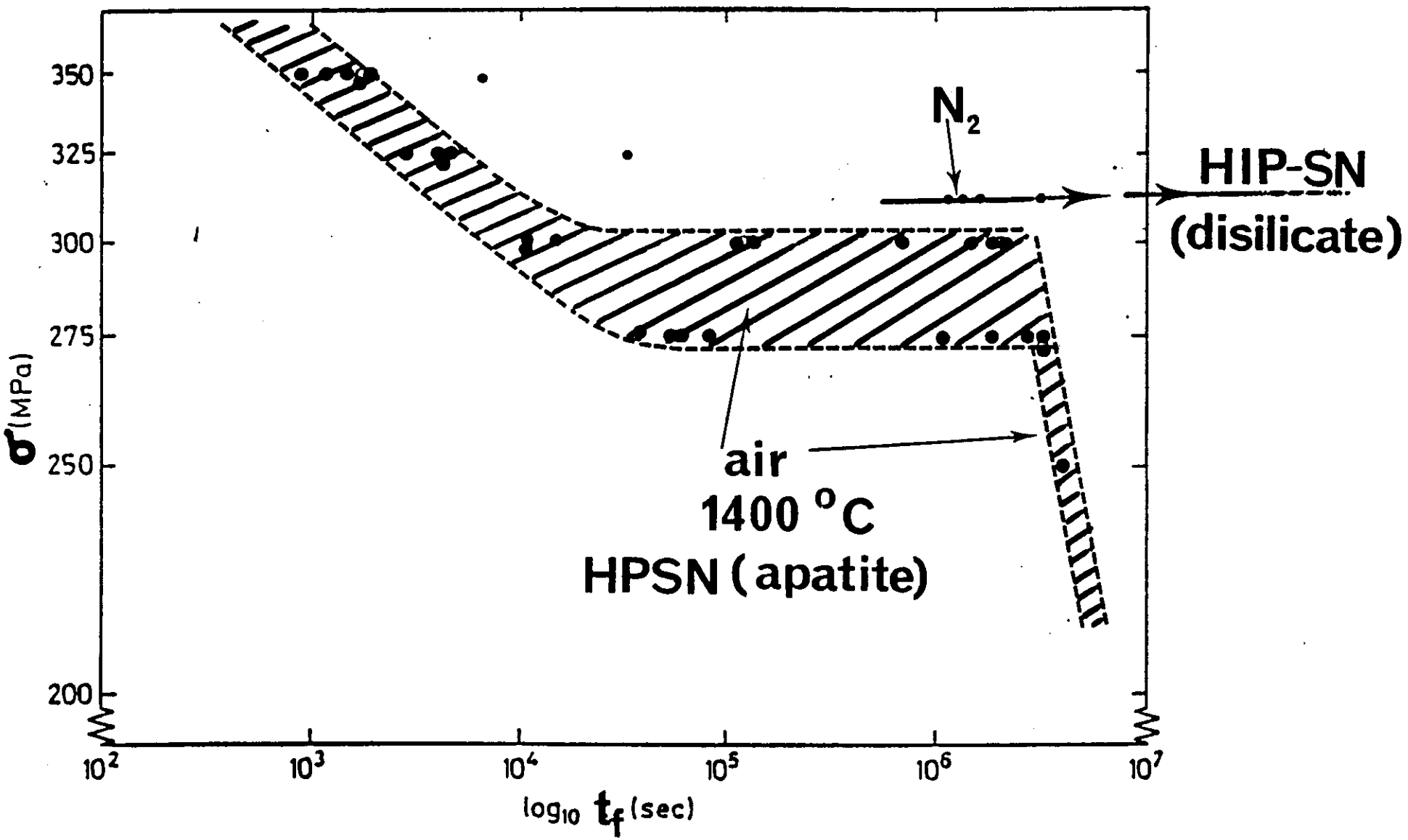
350
325
300
275
250
200
σ (MPa)
10^2
10^3
10^4
10^5
10^6
10^7
$\log_{10} t_f$ (sec)
N_2
HIP-SN
(disilicate)
air
1400 °C
HPSN (apatite)

C. Weber
A. N. H.

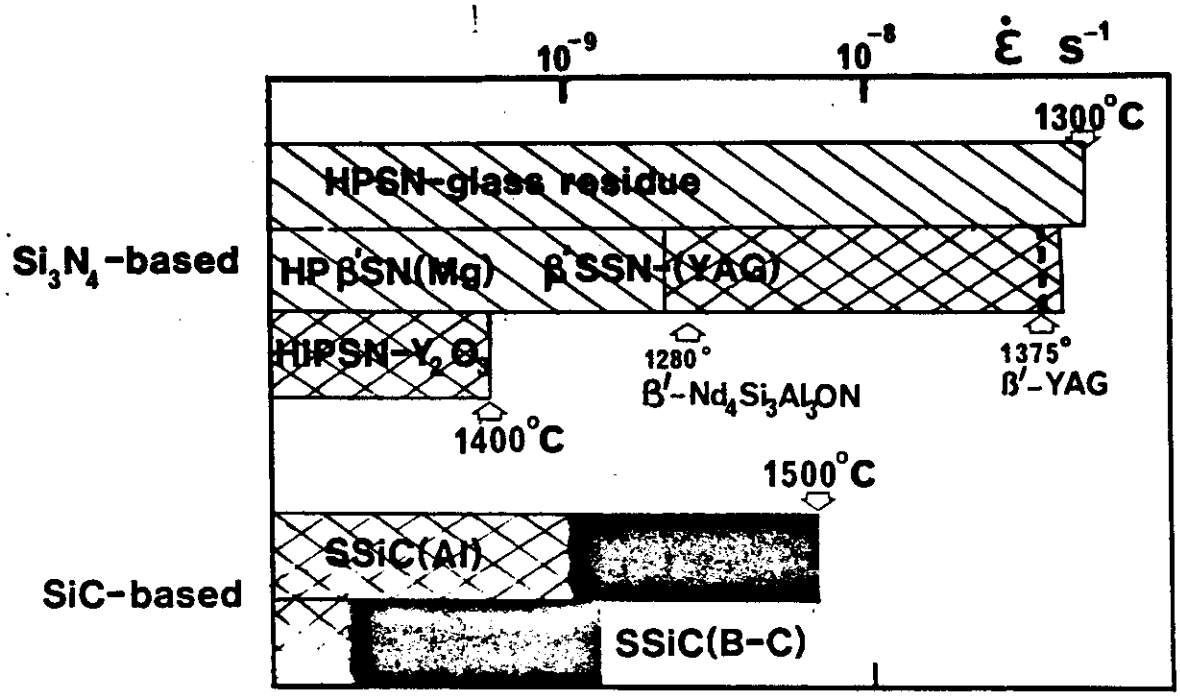

CREEP RATES AT 100 MPa

Ref. 2, 8.

Sialon 201 (β'-YAG) Rolls-Royce Burner Rig. – Salt corr

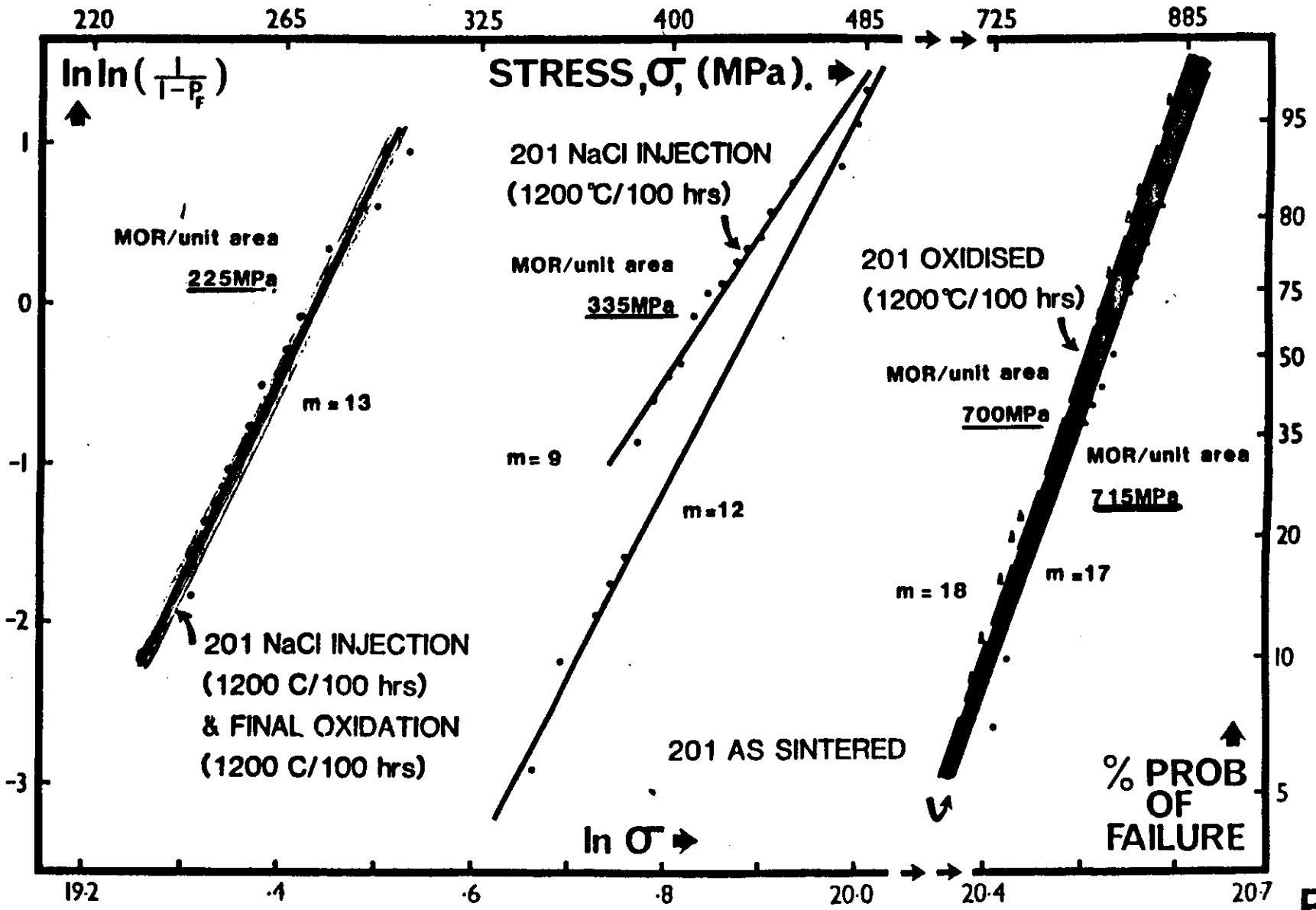

FIG 4

C. Ree
M.Sc.
Univ.

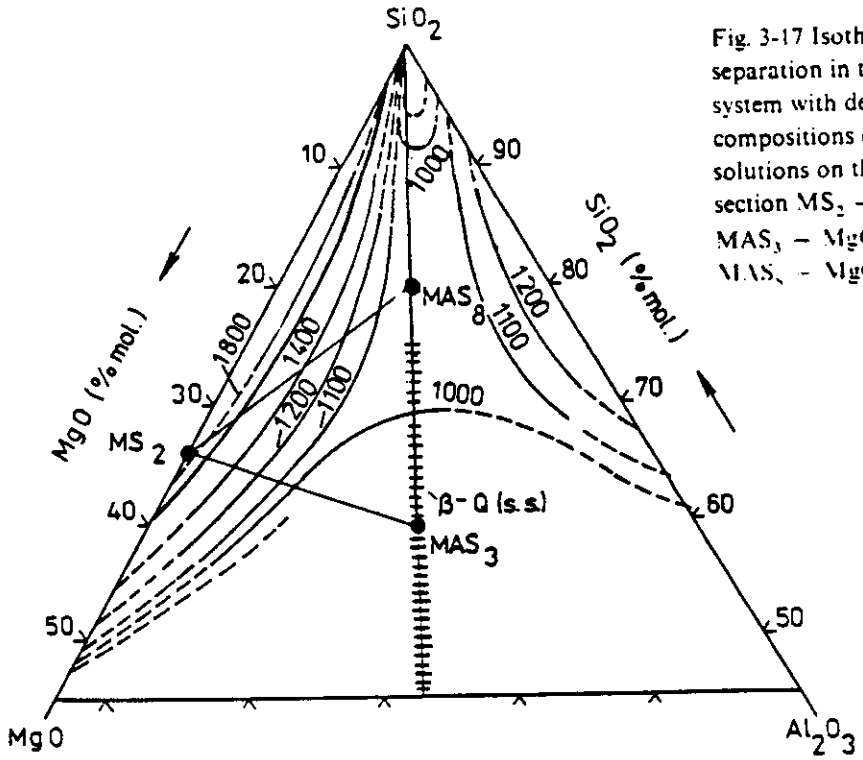

Fig. 3-17 Isotherms of liquid phase separation in the SiO_2–Al_2O_3–MgO system with designation of the compositions of solid β-quartz solutions on the SiO_2–$MgAl_2O_4$ section MS_2 – $MgO{\cdot}2SiO_2$, MAS_3 – $MgO{\cdot}Al_2O_3{\cdot}3SiO_2$, MAS_8 – $MgO{\cdot}Al_2O_3{\cdot}8SiO_2$ [110]

3.3 THE SiO_2–Al_2O_3–Li_2O SYSTEM

The important crystalline phases in the lithium-aluminium-silicate system, i. e. eucryptite ($Li_2O{\cdot}Al_2O_3{\cdot}2SiO_2$), spodumene ($Li_2O{\cdot}Al_2O_3{\cdot}4SiO_2$) and petalite ($Li_2O{\cdot}Al_2O_3{\cdot}8SiO_2$) lie on the connecting line in the ternary diagram inside the glass-forming region. The phase diagram [92, 93] for this pseudobinary system is given in Fig. 3-5. It is apparent from this diagram that, at high temperatures, the low-temperature modifications α-eucryptite and α-spodumene are converted irreversibly into the high-temperature forms (at 972 °C and 500 °C) respectively, and that stable solutions of β-spodumene and β-eucryptite are formed in the nonstoichiometric composition regions. Burger [94] was the first to realize that certain alumino-

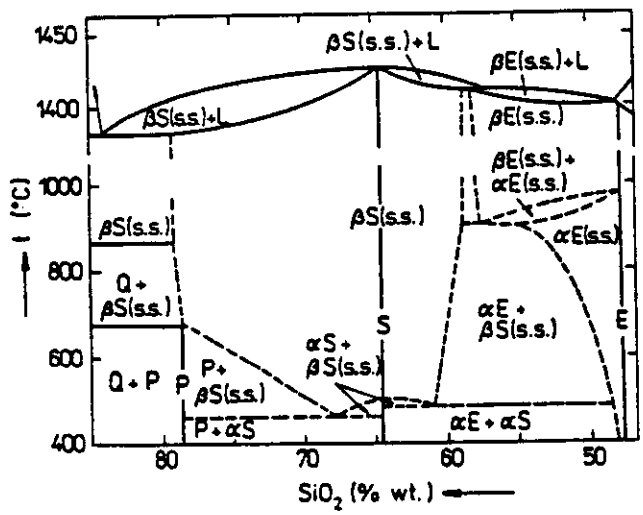

Fig. 3-5 Phase diagram of the SiO_2–$Li_2O{\cdot}Al_2O_3{\cdot}2SiO_2$ system
βP – petalite,
βS – spodumene,
βE – eucryptite, Q – quartz,
s.s. – solid solution,
L – liquid

Ref. 17

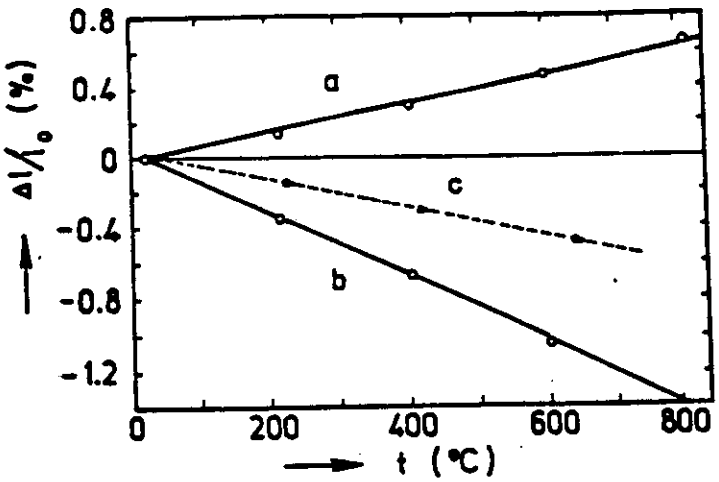

Fig. 3-12 Longitudinal thermal expansion of β-eucryptite
a) in the direction of crystallographic axis a_0,
b) in the direction of crystallographic axis c_0,
c) polycrystalline material [104]

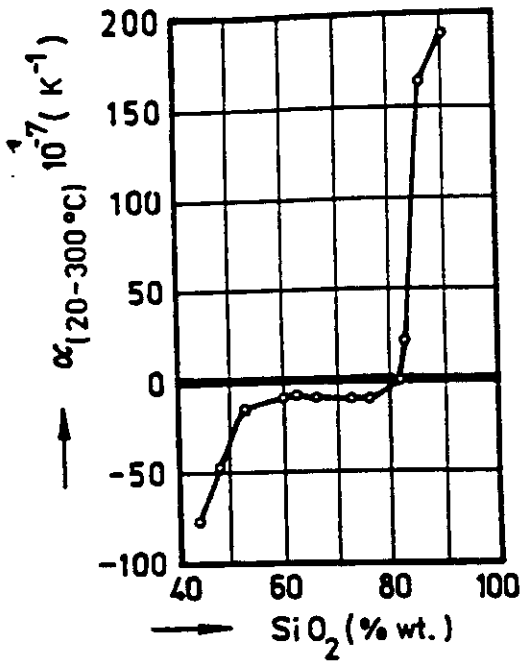

Fig. 3-11 Coefficient of thermal expansion of solid solutions of β-quartz separated from glasses of the SiO_2–$LiAlO_2$ series [101]

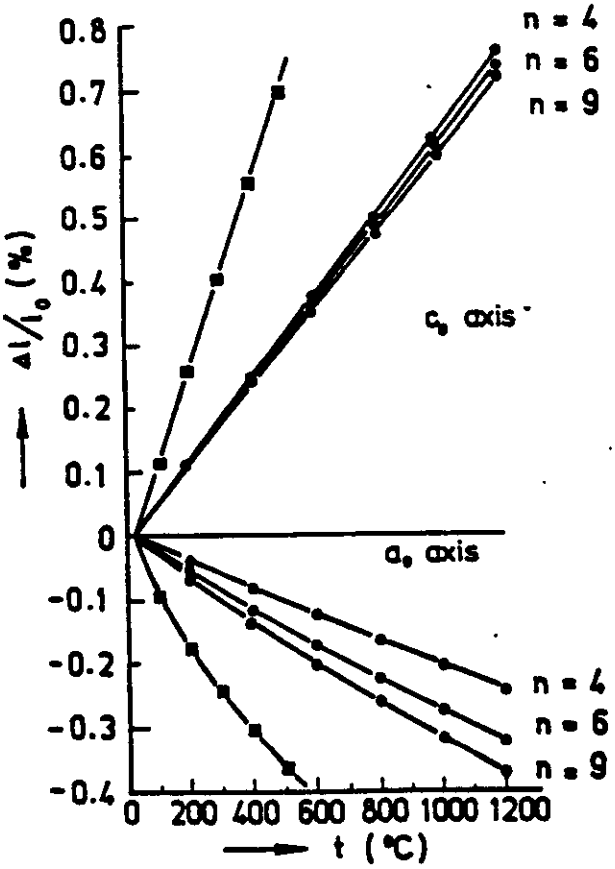

Fig. 3-14a Longitudinal thermal expansion of solid solutions of β-spodumene $Li_2O \cdot Al_2O_3 \cdot nSiO_2$ (●) and keatite (■) in the direction of crystallographic axes a_0 and c_0 [106].

Fig. 3-14b Volume expansion of solid solutions of β-spodumene $Li_2O \cdot Al_2O_3 \cdot nSiO_2$ [106]

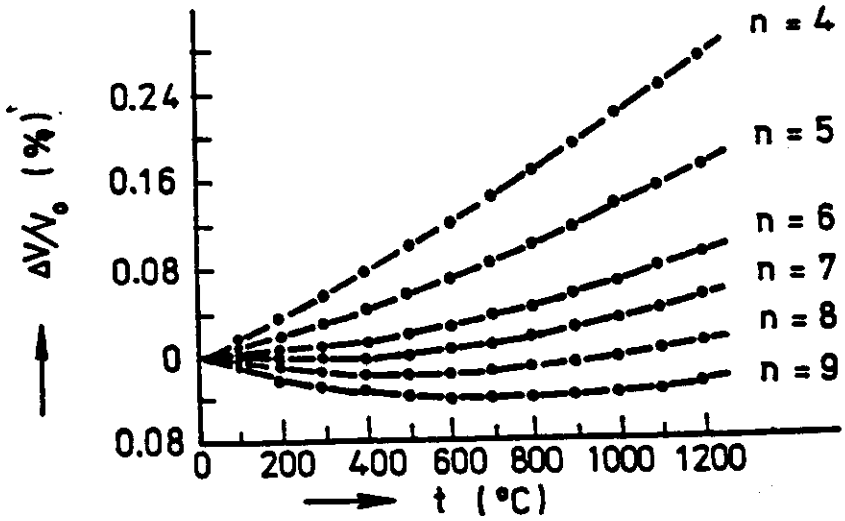

Ref. 17

	Glass-ceramic				
Compositional data	M1	M2	M3	M4	M5
MgO	15	12	14	12	22
Al_2O_3	20	26	30	26	22
Nucleant	TiO_2	TiO_2	TiO_2	TiO_2+ ZrO_2	ZrO_2
Properties X-band					
ε					
20°C	5.65	5.91	6.39	5.60	8.5
400°C	5.78	5.90	6.29	5.65	8.8
tan δ x 10^4					
20°C	3	5	5	4	60
400°C	20	43	43	25	172
Density $g.cm^{-3}$	-	-	-	-	3.18
Strength MPa	350	162	127	270	750
Thermal expansion coefficient α x 10^7					
20-500°C	53	32	24	31	82

Properties of selected Li_2O-Al_2O_3-SiO_2 glass-ceramics

	Glass-ceramic					
Compositional data	L1	L2	L3	L4	L5	L6
Total alkali	14%	12%	10%	15%	10%	4%
Al_2O_3	10%	10%	10%	5%	10%	20%
Alkaline earths	-	2%BaO	5%	-	9%	-
Nucleant	P_2O_5	P_2O_5	P_2O_5	P_2O_5	P_2O_5	TiO_2+ ZrO_2
Properties X-band						
ε 20°C	5.63	5.68	5.66	5.21	5.97	5.91
400°C	6.21	6.15	5.98	-	6.31	-
tan δ x 10^4						
20°C	106	93	68	138	107	1300
400°C	208	168	-	-	110	-
Density $g.cm^{-3}$	2.44	2.47	2.51	2.40	2.59	-
Strength MPa	255	230	160	380	175	-
Thermal expansion coefficient α x 10^7						
20-500°C	52	45	45	93	50	~0

Ref. 19.

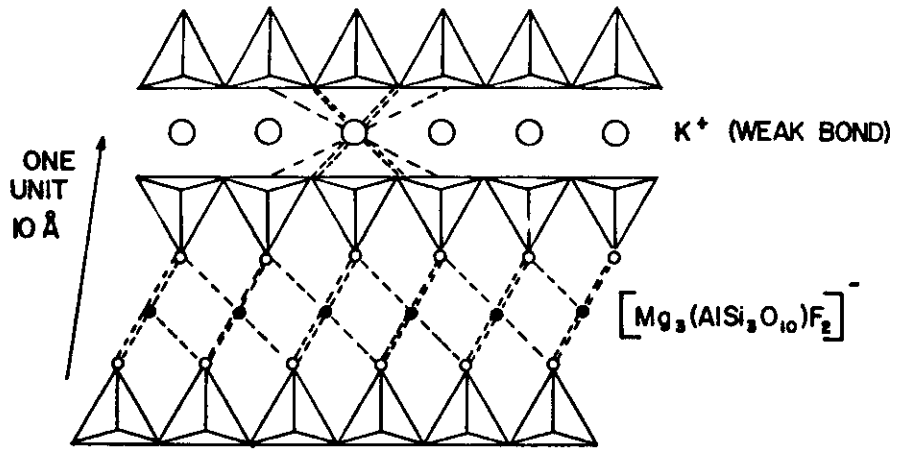

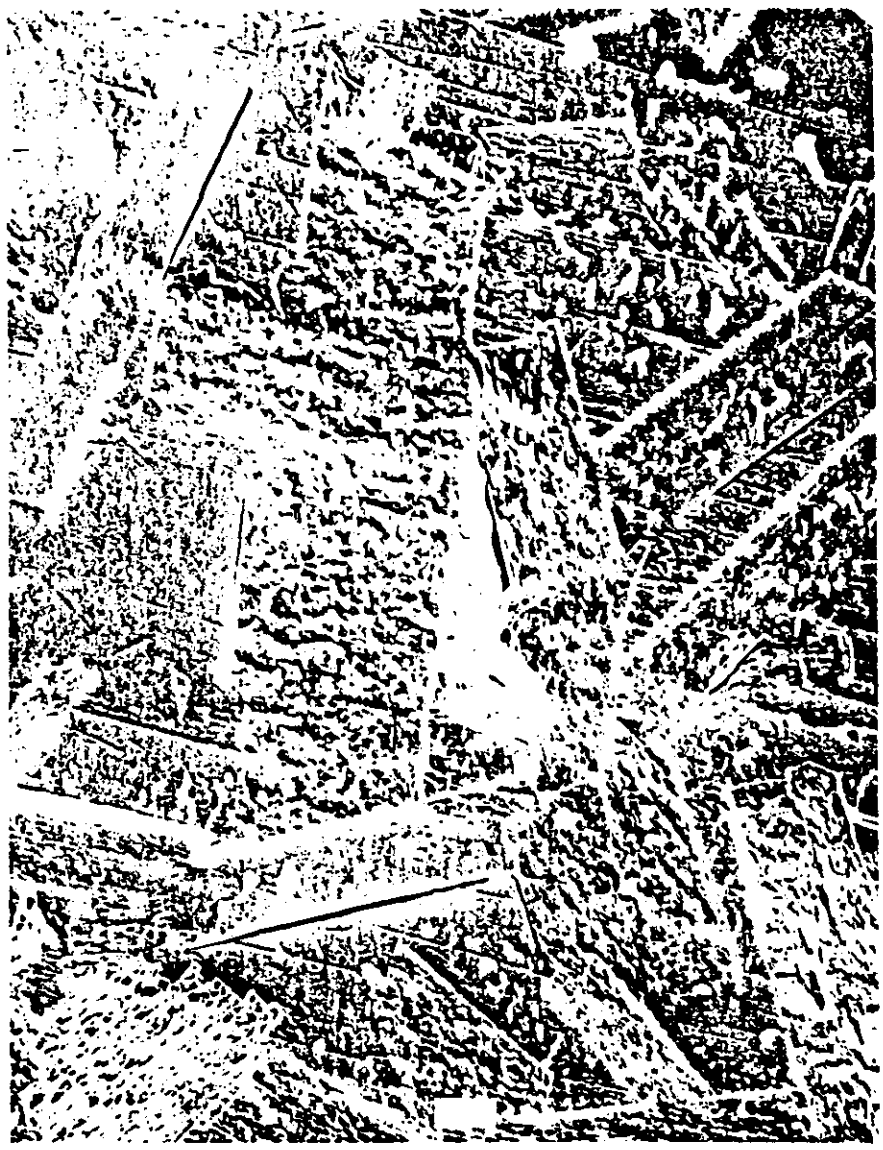

Fig. 13 Cracks developed along the mica-glass interfaces due to the mismatch in thermal expansion coefficients between the glass and the mica crystals. Bar = 1 μ.

Ref. 17.

COMPOSITE CERAMIC MICROSTRUCTURE

examples

Random Whiskers

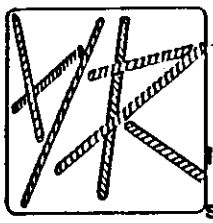

Infiltrate via liquid/glass, solid(sinter)

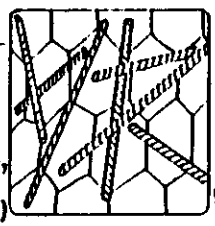

βSiC in Si_3N_4, Al_2O_3 ... or glass-ceramic

or vapour(CVI)

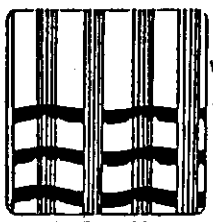

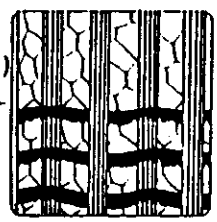

Nicalon (Si/C/O) in glass-ceramic or CVI SiC

Semi-Continuous Fibres (unidirectional or woven)

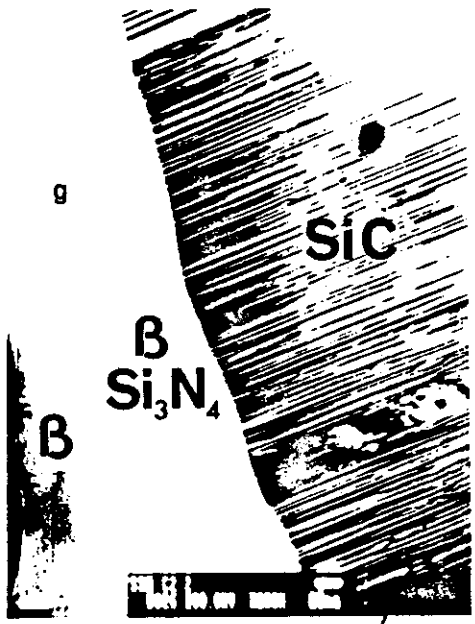

WHISKER

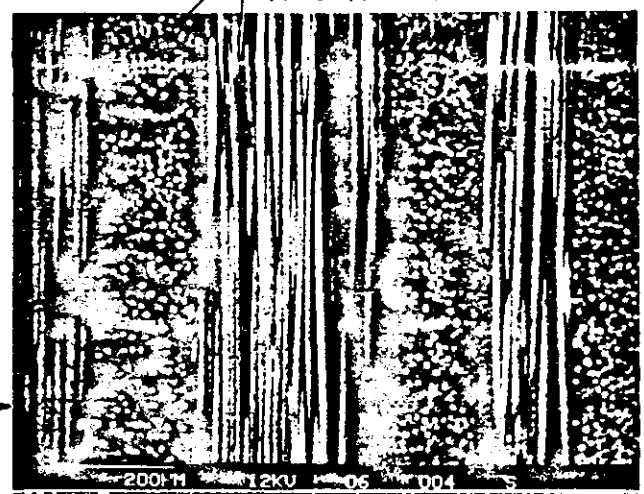

CROSS-PLIED NICALON

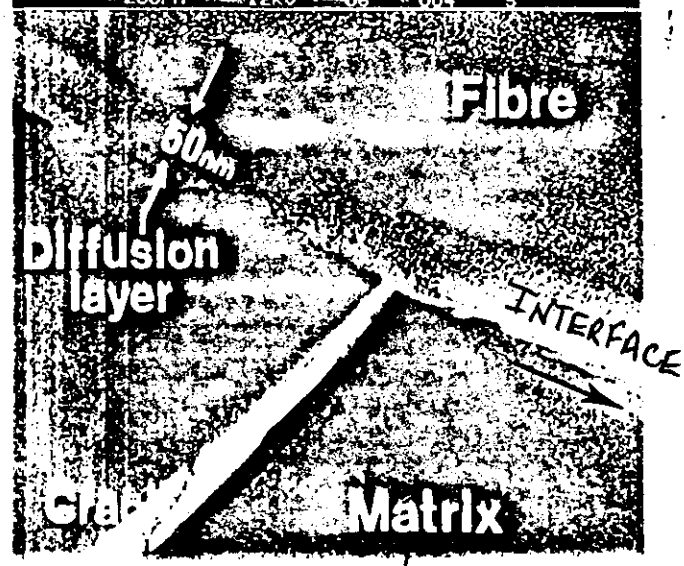

PYREX GLASS

Ref. 2.
+ unpublished work - V. Mwa

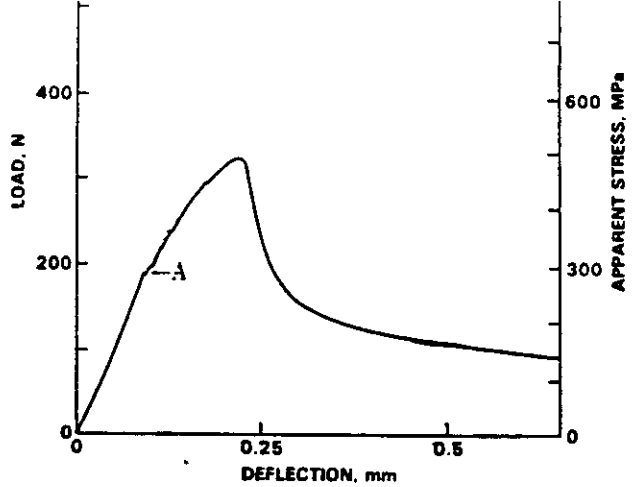

Figure 1 Stress-elongation curve for unidirectional composite comprised of an LAS glass-ceramic matrix reinforced with ~50 vol% Nicalon silicocarbon filaments when tested in tension parallel to the filaments. Point A marks the onset of matrix cracking. (Adapted from Reference 22a.)

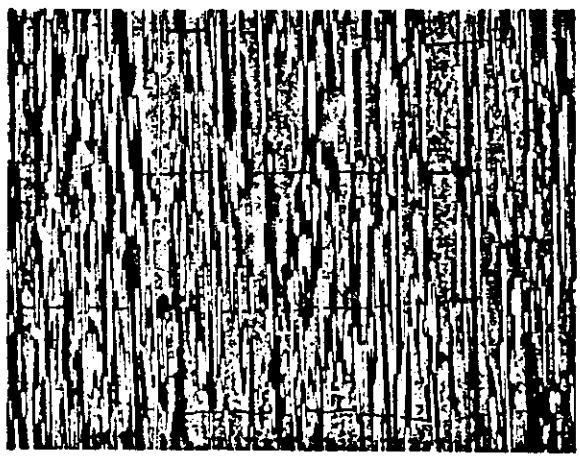

Figure 2 Appearance (22a) of the cracks that develop in the matrix normal to filaments when the composite in Figure 1 is stressed to point A. Note that the filaments remain intact.

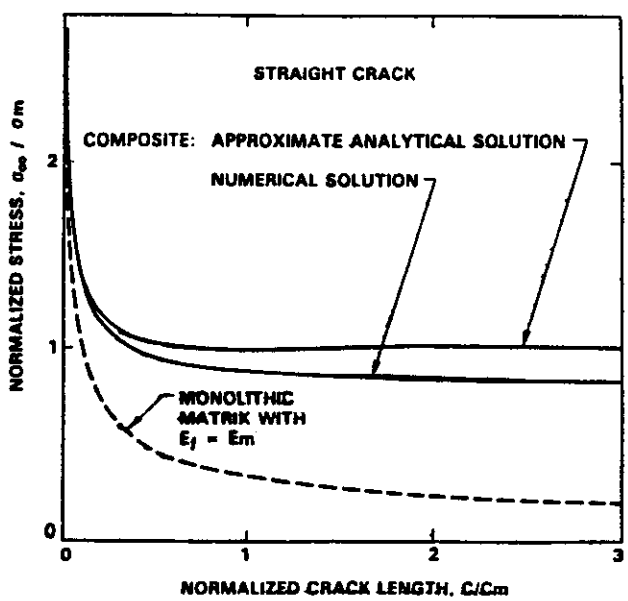

Figure 7 Plot (34) of the normalized (dimensionless) applied tensile stress needed to allow the fiber-bridged matrix crack to grow as a function of the dimensionless matrix crack length.

after W. Hillig

CMC FABRICATION

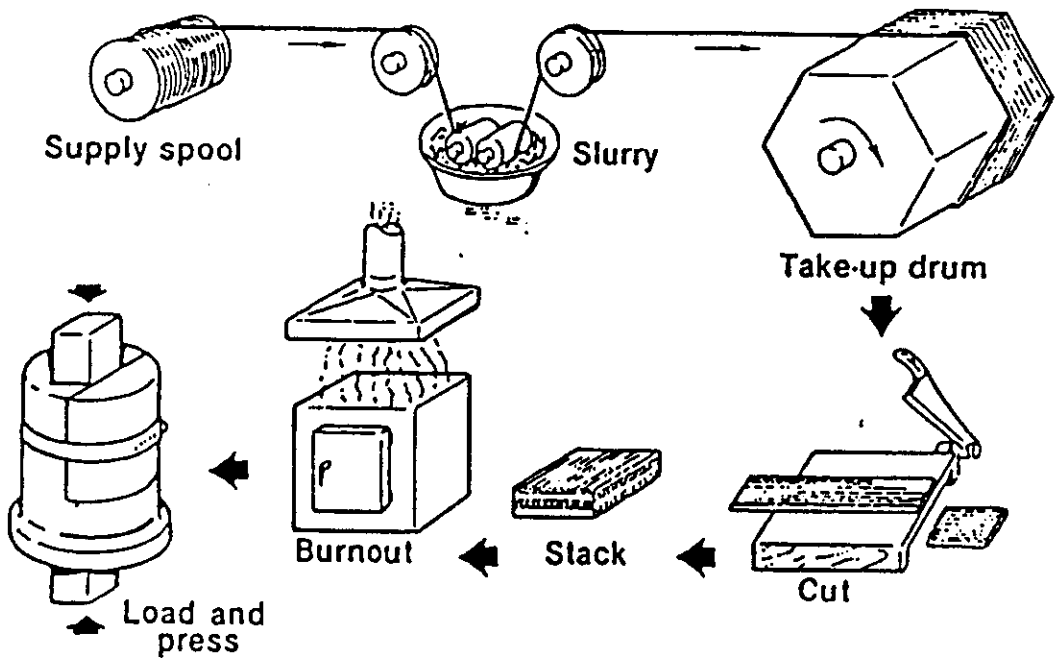

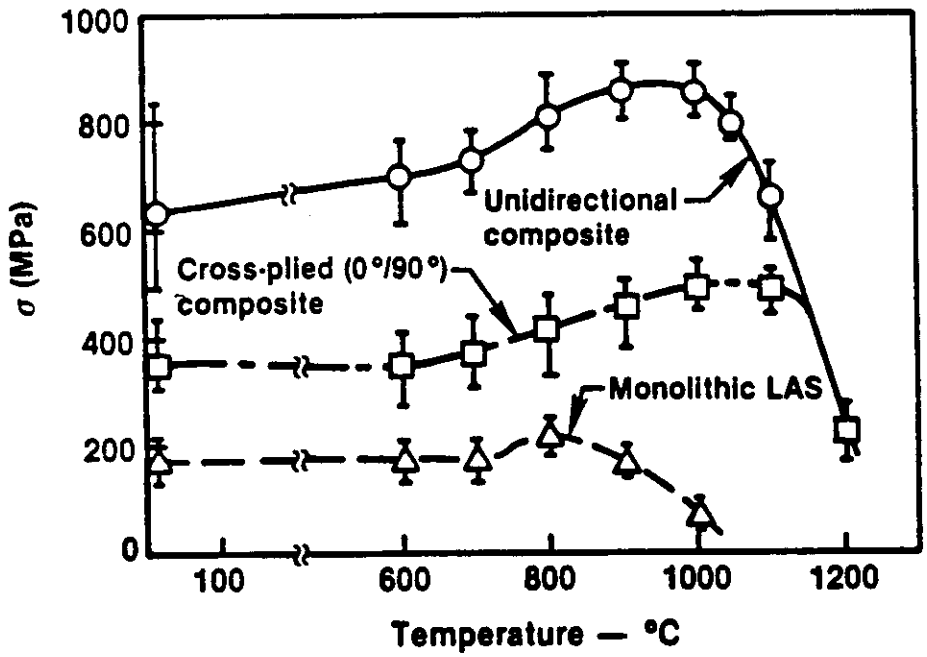

NICALON/LAS

FIG. 19

in Ref. 19 (Prev

Glass and Glass-Ceramic Matrices of Interest

Matrix Type	Major Constituents	Major Crystalline Phase	Thermal Expansion Coefficient ($C^{-1} \times 10^{-6}$)	Ultimate Maximum Use Temp. °C (based on melting or softening)
Glasses-				
Borosilicate	B_2O_3, SiO_2	-	3.3	600
Aluminosilicate	$Al_2O_3 MgO$, CaO, SiO_2	-	8.9	700
High Silica	SiO_2	-	0.6	1150
Glass-Ceramics-				
LAS	Li_2O, Al_2O_3, SiO_2 (1 1 4)	β-Spodumene	0.9	1000
MAS	MgO, Al_2O_3, SiO_2 (2 2 5)	Cordierite	2.6	1200
BMAS	BaO, MgO, Al_2O_3, SiO_2 (1 2 3 9)	Barium Osumilite	2.7	1250
Ternary Mullite	BaO, Al_2O_3, SiO_2	Mullite	4	1500
CAS	$CaO.Al_2O_3.SiO_2$ (1 1 2)	Anorthite	4.5	1550
BAS	BaO, Al_2O_3, SiO_2 (1 1 2)	Hexacelsian Celsian (Monoclinic)	8.0 3.0	1700

SiC FIBRES

NICALON
or
TYRANNO
(NON-
CRYSTALLIN

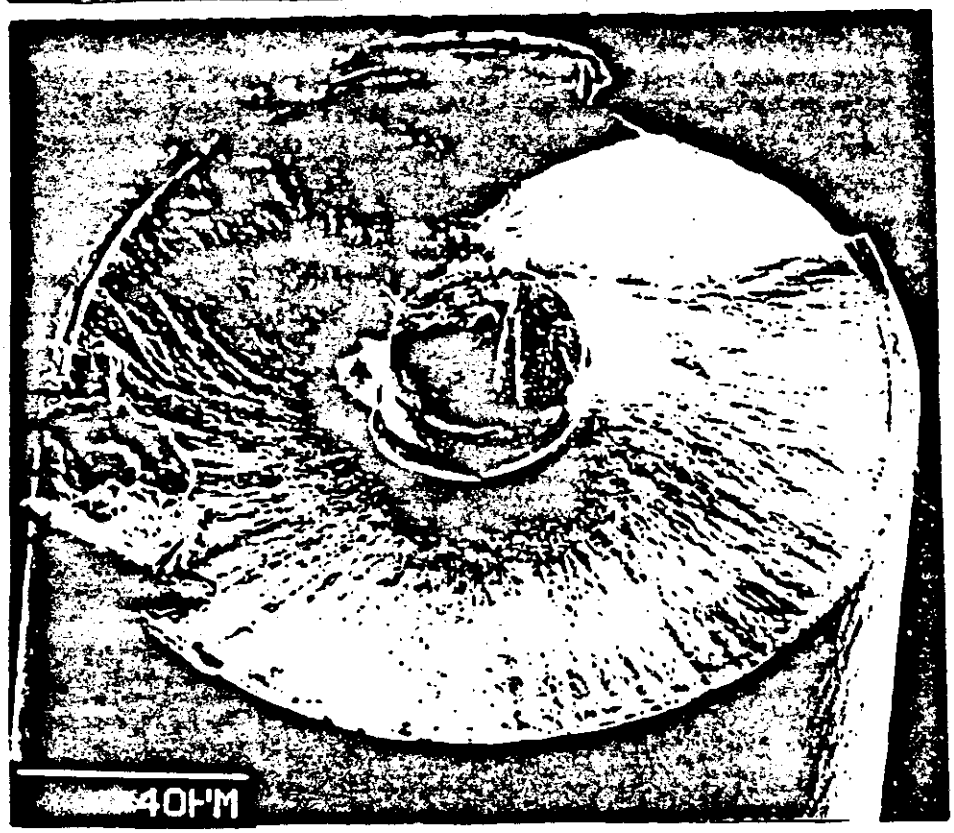

ARCO
SCS 6

C-core,
CVD SiC
(crystallin
outer C
coating.

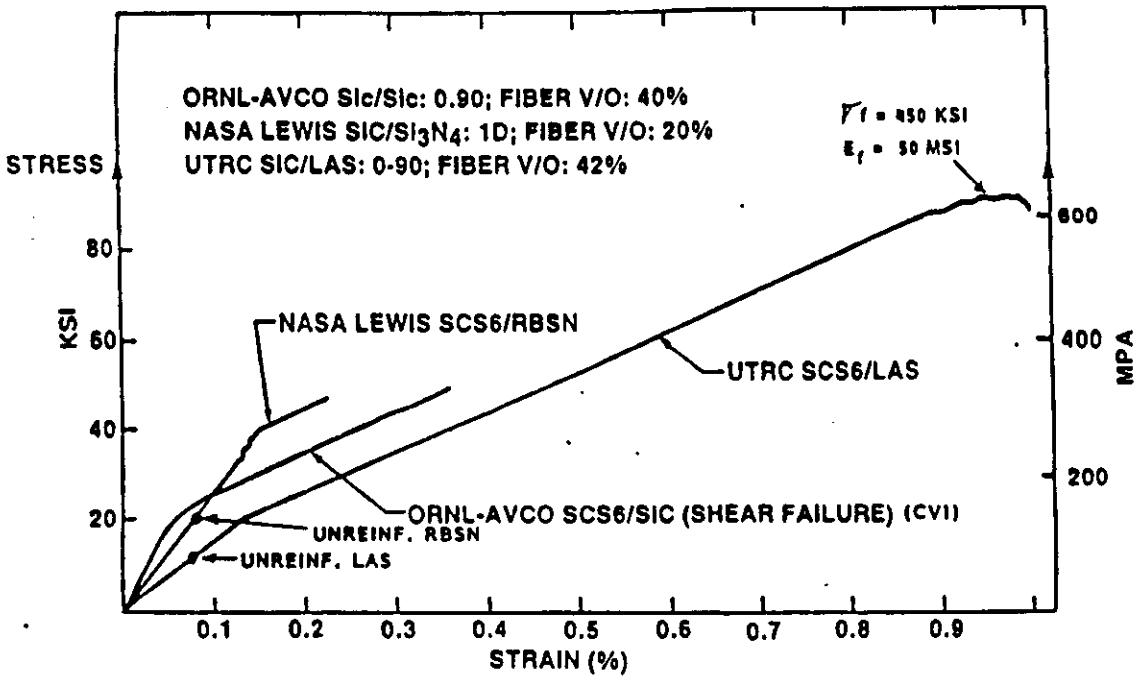

FLEXURAL STRESS — STRAIN BEHAVIOR OF REINFORCED AND MONOLITHIC RB Si_3N_4*

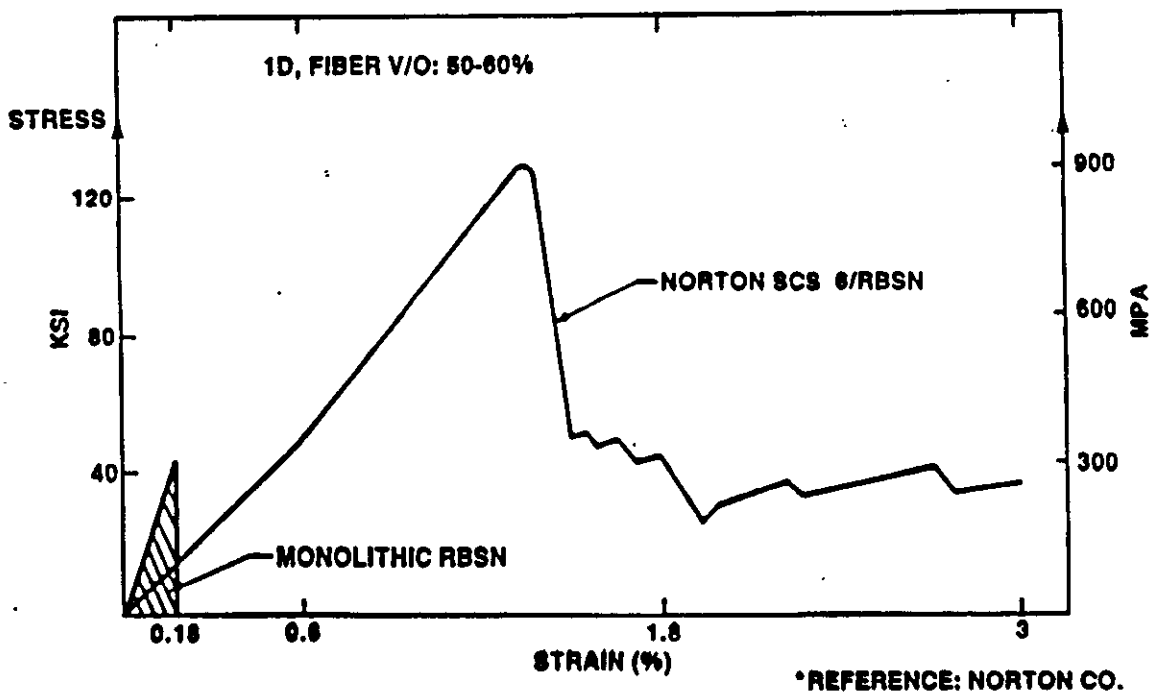

*REFERENCE: NORTON CO.

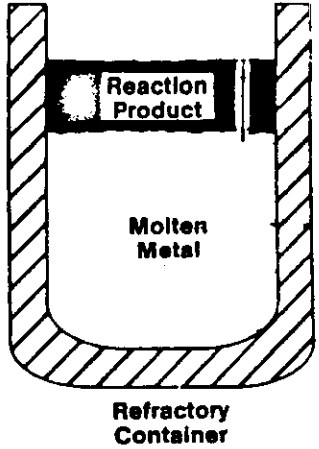

LANXIDE PROCESS

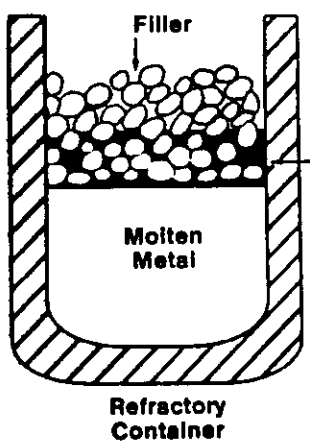

matic of the matrix formation reaction illustrating the ard growth of a ceramic/metal reaction product from a en metal exposed to a vapor phase oxidant.

Fig. 2. Schematic of the formation of a ceramic composite by t outward growth of a ceramic/metal reaction product mat through a mass of filler material.

3

)SITE FO
mic matrix
ert filler ma
adjacent to
ie outward
t reaction pr
, 2). A key
erials are r
uring the ma

Figs. 3 throu
h as Al_2O_3 ar
ade using bo
Fig. 7 shows t
rosswoven fib

of these mate
ate properties
the selection

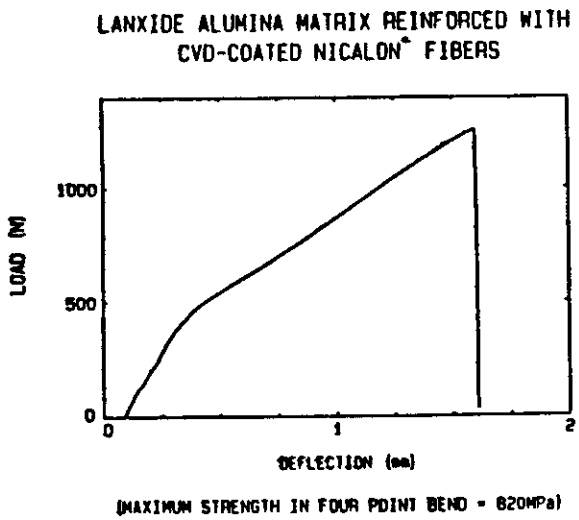

Fig. 7. Load-deflection curve recorded during flexure testing of an alumina composite containing CVD-coated Nicalon® fibers.

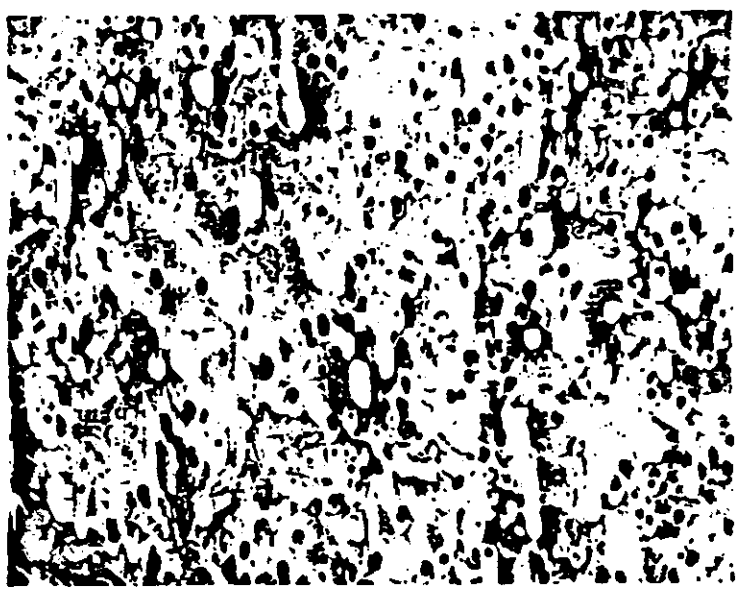

Ref. 2

Fig. 8. Scanning electron micrograph of the fracture

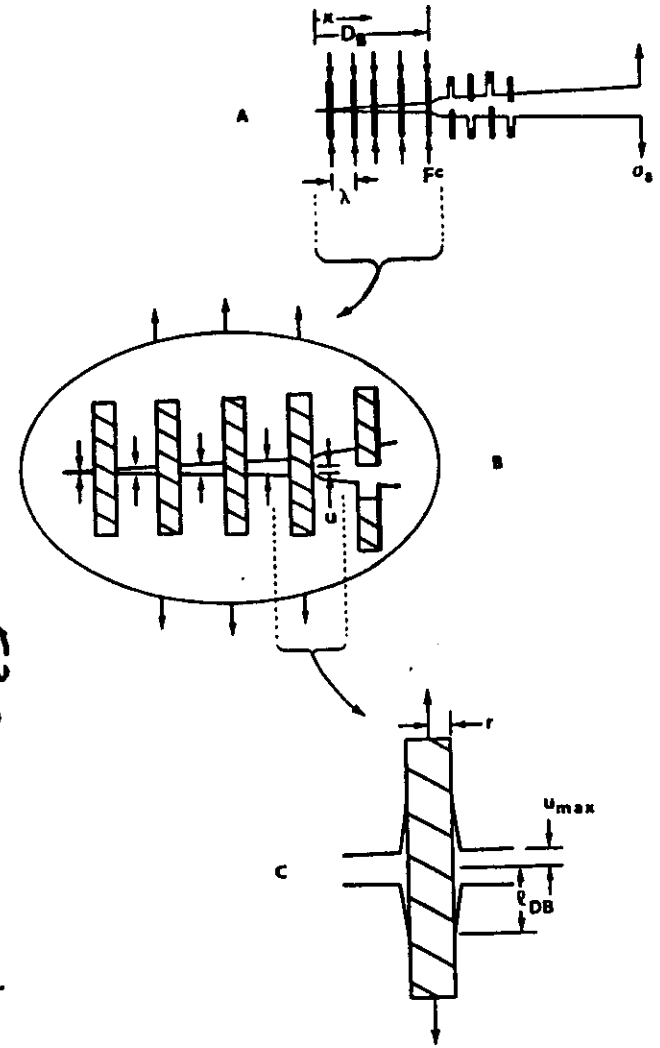

Fig. 1. The presence of a whisker bridging zone behind the crack tip modifies the crack-opening displacement. In the presence of bridging whiskers, closure forces (F^c) and stresses are imposed on the crack surfaces, A. The size/length of the zone (D_B) and the total stress imposed on the crack define the toughening contribution. For a fully developed zone in mechanical equilibrium, the applied tensile stress acting on the bridging zone just equals the closure stress, B. At $x = D_B$, the tensile stress is sufficient to cause whisker failure. The strain (u^w_{max}/l_{DB}) in the whisker at $x = D_B$ is then equal to σ_f^w/E^w; the displacement in the whisker equals the crack opening displacement, C.

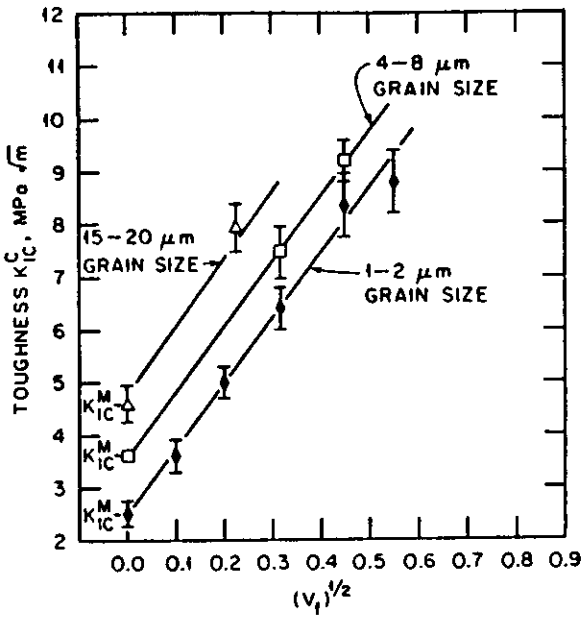

Fig. 8. The overall toughness of the SiC whisker (0.4-μm radius) reinforced alumina composites increases with increase in the matrix toughness. Increasing the grain size of the alumina matrix enhances the matrix toughness and that of the composite. The increase in both the matrix and composite toughnesses with increased grain size is consistent with matrix bridging effects.

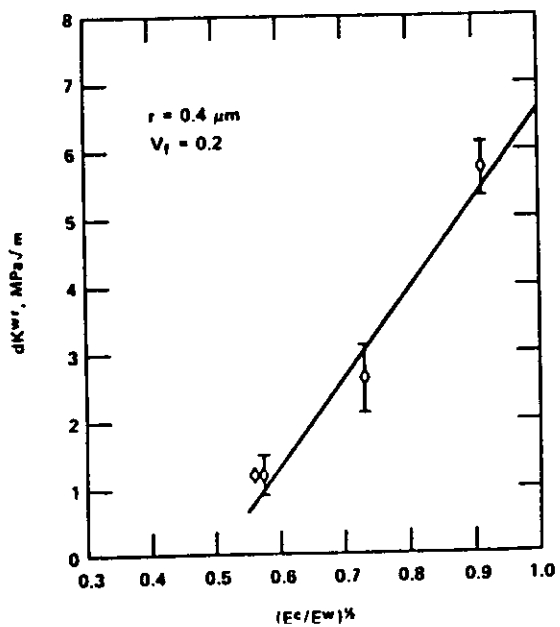

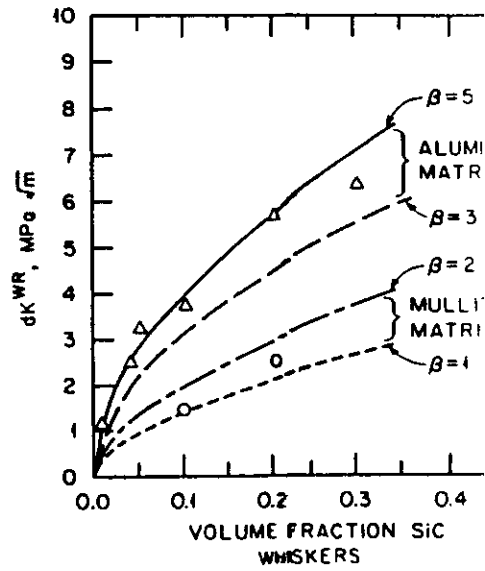

Fig. 9. Using the solution provided by Eq. (13), dicted toughening response in alumina- and mullit composites is found to be in excellent agreement with perimental observations. The predicted curves are sho the range of $l_{DB}/r = l_{PO}/r$ ratios found experimenta ploying the 0.4-μm-radius, low-surface-oxygen-cont whiskers for a whisker strength of 10 GPa.

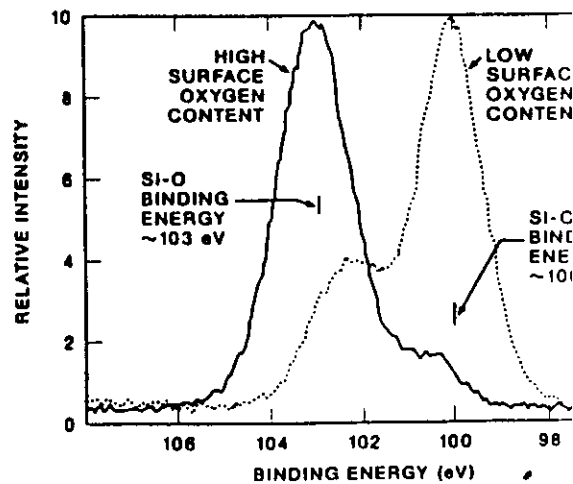

Fig. 5. X-ray photoelectron spectra show that SiC whiskers surface oxygen content exhibit a strong Si–O signal versus t Si–C signal for whiskers with low surface oxygen content.

FIGURE (3)

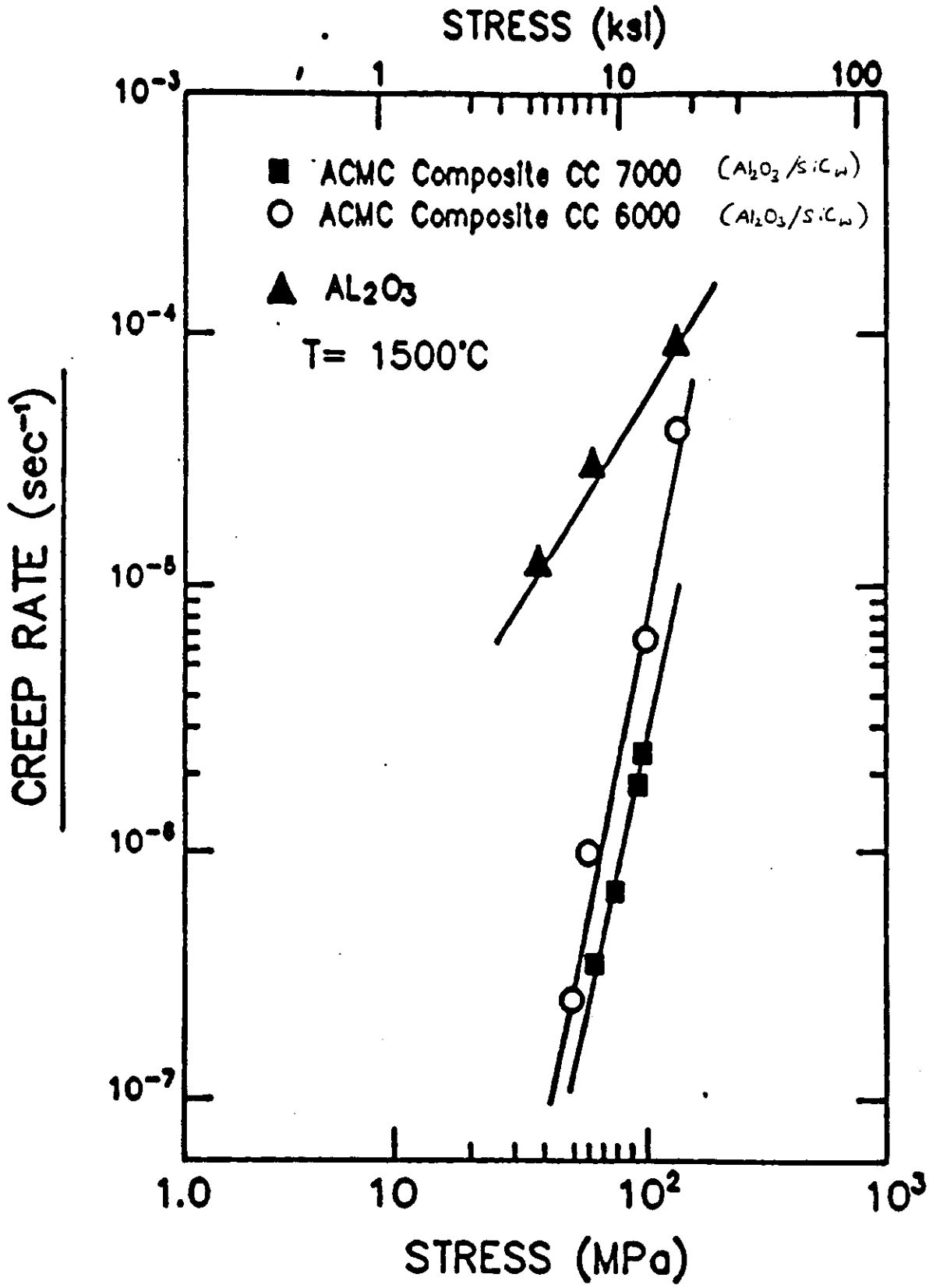

CREEP RATE VERSUS STRESS FOR SELECTED CERAMICS

Advanced Composite Materials (
1525 S. Buncombe Road
Greer, South Carolina 29651

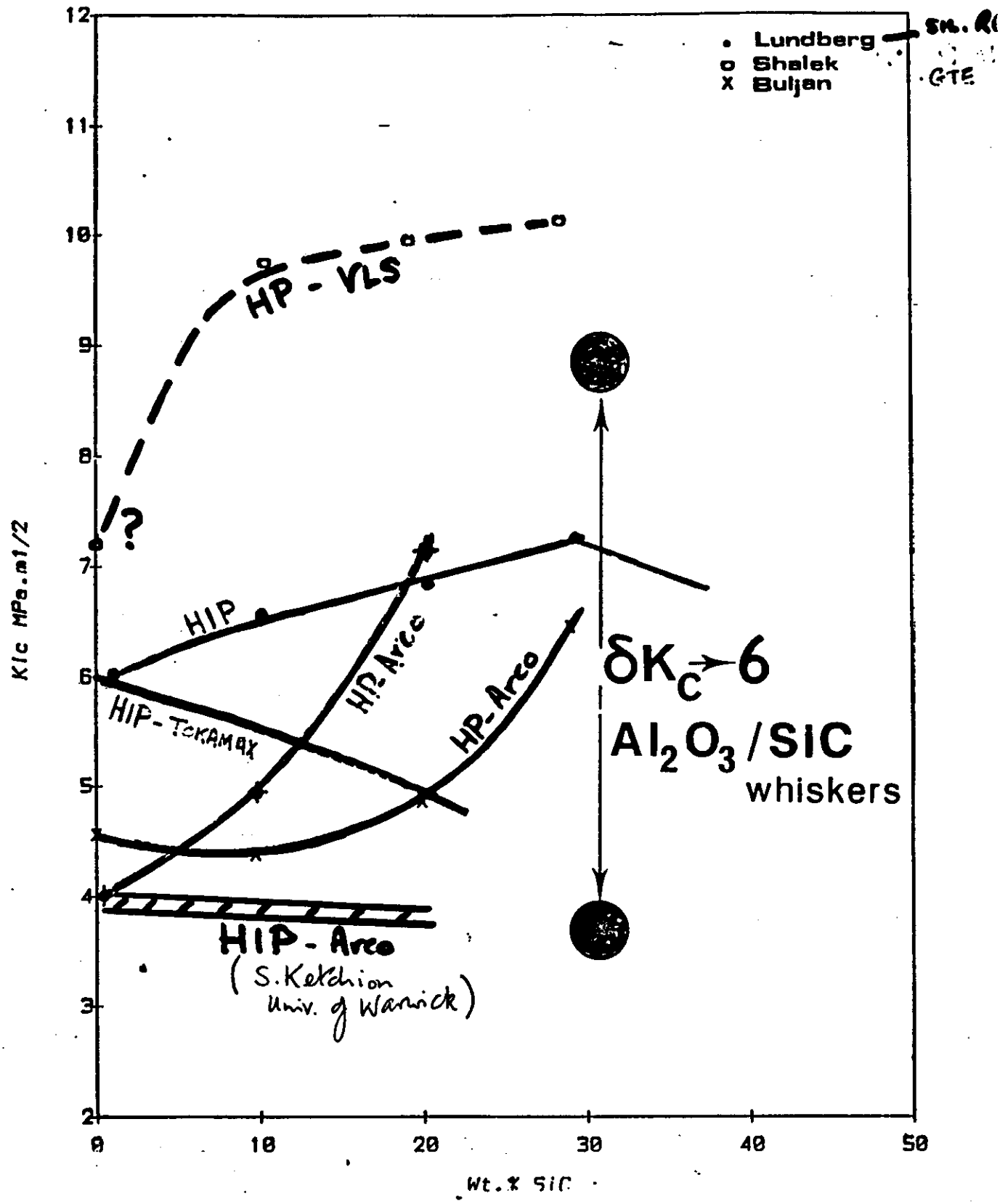

FRACTURE TOUGHNESS OF SIC-Si3N4 COMPOSITES

SiCw/MAS
GLASS-CERAMIC

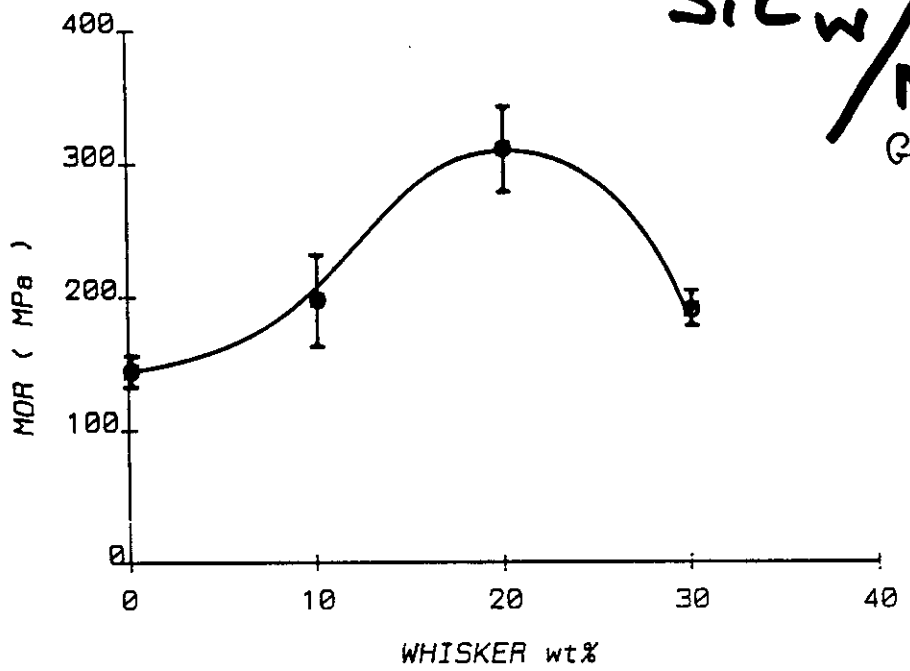

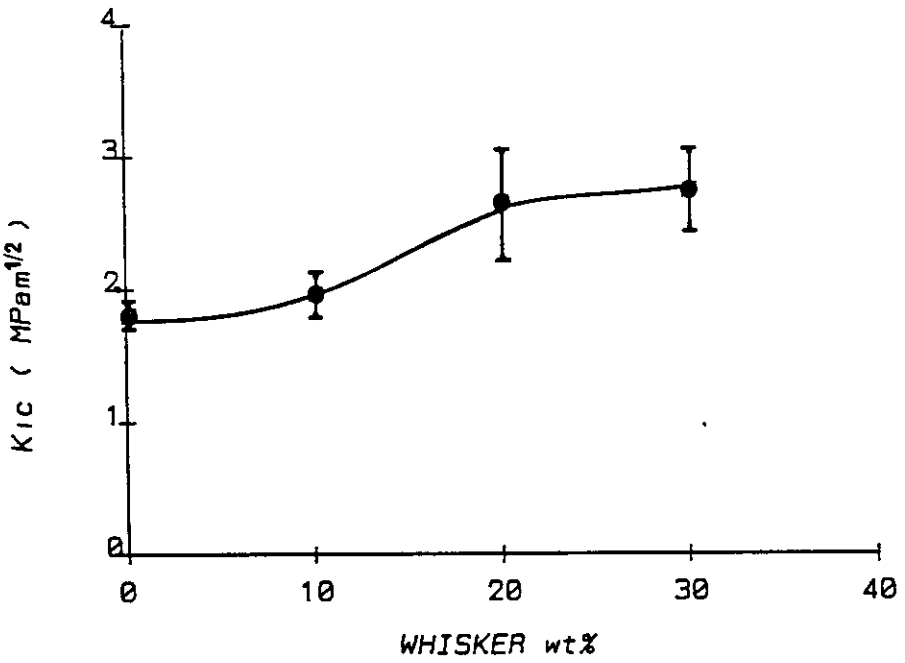

Fig.5.1 MOR & Kic VS WHISKER CONTENT

Ref. Li Jie
M.Sc. Thesis
Univ. of Warwick

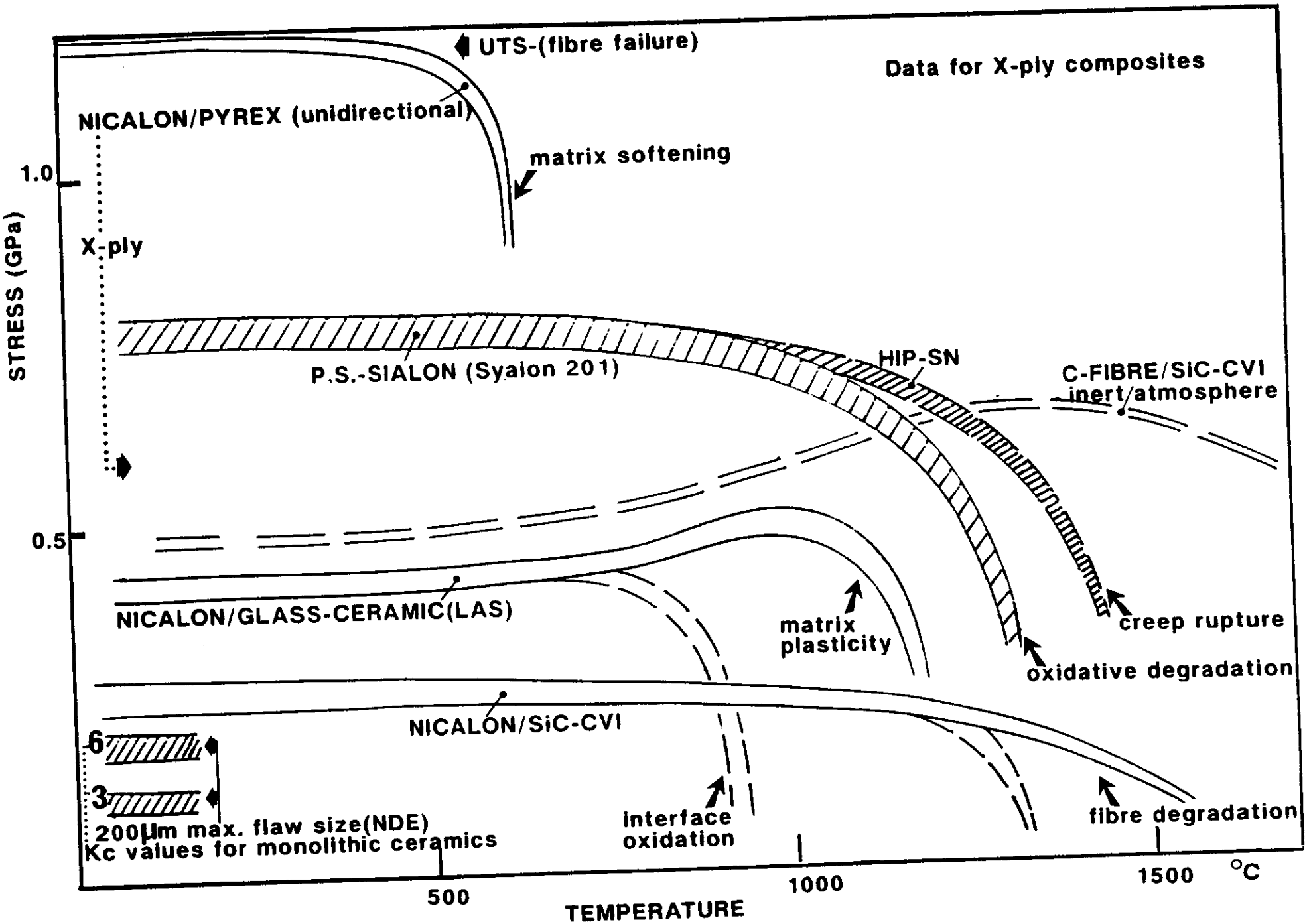
Data for X-ply composites
UTS-(fibre failure)
NICALON/PYREX (unidirectional)
matrix softening
1.0
X-ply
STRESS (GPa)
P.S.-SIALON (Syalon 201)
HIP-SN
C-FIBRE/SiC-CVI
inert/atmosphere
0.5
NICALON/GLASS-CERAMIC(LAS)
matrix
plasticity
creep rupture
oxidative degradation
NICALON/SiC-CVI
6
3
200µm max. flaw size(NDE)
Kc values for monolithic ceramics
interface
oxidation
fibre degradation
500
1000
1500
°C
TEMPERATURE

Ceramics: applications and limitations

M H LEWIS

Within the past decade a number of significant advances have been made in the development of new ceramics which has been stimulated by the inadequacy of metallic alloys or traditional ceramics in meeting the needs of newly-developing technologies. This paper surveys some of the current and potential applications of the new ceramics in relation to their microstructure and properties. The main emphasis is on monolithic ceramics based on Si_3N_4 and SiC, which have important applications in high-temperature energy conversion systems, and on the ZrO_2-toughened ceramics, currently restricted to a lower temperature regime. Ceramic/ceramic composites are briefly reviewed as an important new class of material which may overcome some of the engineering design/reliability problems associated with brittle fracture.

The author is with the Centre for Advanced Materials Technology, Department of Physics, University of Warwick.

INTRODUCTION

The name 'ceramic' has traditionally been associated with the chemically and microstructurally complex products of 'firing' natural silicate minerals following a convenient shaping operation in which the silicate particles are held in a fluid medium. A large volume of the ceramic industry, based on the need for cheap sources of thermal or electrical insulation, will continue in this 'traditional' ceramic area. However, there has been an increasing requirement for operation of ceramics in an environment of greater severity which has stimulated the development of high-purity synthetic ceramics with enhanced chemical, thermal or mechanical properties. These are the oxide refractories, based mainly on Al_2O_3 MgO or ZrO_2, and more recently the nitrides or carbides of silicon and boron and the silicides or borides of selected transition elements (e.g. $MoSi_2$, TiB_2).

In the 1980's we are witnessing a new era in the development of structural ceramics based principally on the evolution of microstructures with special mechanical or thermo-mechanical properties. A well-publicised example of a recent 'high-technology' ceramic application is that of the thermal protection system of the space shuttle. The requirement for low density and thermal conductivity, high thermal-shock resistance together with a retention of moderate strength and rigidity has been met by a combination of intrinsic solid properties and microstructural design. Thus the insulating layer, which has to withstand sudden re-entry temperatures up to 1400°C and large 'g' forces, consists of micron-diameter SiO_2 glass fibres in a random array, leaving >90% porosity (Fig.1). The necessary intrinsic properties are conferred by the disordered (glassy) SiO_2 structure which has 1/10 of the thermal conductivity of crystalline SiO_2 and an extremely small thermal expansion coefficient (0.5×10^{-6} compared e.g. to Al_2O_3 - 8.8×10^{-6}). The low density - high porosity microstructure enables a further large reduction in thermal conductivity and rigidity is provided by high-temperature diffusional bonding between the glass fibres.[1]

This introductory example of the evolution of a ceramic with appropriate macroscopic properties is a simple illustration of the interaction between intrinsic phase-properties and microstructural 'engineering'. Similar principles apply to the wide variety of phase combinations and morphologies found in the more complex microstructures of the new 'engineering

Table 1

Estimated energy gain in using ceramic components in heat engines. (Ref.2)

Type of engine	% Reduction in fuel
Automotive turbine 150 h.p., 1370°C inlet temperature.	27
Truck diesel (adiabatic turbo-compound) 500 h.p., 1210°C max. component temperature.	22
Passenger car diesel (no cooling) 80 h.p., 800°C max. component temperature.	10-15

Table II – Si_3N_4 – based ceramics

Major phase : normally βSi_3N_4 or substituted-derivative $\beta'(Si_{3-x}Al_xO_xN_{4-x})$

Type	Example of Composition and Source		Microstructure
HPSN or HIPSN	1% MgO additive	Norton NC132	0-3% mainly glassy intergranular residue
	2-5% Y_2O_3 additive	Battelle-U.S.A.	
SSN	5% MgO + 9% Al_2O_3	Kyocera SN205	5-10% glassy or crystalline matrix + β'
	6% Y_2O_3 + variable Al_2O_3/AlN	Lucas-Cookson-Syalon 101/201	βSi_3N_4 + glass
	6% Y_2O_3	GTE PY6	
RBSN	Nitriding of Si during sintering without additives	Norton NC350	60-90% αSi_3N_4
		AED 'Nitrasil'	10-40% βSi_3N_4
			5% Si
			15-30% porosit
SRBSN	Similar to RBSN, followed by high-temperature sinter (with additives)		Similar to SSN

Table III - SiC-based Ceramics

Major phase : either αSiC (hexagonal polytypic) or βSiC (cubic)			
Type	**Example of Composition and Source**		**Microstructure**
HP SiC	1% B_4C or Al/Al_2O_3	Norton NC203 Elektroschmelzmer Co. FRG	αSiC + up to 3% intergranular residue with Al/Al_2O_3 additions
SSiC	0.5–1% B + C or Al+C additives	Kyocera SC201 Carborundum Co. G.E. 'Sintride'	" " βSiC
SiSiC	'Siliconized' : wide range of composition and sintering process e.g. SiC + graphite preform + reaction with Si in liquid or vapour state	Norton NC435 Coors	α + β SiC + ∿ 10% free Si

Table IV - ZrO_2-toughened ceramics

Type	Example of Composition and Source	Microstructure
TZP	2–4% Y_2O_3/ZrO_2 sintered 1350–1500°C NGK Z191	Fine-grained, fully tetragonal polycrystal
PSZ	8–10% MgO/ZrO_2 sintered 1650–1850°C, heat-treated 1100–1450°C Feldmuhle ZN40, Coors	Tetragonal ZrO_2 precipitates in cubic matrix

Property Comparison

Type	MOR (MPa)	K_{1c} (MPa $m^{½}$)
TZP	1000–2500	7–12
PSZ	600– 800	6– 8
ZT(Al_2O_3)	500–1300	5– 8
CSZ (fully cubic)	200	3
SSN	500– 800	5– 8
SSiC	400– 600	3– 5

ceramics' discussed in this paper. The emphasis will be on structural ceramics in which the development of exceptional mechanical or thermo-mechanical properties is of prime concern.

2. THE PROCESSING CONSTRAINT

The idealised sequence of phase selection and microstructural engineering, outlined above, is frequently inhibited via kinetics or thermodynamics (phase equilibria) associated with the ceramic fabrication process. A melting/casting/thermal-mechanical process commonly used in metallurgical practice is inappropriate for ceramics in view of their high melting temperatures or decompositional problems, susceptibility to thermal shock and resistance to plasticity. The nearest approach is that of silicate glass melting, shaping and controlled crystallisation typified by the 'glass ceramic' processing route. More frequently ceramics are formed by the consolidation of pressed particle aggregates known generally as 'sintering'.

The simplest sintering mechanism is that in a monophase ceramic with transport of matter by solid-state diffusion from particle-contacts along grain-boundaries to inter-particle pores. The thermodynamic 'driving-force' for transport is the reduction in free surface energy associated with porosity. To accelerate the sintering process or to achieve a theoretical density (i.e. zero porosity) ceramic it is common practice to make impurity additions to the particle compact. The role of these sintering catalysts is obscure in many systems; various hypotheses involving enhanced diffusion, modified interfacial/surface energy ratios or grain-boundary 'pinning' have been proposed. However, the better spatial resolution of microscopic and analytical techniques over the past decade has established that monophase solid-state sintering is relatively rare. Frequently, sintering additives are the basis for minor intergranular liquids which provide rapid transport paths during densification by a solution-reprecipitation mechanism.

Liquid-phase sintering (l.p.s.) assumes a greater importance in systems with low diffusivity or those susceptible to decomposition. These are normally ceramics in which the major phase has a high degree of covalent bonding such as silicon nitride or silicon carbide, which are prominent examples of the new engineering ceramics. A number of oxides also utilise l.p.s. in fabrication; the restriction in sintering temperature required to develop appropriate phase-mixtures of ZrO_2 polymorphs in some of the new 'toughened' ceramics dictates the use of silicate impurity-based liquids.

The consequence of liquid phase sintering is the presence of intergranular residues which inevitably impair mechanical properties. This processing constraint is a central problem in the ability to microstructurally engineer ceramics for elevated temperature use. Many sintering liquids are silicate based and are transformed to the glassy state on cooling. Procedures for minimising the intergranular glass volume or tailoring glass compositions for subsequent crystallisation are described below in relation to the new high-temperature nitride and oxynitride ceramics. Heat treatment procedures are also used to induce solid-state phase transformations in various 'toughened' ZrO_2-based ceramics. The capacity for significant property modification via. post-sintering phase-transformations has, in comparison with metallic materials, only recently been identified and is typified by some of the new ceramics.

3. THE REQUIREMENT FOR NEW ENGINEERING CERAMICS

The most rewarding but difficult areas for application of the new structural ceramics are within energy-conversion systems such as the advanced gas-turbine or the turbo-compound diesel engine. The main attraction of ceramics in heat-engine design is the ability to operate at higher temperatures with the elimination or reduction of forced cooling. This translates into greater thermodynamic efficiency and hence decreased fuel consumption (Table 1). Supplementary advantages over cooled metallic alloy components are the reduced inertia (due to a density reduction of 0.5x), important in higher-performance engines. Ceramics, unlike high-performance alloys, rarely contain 'strategic' elements and frequently are composed of the light elements which are abundant in the earth's crust and atmosphere.

The more mundane applications areas for ceramics rely not on their ultimate temperature capability but on their hardness, wear resistance and chemical durability. These are also the main areas of current application whilst the more difficult heat-engine applications remain at a development stage.

Some ceramic component applications are illustrated in Fig.2. Fig.2a illustrates the best-known use of nitride ceramics in high-speed metal cutting under conditions where tool-tip temperatures subject the conventional tungsten-carbide inserts to rapid wear. A comparison of tool lifetimes in the cutting of cast iron is made in Fig.2a.[3] The benefits in machining of certain superalloys are even greater.[4] In this application there is evidence of tip temperatures in excess of 1000°C such that the retention of hardness and wear resistance at elevated temperatures is also important. Similar properties are required in applications involving metal-forming (e.g. extrusion dies) or as high-temperature bearings and seals (Figs.2b). Thermal shock resistance and chemical durability are important in molten metal handling.

The new ceramic applications, especially those in heat-engines have been made possible by the development of ceramics with an appropriate combination of properties. Two

Fig. 1. Scanning electron micrograph of the thermal-protection layer of a space shuttle (courtesy Dr. D J Green).

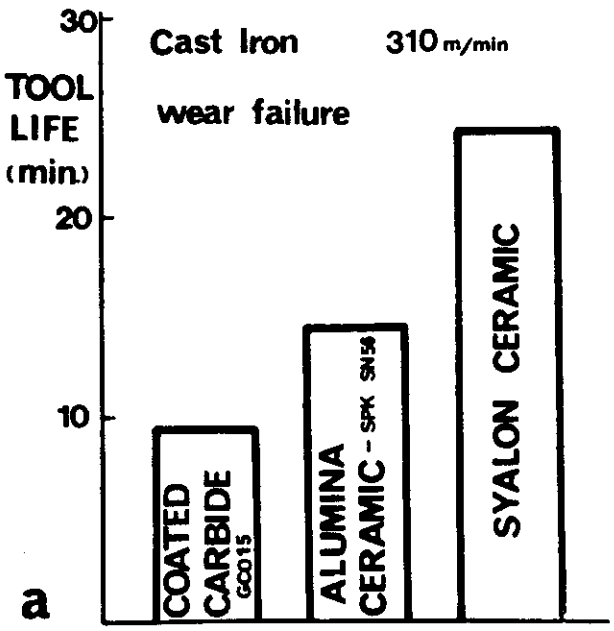

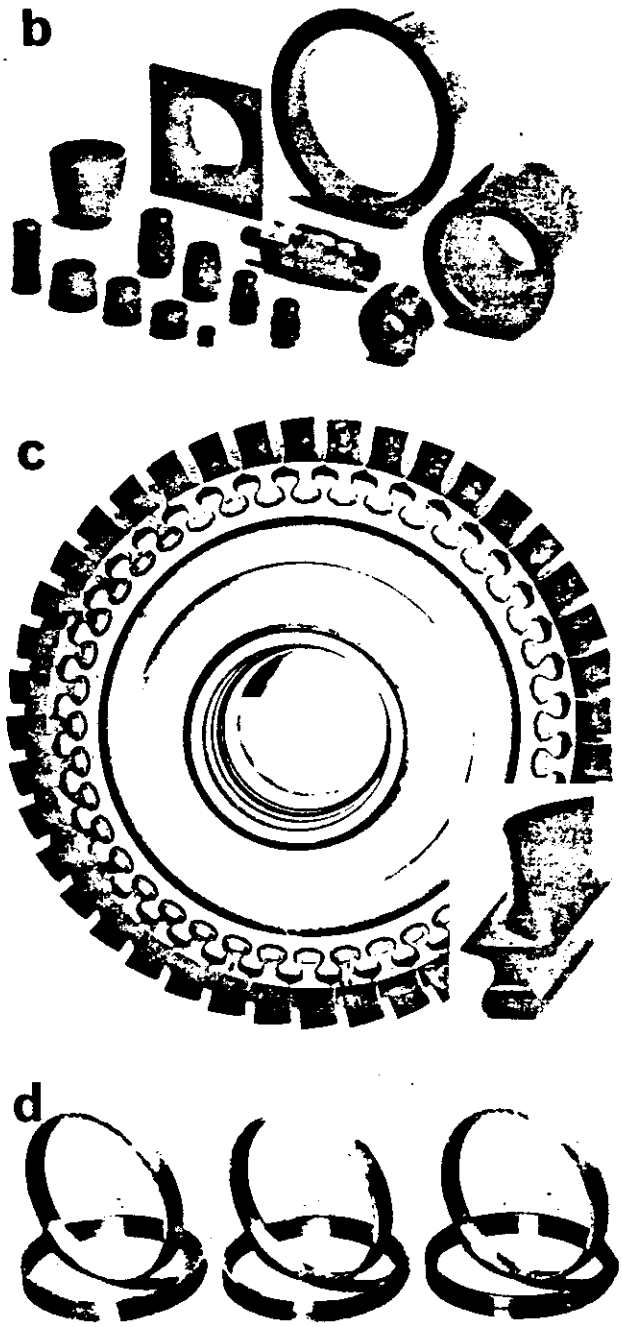

Fig. 2. Ceramic components, illustrating some of the existing and potential applications for new engineering ceramics :
(a) Metal machining, with an example of improved tool life for a Syalon ceramic tool-tip.
(b) Various seals, bearings, crucibles and tube-drawing mandrels in Syalon ceramic (courtesy Lucas-Cookson-Syalon).
(c) (d) Turbine blades and shroud rings in Syalon ceramic (courtesy Rolls Royce and Lucas-Cookson-Syalon).

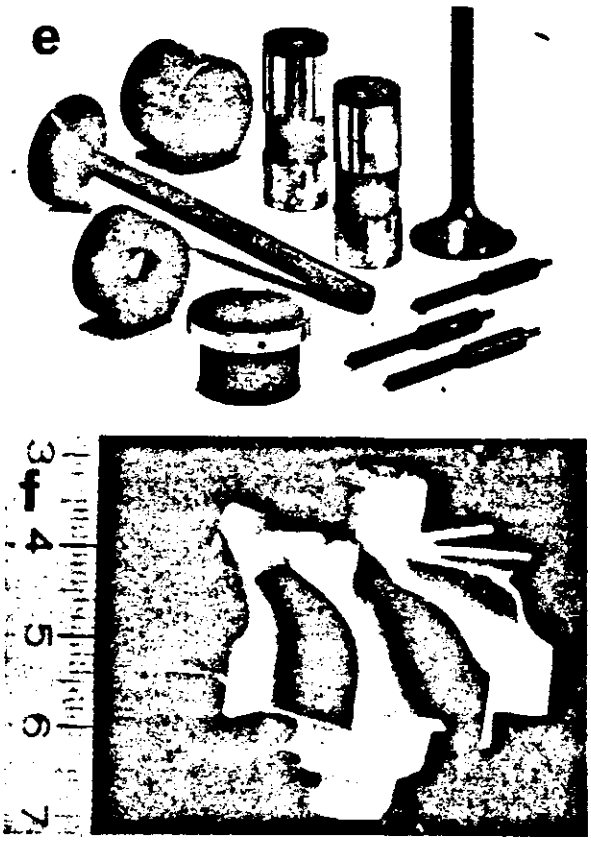

Fig. 2 (e) Reciprocating engine components (valve components, diesel inlet port, etc. - courtesy Lucas-Cookson-Syalon). (f) Turbo-charger rotor.

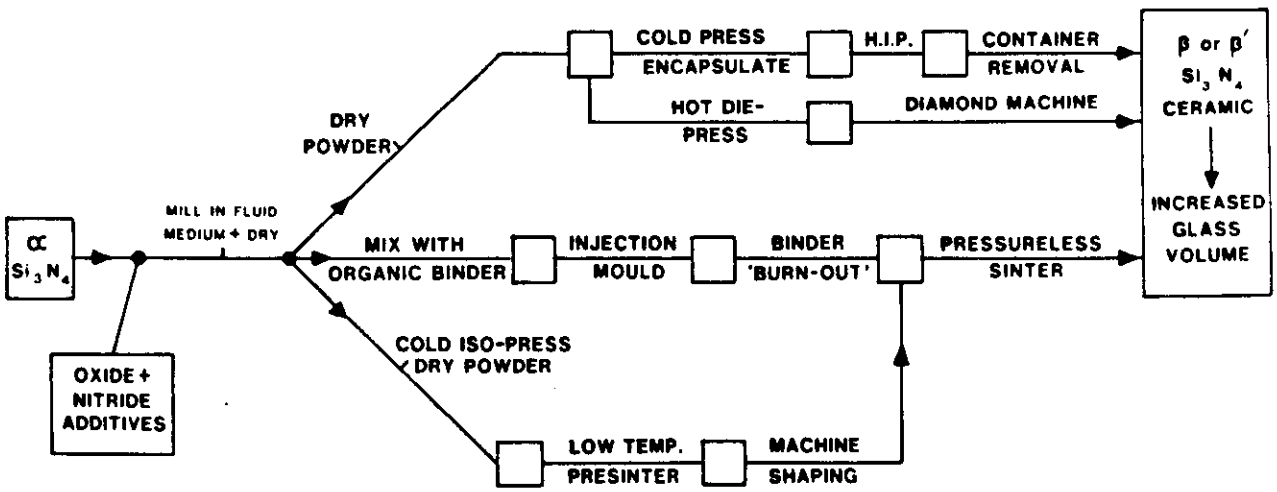

Fig. 3. Fabrication routes for Si_3N_4 ceramics.

main types of monolithic ceramic may be identified:

(i) Ceramics containing Si_3N_4 or SiC as major phases.

(ii) Ceramics in which ZrO_2 is a major or dispersed phase.

Type (i) ceramics are the main contenders for high-temperature applications (>1000°C) in heat engines and have a property combination of high modulus, hardness, creep resistance, low thermal expansion and hence thermal shock resistance. Good oxidation resistance is conferred via a 'self-healing' SiO_2 based oxidation layer. These properties are intrinsic to the major phases βSi_3N_4 or the substituted 'Sialon' derivatives ($\beta' Si_{3-x}Al_xO_xN_{4-x}$) and either the cubic βSiC or hexagonal αSiC. However, significant property variations are introduced via minor intergranular phases and other microstructural differences which are a consequence of the fabrication process. These microstructure/property relations are discussed in Section 4. Examples of heat-engine components made from this type of ceramic are shown in Fig.2e-h.

Monolithic ceramics suffer from the problem of low fracture-toughness and hence are sensitive to the presence of stress concentrations from point loading and from surface or internal flaws of a size which would be unimportant for metallic alloys. Hence one of the most important ceramic developments in the past decade has been the evolution of a range of ceramics of type (ii) - based on ZrO_2 toughening. These are focussed on the initial discovery[5] of a large increment in strength for the cubic-stabilised ZrO_2 polymorph when heat-treated to contain precipitates of the lower-temperature tetragonal form. This phenomenon has been ascribed to transformation of the metastable tetragonal precipitates to the monoclinic form in the stress field of a propagating crack. The transformation is martensitic and the shapechange is a source of internal stress which modifies the stress field of a crack such that a higher applied stress is required for fracture.[6] It is now recognised that the toughening may be a superposition of different mechanisms, such as crack deflection or microcracking associated with precipitates in addition to stress-induced transformation. The dominance of particular mechanisms depends on the microstructure; in addition to the tetragonal precipitate-containing form (called partially stabilised zirconia - PSZ) high strength and toughness may be achieved with a fine-grained, fully tetragonal, polycrystalline structure (TZP). ZrO_2-toughening may also be applied to other ceramic matrices, such as Al_2O_3, which contain a dispersion of tetragonal or monoclinic zirconia particles.

Apart from enhanced toughness, ZrO_2-based ceramics have emerging applications where their low thermal- conductivity and compatibility of thermal-expansion with metallic alloys is especially valuable. For example, in development of heavy-duty uncooled (adiabatic) diesel engines when recovery of heat-energy in exhaust gases is required (e.g. using the turbo-compound principle) the thermally-insulating properties of ZrO_2 ceramic coatings on cylinder walls, exhaust manifolds etc. have been used. ZrO_2 coatings are also in use in turbine combustors but with the proposed increases in inlet temperature ZrO_2-based ceramics, either as coatings or in the 'toughened' monolithic form, will find little application due to their instability on high-temperature cycling.

Finally, the emergence of a new class of ceramic in the past few years has aroused considerable interest due to enhanced fracture-toughness. This is the ceramic/ceramic composite which is normally that of oriented fibres or whiskers within a ceramic matrix. The type of composite most intensively studied is based on a silicate glass or glass-ceramic matrix[7] and hence has limited high-temperature capability. High-quality fibres are not easily available; those most frequently used are SiC or carbon. The development of low-temperature infiltration techniques for refractory matrices, hence avoiding fibre/matrix reactivity during sintering, appears to have promise[8] but the long-term high-temperature properties of these composites have yet to be demonstrated.

4. THE Si-BASED CERAMICS

4.1. Si_3N_4; fabrication and microstructure

A range of Si_3N_4-based ceramics is exemplified in Table II, identified by acronyms frequently used in the literature. Apart from the low- density reaction-bonded form (RBSN), they all contain βSi_3N_4 as a major phase (>90%). 'Syalon' ceramics contain the derivative β' phase but normally at a very low substitution level such that its intrinsic properties are unchanged. Hence commercial pressureless-sintered products, such as the Syalon ceramics are included within the sintered silicon nitride (SSN) category. They are distinguished by the use of lower-melting ternary eutectic sintering liquids of the type Y_2O_3-Al_2O_3- SiO_2, which result in higher sintered densities than the binary type (Y_2O_3-SiO_2) or the latter require hot die-pressing (HPSN) or hot isostatic pressing (HIPSN). In all processes the SiO_2 component of the sintering liquid derives from that present on the surface of α-Si_3N_4 - the main ingredient of the initial fine-particle mixture. The use of α-Si_3N_4 is beneficial not only for its fine particle size and microhomogeneity in SiO_2-distribution but also in providing a chemical component of 'driving-force' for the solution-reprecipitation sintering reaction.

Alternative ceramic-fabrication sequences in achieving shaped components are exemplified in Fig.3. In general the application of pressure during sintering requires smaller liquid volumes and hence reduced silicate

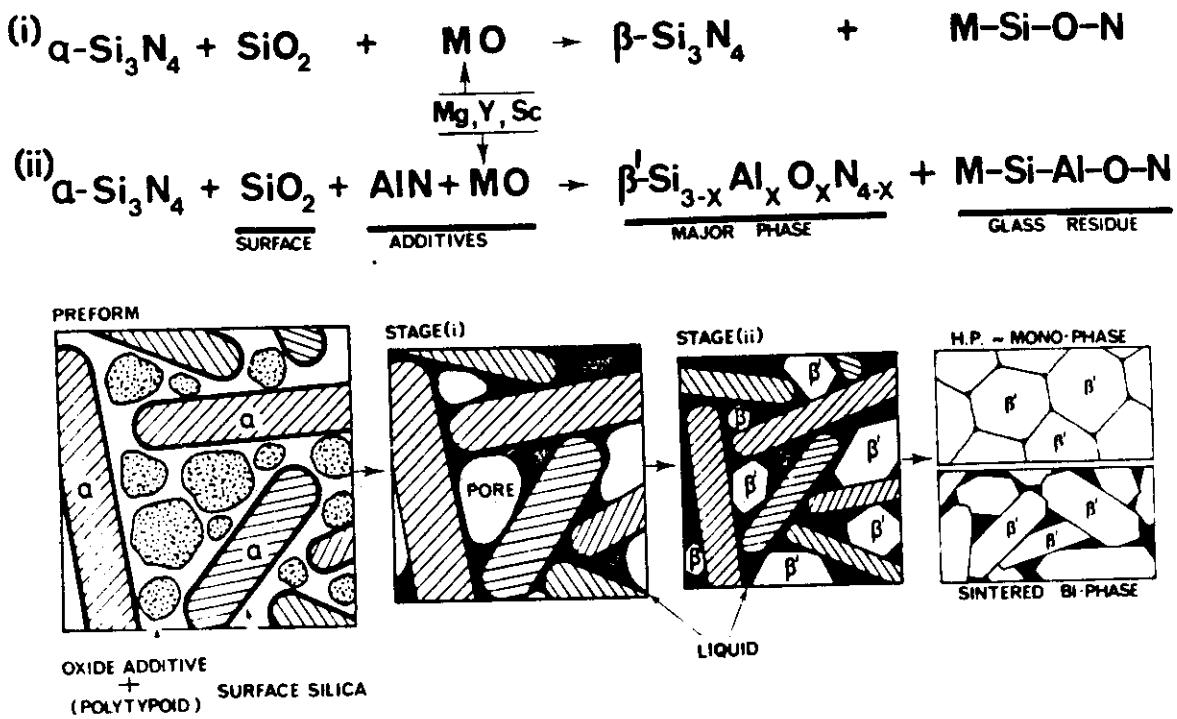

Fig. 4. Sintering reactions and the evolution of microstructure for HPSN and SSN ceramics.

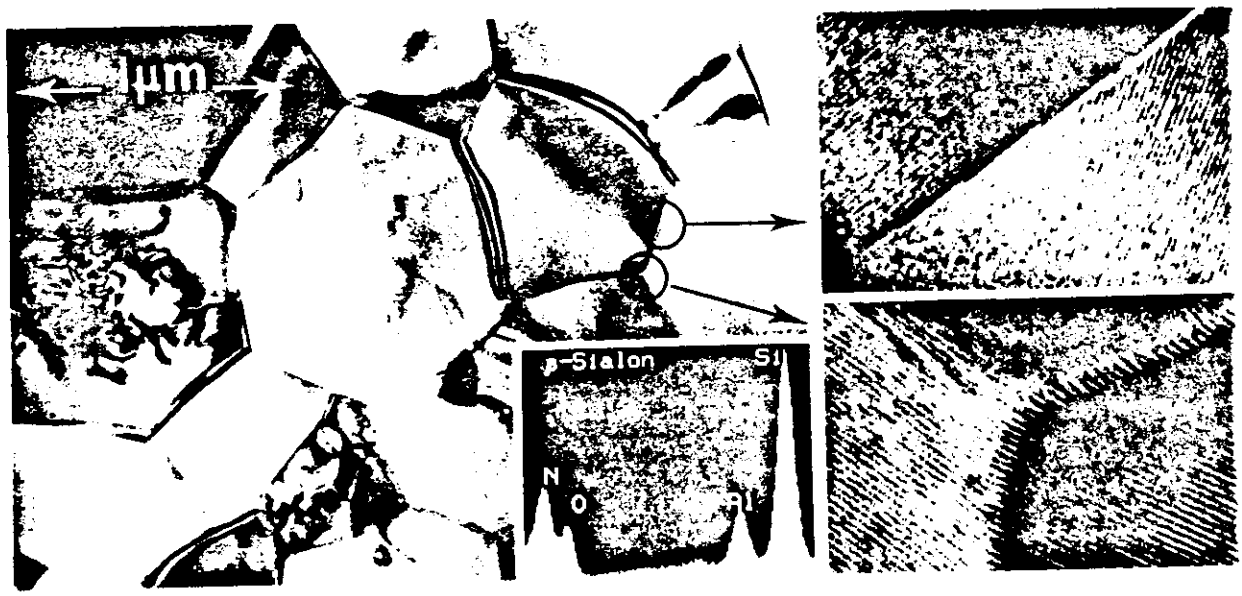

Fig. 5. The microstructure of a hot-pressed Si_3N_4 ceramic, with the absence of residual intergranular glass revealed by high-resolution 'lattice' imaging in TEM.

glassy residues. However, the formation of high-density complex shapes by HIP necessitates encapsulation (e.g. with a high-SiO_2 glass) to isolate the ceramic from the high-pressure gas (200MPa) and enable pore closure. HIP also requires a preformed shape via cold die-pressing, injection-moulding, slip-casting or 'green'-machining before encapsulation. These shaping processes are also necessary for pressureless- sintering, normally carried out in 1 atmosphere of N_2 gas at 1700-1800°C. In all cases the sintering shrinkage of 20-30% presents a major problem in dimensional tolerance of finished components.

Sintering reactions and evolution of microstructure are shown schematically in Fig.4 for a hot-pressed (HP) product with minimal liquid and a pressureless-sintered (β-liquid) bi-phase microstructure. Electron-micrographs of these extremes of micro- structure are exemplified by 'Sialon' ceramics (Figs. 5 & 6). The H.P. sialon is a monophase ceramic sintered with a small transient liquid volume (in this case based on $MgO-Al_2O_3-SiO_2$). The P.S. ceramic has 5-10% of a $Y_2O_3-Al_2O_3-SiO_2$ eutectic liquid which cools to the glassy state as a semi-continuous matrix for $\beta'Si_3N_4$ crystals. However, in ceramics designed for high-temperature application (>1000°C) it is necessary to increase the glass-softening point and, preferably, to induce total crystallisation of the glass matrix. In β' ceramics control of glass matrix and viscosity is achieved by substitution of part of the added Al_2O_3 by AlN (added as a 'polytypoid' phase containing substituted Si and O). The increased N/O ratio in the glass also makes it susceptible to crystallisation of the mixed oxide 'yttro-garnet' (YAG) rather than a silicate phase. Excess Si and N is accommodated in β' and, with carefully tailored initial compositions and post-sintering heat-treatments, the product is a fully-crystalline bi-phase (β'+YAG) ceramic typified by the '201' type of Lucas-Cookson-Syalon.

The earlier commercial silicon nitride ceramics were based on simultaneous nitriding and sintering of compacted silicon powder (reaction-sintering). These RBSN's (Table II) have high porosity levels and hence low strength, but exhibit negligible shrinkage during reaction sintering at 1400°C. More recently a hybrid fabrication route of reaction-sintering followed by high-temperature sintering has been explored (SRBSN - Table II). Final microstructures are generally similar to SSN but the smaller total shrinkage (10%) is beneficial in ceramic shaping.

4.2. Si_3N_4: properties

A survey of mechanical behaviour for selected fully dense high-strength nitride ceramics is contained in Figs.7-10. There is a division in mechanical behaviour from that of a brittle, high modulus, solid at temperatures below 1000°C to a solid which undergoes creep deformation and time-dependent fracture at higher temperatures. The transition is linked to the softening temperature of intergranular glassy residues which increases with N/O ratio and with metallic additive valence (e.g. MgO to Y_2O_3).

In the low-temperature range brittle failure is initiated at pre-existing stress-concentrating flaws. The bend strength (modulus of rupture - M.O.R.) is typically in the range 600-1000 MPa and, as in all brittle solids, is determined by the combination of an intrinsic microstructure-dependent parameter K_{1c} (the fracture-toughness) and the maximum flaw 'size' $\sim c$ via the relation $MOR = \frac{1}{Y}\frac{K_{1c}}{\sqrt{c}}$ is a geometrical 'flaw shape' parameter. This ideal relation is plotted in Fig.7 and gives an approximate range of flaw sizes in the more recent high-strength nitrides. Values of K_{1c} used in Fig.7 are typical of the Syalon range of pressureless-sintered ceramics in which β' grains, crystallised in a liquid matrix, have an elongated prismatic shape.[9] HP ceramics generally have lower values (K_{1c} 3-5 MPa $m^{\frac{1}{2}}$) due to their more equiaxed grain shapes, thus giving a smaller intergranular crack-deflection/'pull-out'component of fracture-toughness. In monolithic nitride ceramics there is little prospect of large increases in K_{1c} such that enhanced M.O.R., together with reduced statistical spread (measured via the Weibull modulus)[10] must come from improved purity, homogeneity in powder processing and sintering to theoretical density. This is relatively difficult in multi-component nitride/oxide systems. Impurity inclusions normally derive from fragments of ball-milling media (e.g. Al_2O_3) or from transition elements (e.g. Fe) within Si_3N_4 powders which form silicides on sintering.

The achievement of MOR values above 1 GPa requires a maximum flaw size <30μm according to the idealised relation in Fig.7. However, it is now realised that surface machining produces an array of surface flaws which contain residual stresses due to a mismatch between the plastically-deformed surface layer and the underlying ceramic.[11] The residual stress supplements the applied stress in crack-opening such that flaws which are much smaller than the stress-free critical size, defined by Fig.7, may result in failure. The failure stress is then a function of the residual stress, determined by severity of machining and ceramic hardness, in addition to K_{1c}.[11]

The transition to 'high'-temperature mechanical behaviour in nitride ceramics containing intergranular glass residues is typified by a precipitous fall in MOR, normally accompanied by a transient rise in K_{1c} (Fig.8). The transition is linked to the glass softening temperature with grain-boundary sliding and viscous deformation of glass bridging crack surfaces all contributing to enhanced K_{1c}. In this regime fracture is not always initiated at pre-existing flaws but, at lower stresses, is associated with the accumulation of creep-cavitation damage i.e. failure is time and strain-dependent.

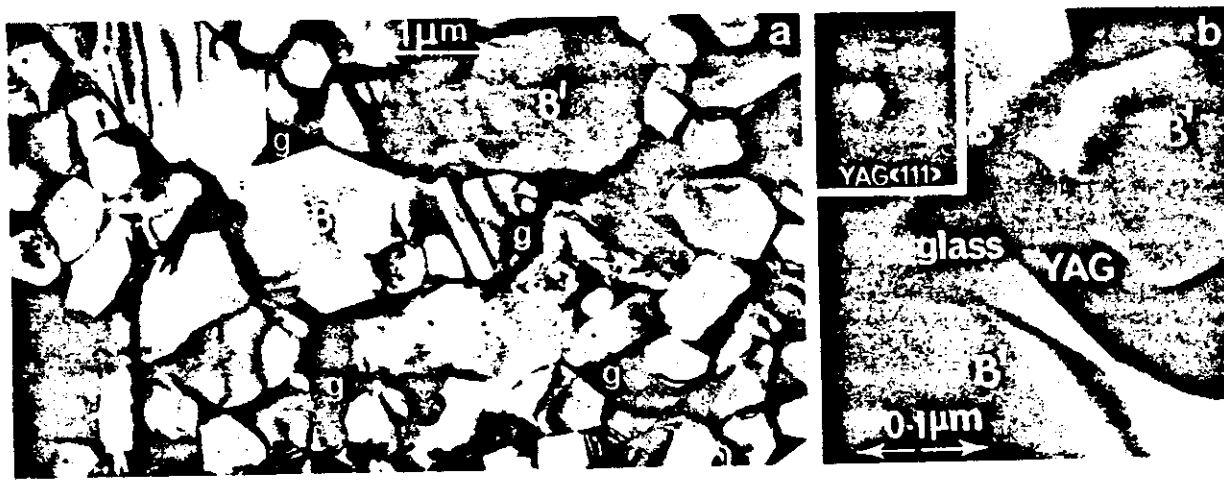

Fig. 6. The microstructure of a SSN ceramic, composed of faceted Si_3N_4 crystals within a ternary- eutectic (Y_2O_3-Al_2O_3-SiO_2) glass matrix containing nitrogen. At high-nitrogen content the matrix crystallises to yttro-garnet (YAG) - Fig.6b.

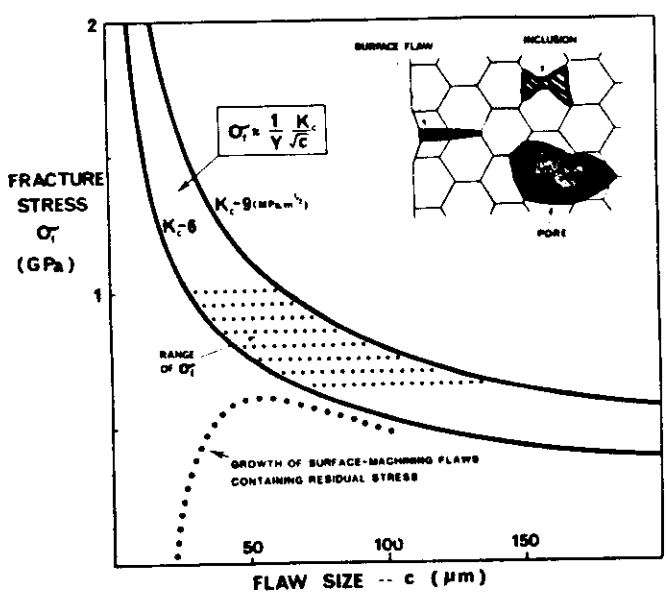

Fig. 7. A simplified fracture-stress (MOR) - flaw size relation plotted for a range of fracture-toughness (K_C) measured in the best SSN ceramics and compared with the experimentally-measured range of MOR. Machining flaws contain residual stresses which may result in a precursor crack growth of small flaws to a reduced failure stress (dotted curve).

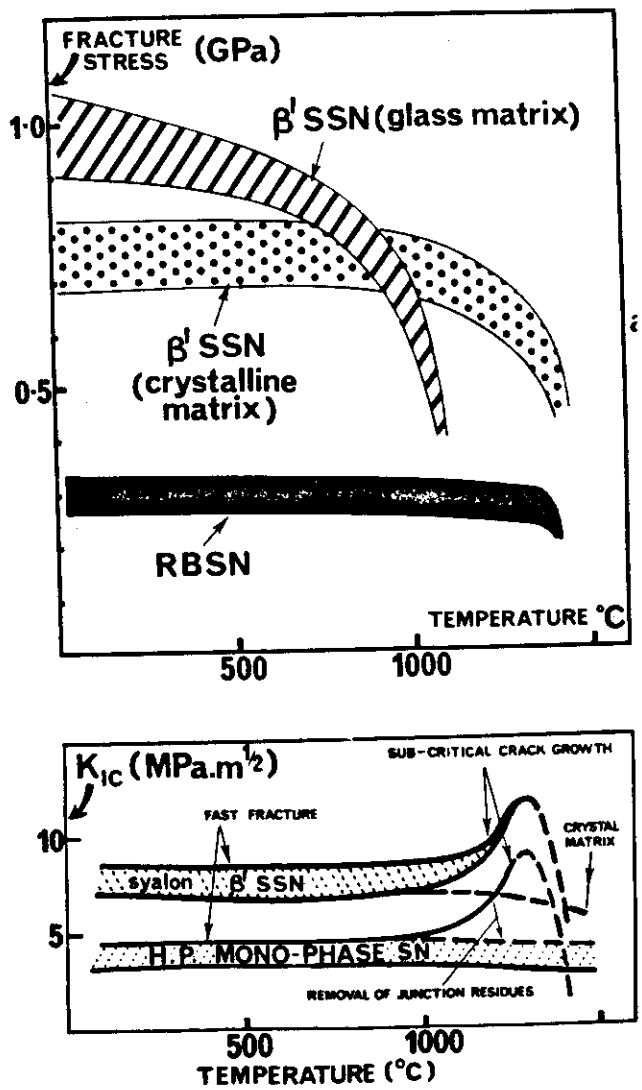

Fig. 8. MOR and K_{1C} - temperature relations for Si_3N_4-based ceramics. The susceptibility to sub-critical crack growth is dependent on elimination of residual glass junctions which form cavity nucleation sites.

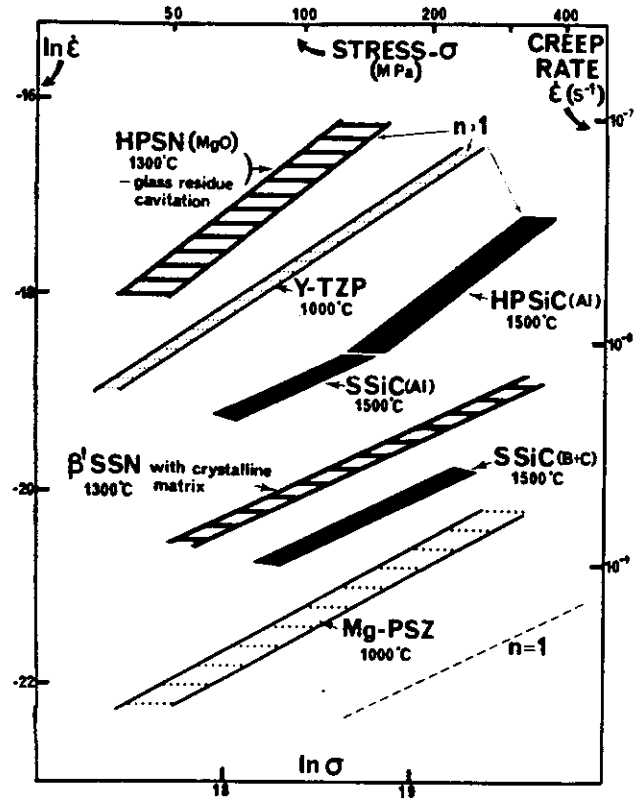

Fig. 9. A comparison of pseudo-steady-state creep rates for a range of Si-based and ZrO_2-toughened ceramics within differing temperature intervals. The stress-exponent (n) of the creep rate is frequently=1, indicative of a diffusion-controlled mechanism.

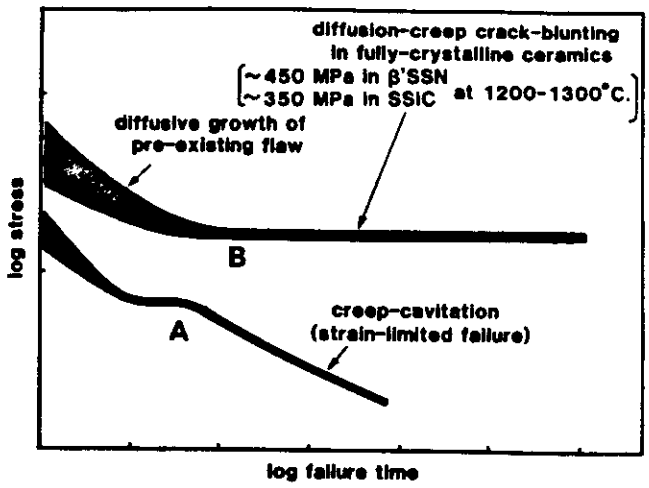

Fig.10. Stress(creep)-rupture behaviour for Si-based ceramics. A high-stress crack-blunting theshold is typical of completely crystalline ceramics undergoing diffusional creep (type B) and is predicted from crack-growth data (Refs.13,14). Type A behaviour is typical of ceramics containing glass residues which undergo creep-cavitation; a limited blunting threshold is followed by fracture due to coalescence of creep-damage (strain-limited failure).

There have been significant advances in the control of high-temperature deformation and fracture via the increased flexibility of micro-structural engineering in the Si-Al-O-N system. This is based on the suppression of creep cavity nucleation when grain-junction glass is below a critical size and is achieved by adjustment of composition and post-sintering heat-treatment to approach the fully crystalline state discussed in 4.1. This microstructure change is also associated with a reduced creep rate with a 'Coble' mechanism controlled by grain-boundary diffusion (Fig.9). Terminal steady-state creep rates at 1300°C are similar for H.P. monophase and P.S. bi-phase ceramics.[12] Creep-rupture data, available only for a limited range of nitride ceramics, indicate a behaviour summarised in Fig.10. At high stresses failure originates from pre-existing flaws with crack-propagation in fully-crystalline ceramics which has been modelled via diffusional growth.[13,14] There is increasing evidence for a threshold stress, below which the 'blunting' of pre- existing flaws occurs by diffusional creep or viscous flow of intergranular glass, depending on the microstructure. This blunting threshold has been identified in fully crystalline Si-Al-O-N ceramics from crack-velocity/K_I data[13,15] and from creep-rupture tests the plateau is believed to extend to very long times in the absence of creep-cavitation. In those ceramics (typified by commercial HP nitrides of the type NC132) where intergranular cavities nucleate below the threshold stress failure is strain controlled via coalescence of cavitation-damage. This behaviour has also been identified in oxides[16] and may be of general application to ceramics. The transition from type A to type B creep-rupture behaviour is critically dependent on micro-structure (i.e. intergranular glass volume and composition) but may also be a function of temperature.

High temperature oxidation-resistance in

Si_3N_4 ceramics is conferred by a passive SiO_2-rich oxidation film, normally in the viscous liquid state at high temperatures. The intrinsic oxidation rate of βSi_3N_4, controlled either by oxygen diffusion through SiO_2 or by the solution rate of Si_3N_4 in SiO_2, is very low even at temperatures >1400°C. The main problem is due to out-diffusion of metallic ions from the intergranular phase which reduces the SiO_2 film viscosity and hence increases the oxygen diffusion rate or Si_3N_4 solubility.[17] For PS ceramics in which the glassy-matrix forms a large reservoir and rapid diffusion path for metallic ions, oxidation resistance above 1200°C is poor. In addition the metallic-ion rich films are susceptible to crystallisation and spalling, especially on thermal cycling. Matrix-phase crystallisation is a partial solution to this problem; for example, YAG or $Y_2Si_2O_7$ matrices in Syalon ceramics confer 1300°C oxidation rates comparable with HP monophase ceramics (Fig.11). Above 1300°C oxidation rate is sensitive to matrix crystal chemistry; most metallic oxides, such as YAG react with SiO_2 to form a eutectic liquid which is accompanied by reversion to high oxidation rates.[18] An extension of application temperature to 1400°C is possible by surface coating (e.g. with CVD Si_3N_4 or SiC) or via controlled sub-surface transformation of the type :

$$Si_3N_4 + SiO_2 \rightarrow 2Si_2N_2O$$

following out-diffusion of metallic ions from the intergranular glass.[18] Si_3N_4/Si_2N_2O phase combinations (or their substituted derivatives β'+O') have excellent oxidation resistance. Fig.11.

4.3. SiC ceramics

Ceramics in which the hexagonal αSiC or cubic βSiC is a major phase have increasing potential as engine components in competition with Si_3N_4. Important steps in the development of dense SiC ceramics were, firstly, the identity of sintering additives for hot-pressing[19] and, later, the ability to pressureless sinter ultrafine βSiC powders.[20] The broad division of ceramic type, presented in Table III, is similar to that for Si_3N_4-based ceramics, viz hot- pressed (HPSiC), pressureless-sintered (SSiC) and a type of 'reaction-sintering' between a graphite-containing preform and silicon introduced as a liquid or vapour (siliconized SiC).

Sintering additives for HPSiC are either B+C (added as B_4C) or Al_2O_3. The latter results in microstructures and properties similar to HPSN, dominated by intergranular (alumino silicate) residues at high temperatures. Fully dense fine (1-2μm) grain-size microstructures provide high MOR values (600-800 MPa) below 1000°C with subsequent rapid degradation beyond the (1200°C) silicate softening temperature (Fig.12). The function of B+C additives (0.5-1%) in both HPSiC and SSiC ceramics is believed to be the removal (via C) of the SiO_2 surface contaminant on SiC powders and the catalysis (via B) of surface/grain-boundary diffusion, hence accelerating densification. Pressureless-sintering requires slightly higher temperatures coupled with ultra fine, low oxygen, SiC powders (both α and β powders and products have been used - Table III). Grain-sizes and porosity levels are higher than for Al_2O_3 additives due to the absence of more efficient intergranular sintering liquids which also inhibit grain growth. As a consequence low-temperature strength is inferior but strength is retained to higher temperatures than for Al_2O_3-additive ceramics or HPSN and SSN (Fig.12).[21] The poor low-temperature strength of SSiC is a combination of large flaw size and relatively low fracture-toughness. Typical values for K_{1c} are 3-4 MPa $m^{\frac{1}{2}}$, probably due to grain size and lack of anisotropy in grain shape in comparison with SSN.

The superior high-temperature properties of (B+C additive) SSiC reflect the absence of liquid-sintering residues. B+C may be present only as undetectable intergranular segregated atoms following an essentially solid-state sintering process. Equivalent creep rates to SSN are attained at much higher temperatures (Fig.9) and the linear stress dependence indicates a diffusion-controlled mechanism. There are various interpretations of the diffusion process (lattice or grain boundary) and rate-controlling species which appear to be a function of the sintering additives.[22,23] The appearance of a non-linear (frequently non-integral) stress dependence and visible creep-cavitation in Al_2O_3-additive ceramics is explicable via their inter-granular residues and parallels that of inferior HPSN and SSN ceramics, although normally at higher temperatures due to the higher alumino-silicate glass viscosities.[24]

SiC ceramics are less susceptible to time-dependent failure (creep-rupture) than most Si_3N_4-based ceramics up to 1600°C. This stems from the non-cavitating creep-behaviour of (B+C) SSiC such that the low-stress 'strain-limited' failures (Fig.10) are absent. Like the fully-crystalline Si_3N_4 ceramics there is a narrow range of stress within which time-dependent failure is measureable above a crack-blunting threshold (Fig.10). Stress intensity exponents(n) in the crack-velocity relation $V=AK^n$ normally exceed 30 for tests in vacuum or argon[25,26] characteristic of a nearly time-invariant fracture-stress. In oxidising atmospheres the exponent increases, suggesting a crack-growth mechanism associated with an intergranular oxidation-reaction, i.e. stress-corrosion,[27] which is probably sensitive to the segregated species at grain-boundaries. Creep-rupture data for SSiC ceramics is not directly comparable with that for SSN ceramics, due to their substantially lower instantaneous fracture stress. However, in the 1300-1500°C interval current SiC ceramics have a superior performance.

Siliconized SiC ceramics have, until recently, been associated with lower values of MOR and a rapid loss of strength at 1400°C, associated with the melting of unreacted Si

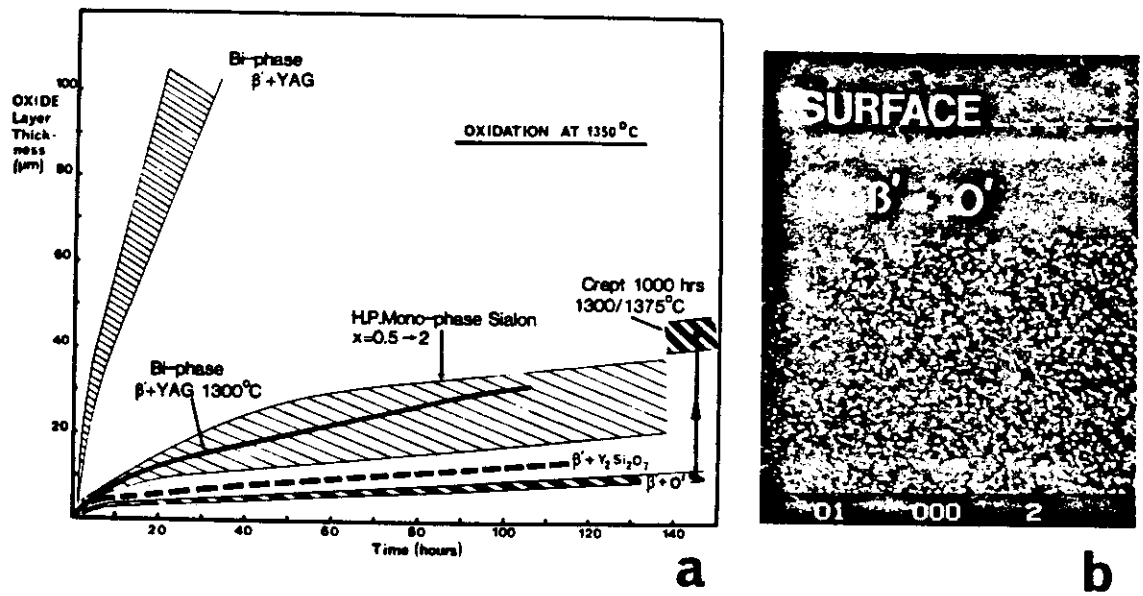

Fig.11. A comparison of oxidation kinetics for β' HPSN and β' SSN ceramics with different phase combinations within near-surface microstructures. The β'+O' (Si_2N_2O) data corresponds to a surface transformation layer illustrated in 11b.

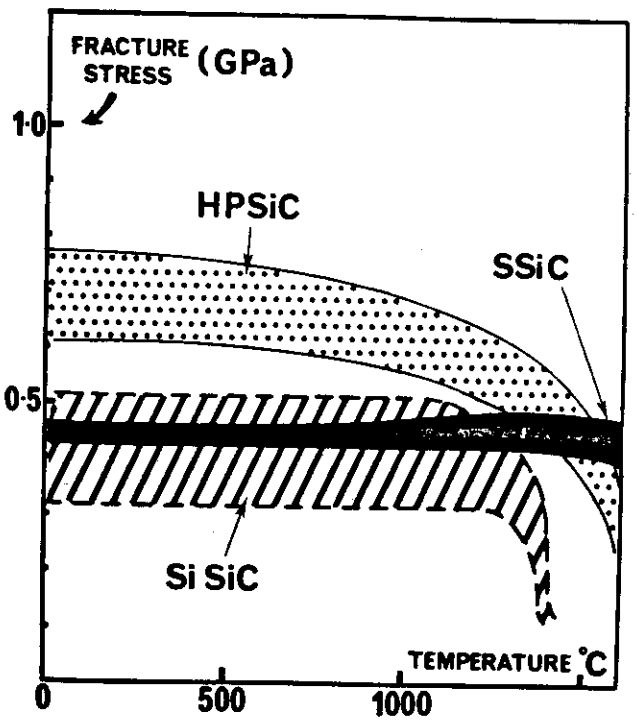

Fig.12. Bend strength (MOR) - temperature relationships for various SiC-based ceramics (see table III).

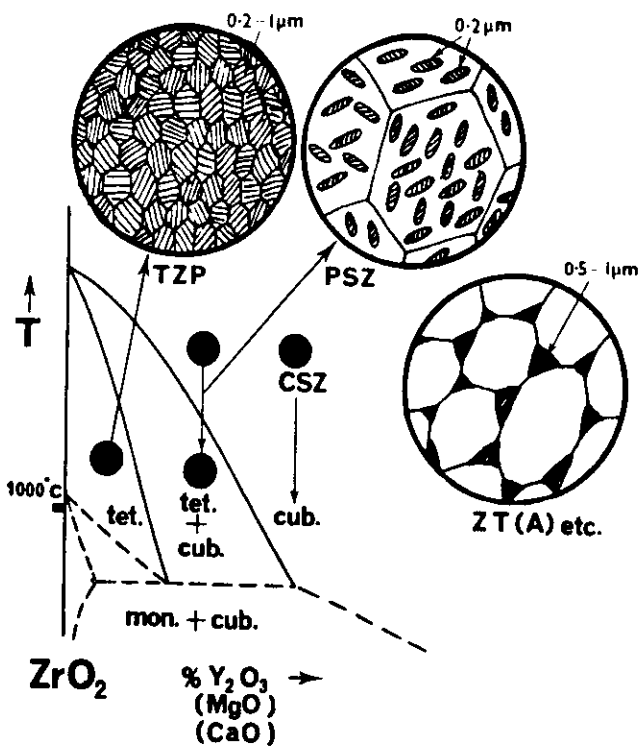

Fig.13. Phase equilibria and related microstructures for ZrO_2-toughened ceramics.

(Fig.12). A new processing technique, in which a porous preform is made by carbonization of a liquid polymer prior to Si-infiltration, has achieved MOR values comparable with the best SSN ceramics.[28] Shaping of components may be carried out at the polymer-precursor stage due to predictable shrinkage on carbonization. Excess Si still provides the limit to high-temperature application, but creep-rupture properties are excellent to ~1300°C.

Apart from their inferior MOR and fracture toughness, SiC ceramics suffer from a relatively poor thermal shock resistance compared to Si_3N_4 ceramics. This is due to a higher thermal expansion coefficient (α) and elastic modulus(E), interpreted via a thermal stress resistance parameter such as $R = \frac{\sigma(1-\nu)}{\alpha E}$, ($\sigma$ = M.O.R., ν = Poisson's ratio). This is one of the main reasons why Si_3N_4-based ceramics have been favoured in turbine applications for highly-stressed components. However, SiC ceramics have found application in combustors, in which temperature variations are not severe, utilising their superior thermal-diffusivity in eliminating 'hot-spots'. The absence of intergranular glassy residues in SSiC results in a superior oxidation resistance compared to SSN ceramics, especially above 1350°C (Section 4.2).

5. ZrO_2 TOUGHENED CERAMICS

5.1. Constitution and Microstructure

The constitution of PSZ and TZP ceramics in relation to phase equilibria is sketched in Fig.13. The cubic polymorph of ZrO_2 is 'stabilized' by the extension of its transformation temperature (cubic - tetragonal) to lower temperatures when in the form of a solid-solution with various metal oxides. MgO CaO and Y_2O_3, which are the most frequently used stabilizing elements, produce different phase-diagrams but share a common feature in the separation of C and T polymorphs by a two-phase (C+T) field which is the basis of PSZ ceramics.[29]

A typical PSZ, alloyed with 8-10 mol.% MgO, CaO or Y_2O_3 would be sintered in the 1650-1850° range to produce large (~100μm) grains of cubic solid solution, cooled and heat-treated in the 1100-1450°C interval to produce coherent precipitates of the tetragonal phase (Fig.14). Precipitate morphology depends on stabilizing oxide (lenticular for MgO, cuboid for CaO, platelet for Y_2O_3) and heat-treatments are critical in relation to precipitate particle size (normally ~0.2μm) such that the constrained tetragonal particles will transform to the monoclinic stable form, at lower temperatures, only in the presence of the crack stress-field.[30] 'Overaging' causes a spontaneous transformation of the larger particles on cooling whilst 'underaging' inhibits crack-tip transformation.

TZP ceramics have lower solute oxide additions such that they lie in the tetragonal single-phase field when sintered in the 1350-1500°C interval (Fig.14c and Table IV). Y_2O_3 (2-4 mol.%) is the favoured solute oxide and there is a critical grain-size for stabilization of a fully tetragonal structure to lower temperatures. This is normally in the 0.2-1μm range but depends on Y_2O_3 concentration and residual grain-boundary phases.[31] These residues are derived from impurity silicates which, together with Al_2O_3 additions and the Y_2O_3 solute, are the basis of a silicate sintering liquid analogous to that used for Si_3N_4 ceramics. Liquid phase sintering is a necessity in the lower-temperature tetragonal phase field.

The dispersion of tetragonal-stabilized ZrO_2 within other ceramic matrices is the basis of a third class of microstructure which exhibits ZrO_2-toughening phenomena (Fig.13). The tetragonal particles may be either intra or intergranular dispersions but the latter, exemplified by zirconia-toughened Al_2O_3 (ZTA - Fig.14d) is most effective and conveniently derived from normal ceramic processing.[32] The dispersed tet-ZrO_2 particle sizes are also critical in relation to thermal stability and crack-induced transformation. They are in the 0.2-1μm range, the particular optimum value being a function of matrix property and impurity level; for example, in ZTA the critical size is 0.5μm with a related (0.5-5μm) Al_2O_3 grain size.[33]

5.2. Properties and Limitations

Some of the low-temperature properties which emphasise the potential of ZrO_2-toughened ceramics are listed in Table IV. Mean values of MOR and fracture-toughness are far superior to a cubic stabilized zirconia (CSZ) and there is an important increment above the high-temperature monolithic Si_3N_4 and SiC ceramics. The high values of K_{1c} stem from both transformation of metastable tet-ZrO_2 in the crack stress-field and from transformation-induced microcracking, the relative importance of these mechanisms varies with type of microstructure (PSZ, TZP or ZTA). MOR is limited by K_{1c}, but also by flaw population via a 'Griffith-type' relation (Fig.7). Hence the highest strengths are recorded for TZP (a remarkable 2500 MPa) due to a combination of K_{1c} and controlled processing of fine powders, avoiding both porosity and heterogeneity.

The impressive low-temperature properties are not retained to elevated temperatures for two main reasons. Firstly, the thermodynamic driving force underlying the transformation-toughening mechanism decays as the equilibrium transformation temperature is approached (~1000°C). This is shown in Fig.15 with an example of a predicted and measured strength-temperature relation for a ZTA ceramic.[32] Secondly, the need for liquid-assisted sintering, especially for TZP, severely impairs high-temperature strength and creep resistance due to normally-glassy intergranular residues (Fig.9). An additional problem concerns thermal cycling; although transformation-toughening is beneficial in reducing thermal-shock damage, there are a number of microstructures (especially Mg-PSZ)

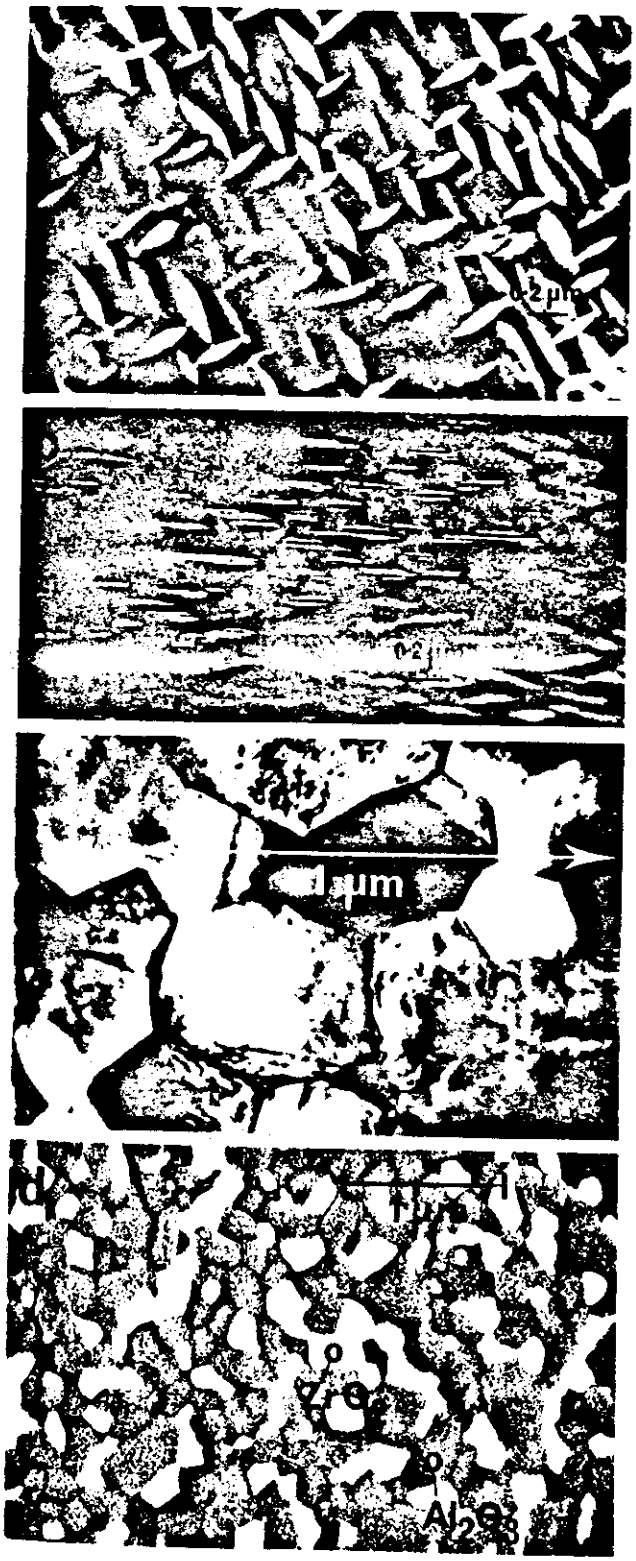

Fig.14. Electron micrographs of ZrO_2-toughened ceramics :
(a) Mg-PSZ with transformation of initially-tetragonal precipitates, adjacent to a crack, revealed by dark-field imaging in (b) using monoclinic reflections. (Courtesy Professor A H Heuer; (b) from Schoenlein and Heuer in 'Fracture Mechanics of Ceramics 6, Plenum Press 1983, (a) from D L Porter, PhD thesis, Case Western Reserve University).
(c) Y-stabilized TZP.
(d) ZT-Al_2O_3 containing intergranular tetragonal ZrO_2 (back-scattered SEM - courtesy Dr. D J Green).

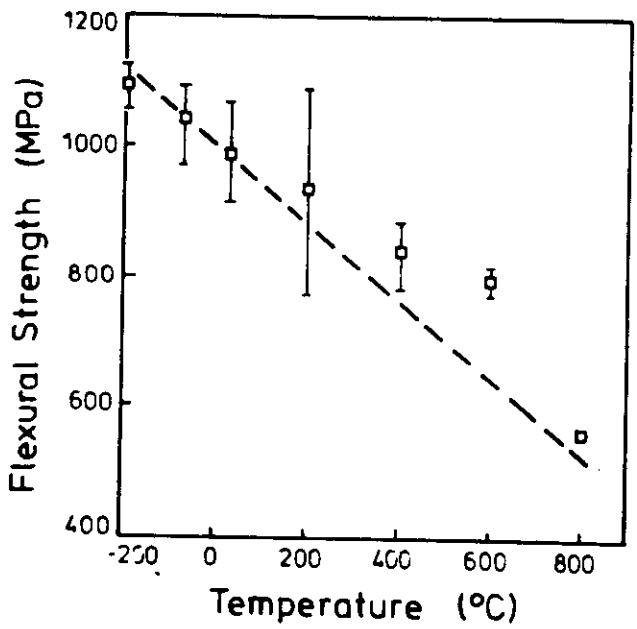

Fig.15. MOR-temperature relation for a ZT-Al_2O_3, illustrating the reduction in strength related to an approach to the equilibrium (tetragonal-monoclinic) transformation temperature (after Ref.6 and 35).

which suffer thermally-induced irrecoverable transformation from tetragonal to monoclinic ZrO_2 when cycled above 800°C. However Y-TZP is stable up to 900°C and hence is favoured in thermal-barrier applications utilising the low thermal conductivity of ZrO_2 and its metallic-range thermal expansion.

There have been various alloy-design strategies used in attempting to extend the application temperature for ZrO_2-toughened ceramics. Using HfO_2 as a stabilising additive equilibrium transformation temperatures up to 1400°C have been achieved, but there are problems in control of sintered microstructure to retain a critical size for the tetragonal phase (e.g. in Hf-ZTA).[34] Alternative strengthening mechanisms, for example, precipitation within the matrix of ceramics such as ZTA have been explored[32] together with a refinement or removal of grain- boundary residues. The latter procedure normally impairs sinterability, especially in TZP but also in PSZ ceramics where impurity SiO_2 (~0.05% on commercial ZrO_2 powders) is recognized as an important liquid sintering catalyst. The most promising high-temperature strengthening mechanism is that using whiskers (normally SiC) dispersed within matrices such as Y-TZP, ZT-Al_2O_3, ZT-mullite or ZT-cordierite.[35] These are essentially a class of ceramic-matrix composites discussed in the next section.

6. CERAMIC COMPOSITES

6.1. Strengthening principles

The principle of load-transfer to high-modulus, high-strength fibres within polymer or metallic matrices is well-established in achieving high-strength, fracture-tough materials. Carbon fibre reinforcement of glass was demonstrated more than 10 years ago[36] but further developments using ceramic matrices have been inhibited by fibre damage or reactivity during processing and a severe limitation to high-temperature properties from atmospheric oxidation of carbon fibres.

A resurgence of interest in composites with ceramic matrices is due partly to the problems of engineering design with brittle monolithic ceramics but also to the availability of a variety of reinforcing phases, for example SiC, Si_3N_4 and Al_2O_3 single crystal whiskers or SiC produced from a polymer precursor as a continuous fibre. A particular stimulus has been the work of Prewo et al at United Technologies Research Center, U.S.A., in demonstrating high-strength and fracture-toughness for silicate glass ceramics reinforced with high-strength (>2000MPa) continuous SiC fibres[7] (a Japanese 'Nicalon' source, which is a microcrystalline SiC interspersed with SiO_2 and free carbon).[38] The approach to an optimum mechanical response of Nicalon-reinforced lithium-aluminium silicate (LAS) glass-ceramic has confirmed the strengthening principles for semi-continuous fibres, illustrated in Fig.16. The important mechanism is that of load- transfer following matrix-cracking which results in a deviation from composite elastic behaviour (Stage I) to a reduced modulus associated with elastic extension of fibres (Stage II). A maximum stress (the UTS) occurs with fibre-bundle failure which may be followed by fibre 'pull-out' (Stage III) which contributes to the total work-of-fracture. The important characteristics of this ideal response are :

(i) A high failure strain and tolerance of overstressing (such as thermal shock or impact loading) which would cause instantaneous fracture in a monolithic ceramic.

(ii) An insensitivity to matrix flaws and hence component size (unlike the 'weakest-link' failure of monolithic ceramics) due to a limitation to crack-tip stress intensity caused by fibre-bridging of crack surfaces.[16]

This ideal composite behaviour is only achieved for unidirectional semi-continuous fibres which are weakly bonded to the matrix. Fibre-matrix reaction which induces primary interface atomic bonding results in a monolithic-type of response. Formation of weak interfaces is a function of processing (e.g. temperature at which initial matrix glass infiltration occurs) and chemical compatibility. There is evidence of a 50nm amorphous carbon-rich interfacial layer in certain optimal SiC-glass ceramic composites (e.g. SiC-LAS)[39] which provides an appropriate combination of weak interface and interfacial shear resistance during load transfer.

Whisker-reinforced composites are normally fabricated by conventional ceramic powder mixing and sintering techniques but hot-die pressing, used to achieve theoretical density, induces a preferred two-dimensional whisker orientation. The induced property-anisotropy does not extend to the ideal fracture behaviour observed for uniaxial semicontinuous fibre reinforcement. However, there are important increments in strength and fracture-toughness which may be attributed to interfacial micro- cracking and whisker pull-out which is also sensitive to whisker-matrix reactivity.[41] Such mechanisms relate to the enhanced K_{1c} levels ascribed to the anisotropy in βSi_3N_4 crystal growth morphology in SSN ceramics. Single crystal whiskers, such as βSiC, used in composites have large anisotropies, typically 0.2-0.5μm x 5-30μm.

6.2. Phase Combinations and Property Limitations

Semicontinuous fibres of C and βSiC are available as refractory reinforcing phases with high-temperature potential within ceramic matrices. Oxide fibres and whiskers are unsuitable due to reactivity with silicate liquids used either as glass-ceramic matrix precursors or as liquid-sintering aids used during conventional ceramic processing. αSi_3N_4 is unstable in most silicate liquids above 1000°C, being susceptible to the dissolution-reprecipitation reaction utilised in βSi_3N_4 ceramic fabrication (section 4). Since carbon is susceptible to oxidation in the uncoated state within silicate matrices the

most recently studied composites are based on βSiC fibres and whiskers.

The problem of infiltration and reactivity during processing has promoted the use of silicate glasses and their crystalline derivatives as suitable matrices for continuous fibres. They may be tailored with a wide range of chemistry, softening point or thermal expansion mismatch with the reinforcing phase. The composites may be fabricated by hot-pressing following infiltration of fibres with a presynthesised glass frit[36,37] or via a sol-gel glass route which has the advantages of improved homogeneity in microstructure and reduced hot-pressing temperature.[42] More refractory matrices have been formed via chemical-vapour-infiltration (CVI), the comparatively low temperature processing then permits a much wider range of both fibre and matrix chemistry.[8,43] The absence of the pre-alignment constraint for whisker-reinforcement permits the use of powder mixing and sintering procedures, for example, βSiC whiskers within Al_2O_3 or Si_3N_4 ceramic matrices.[41,44]

The high values of fracture stress attainable for unidirectional fibre-reinforced SiC-LAS glass-ceramic composites, described above, may be extended to temperatures of ~1000°C (Fig.18a). However, this high temperature data exposes a number of potential limitations of such composites. Firstly, above the matrix- microcracking stress the fibres are exposed to the environment, which causes premature failure in oxidising atmospheres above ~700°C (Fig.18b) probably due to reaction with the carbon-rich interfacial layer.[39] Secondly, there is little data yet available on time-dependent deformation, but the transient increase in fracture strength and K_{1c} between 700 and 1000°C is indicative of matrix plasticity due to residual glass. This is normally associated with creep-cavitation failure in monolithic ceramics. The use of more refractory matrices, such as CVI SiC, reveals an ultimate temperature limitation due to irreversible structural changes within the Nicalon SiC fibres.[21] This is consistent with a reduction in isolated- fibre fracture stress by a factor of 2 following heat treatment at 1300°C for 200 hours[42], believed to result from a recrystallisation/ grain growth process within the $SiC/SiO_2/C$ fibre microstructure.

Encouraging data for βSiC whisker-reinforcement of Al_2O_3[41] and Si_3N_4 [44] has recently been presented. For hot-pressed Al_2O_3 components with >40 vol.% SiC there is a fracture stress increment over a monolithic Al_2O_3 of 500 MPa which is retained to ~1200°C (Fig.19). Fracture toughness increases from 4.5 to 8.5 MPa m and there is a remarkable insensitivity to thermal shock up to the 1000°C test limit.[41] Hot-pressed Si_3N_4 composites with 30 vol.% SiC have been fabricated with 600-700 MPa bend strengths, comparable with monolithic ceramics, but combined with higher Weibull modulus and work of fracture.[44] These composites have a supplementary advantage in being electrically conducting and hence may be spark-machined to component shape. As in the case of fibrous-composites, the time or environmental dependence of high-temperature mechanical behaviour has yet to be proven and it is clear that whisker-matrix interfacial reactivity is sensitive to time and temperature of hot-pressing in addition to composition of liquid sintering aid[45] and whisker surface chemistry.[44]

7. FUTURE DIRECTIONS

Each class of structural ceramic surveyed in this paper, although representing a significant advance in the past decade, is observed to have important limitations within differing regimes of temperature. A simplistic survey of this situation is contained in Fig.20 in which fracture stress is plotted as a function of temperature for examples of the monolithic ceramics.

Engineering design with the Si-based ceramics is inhibited by their relatively low K_{1c} and MOR combined with a spread in property (low Weibull modulus) associated with failure from the dominant flaw. Some improvement has been realised for SSN ceramics due to a natural anisotropy in βSi$_3$N$_4$ crystal morphology and hence enhanced K_{1c}. Comparatively poor low-temperature properties for SSiC ceramics are compensated by the high-temperature increment over SSN ceramics containing liquid sintering residues. The importance of complete crystallisation of intergranular glass in the latter is well- established in relation to creep rate and stress-rupture. For completely crystalline SSN ceramics the temperature ceiling is currently limited by oxidising atmospheres.

Zirconia ceramics offer a valuable increase in K_{1c} and MOR and the toughening principles are also applicable to a variety of, normally oxide, ceramic matrices. The intrinsic limit to transformation toughening and the presence of intergranular sintering residues inhibits their application at temperatures comparable with the Si-based ceramics.

A quantum jump in the performance of monolithic ceramics would occur in combining the advantages of Si-based and ZrO_2-toughened ceramics at high and low temperatures, respectively. However, the development of an optimal microstructure consisting of tetragonal ZrO_2 intergranular particles of critical size within a SSN or SSiC fine-grain polycrystal with no residual glass phase is difficult to achieve, in view of the differing constraints of sintering temperature and chemistry. Similar difficulties occur in attempting to improve the high-temperature performance of ZrO_2-toughened oxides, such as Al_2O_3, mullite, spinel etc.[35], in which higher-temperature sintering is a consequence of the quest for creep resistance via removal of liquid sintering aids. Such difficulties dictate the alternative strategy involving composite ceramics; for example, SiC whisker dispersions within SSN or oxide matrices to improve low

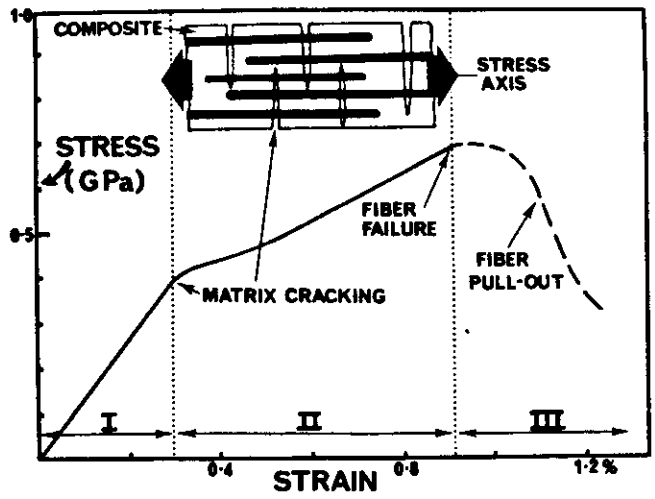

Fig.16. The optimal stress-strain behaviour of a ceramic composite, typified by an LAS glass ceramic containing unidirectional 'Nicalon' SiC fibres (after Ref.7).

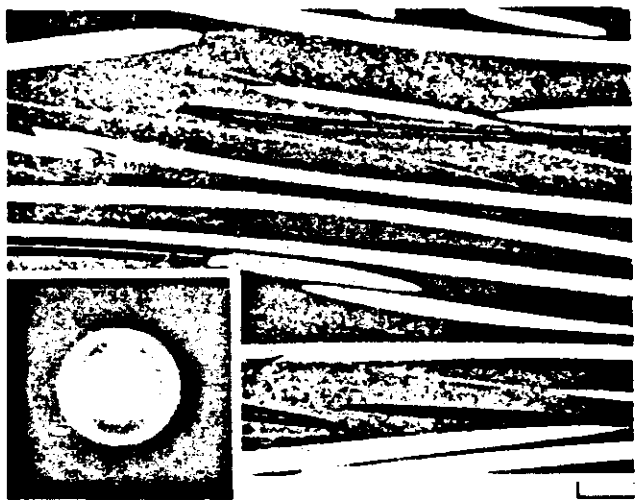

Fig.17. Longitudinal section through a SiC/LAS glass-ceramic (after Ref.7). A transmission electron diffraction pattern (inset) illustrates the microcrystalline state of β SiC which is associated with residual graphite and amorphous SiO_2 in the Nicalon fibers.

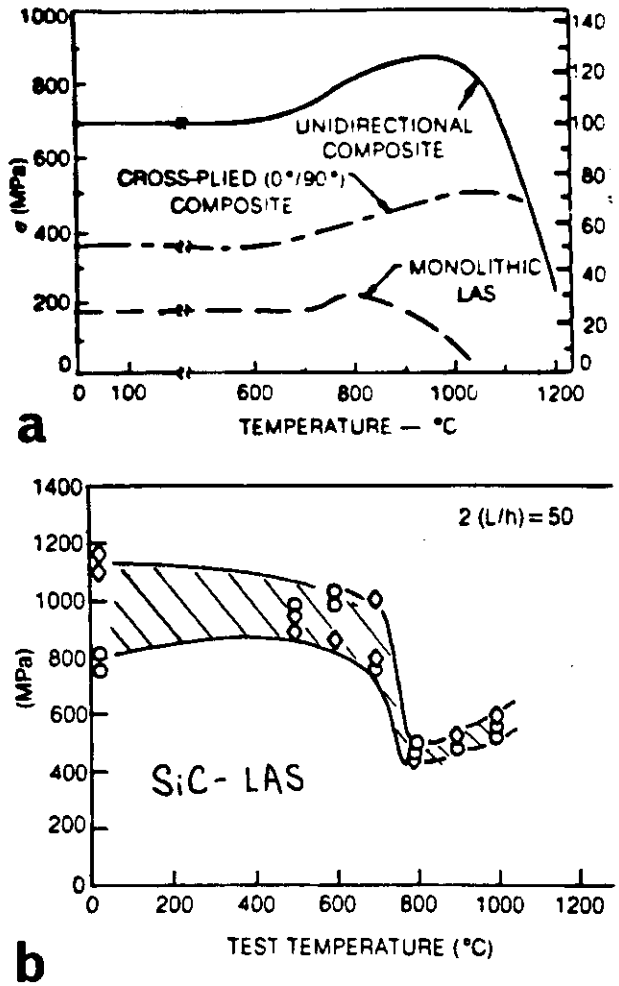

Fig.18. Fracture stress-temperature relation for SiC/LAS composites :
(a) Inert-atmosphere tests
(b) Unidirectional composite tested in an oxidising environment (Ref.40).

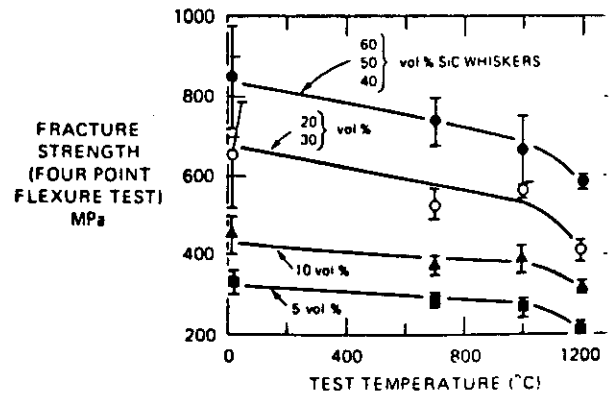

Fig.19. MOR-temperature data for Si whisker-reinforced, hot-pressed Al_2O composites (Ref.41).

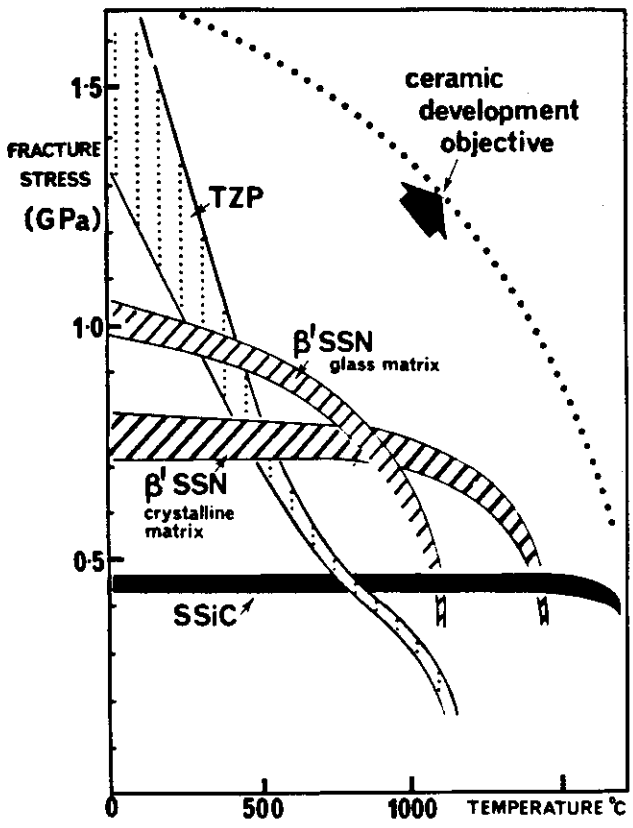

Fig.20. A summary of the limitations of the various types of monolithic ceramic in differing temperature regimes, indicating the need for development of new composite ceramics.

temperature fracture toughness and within ZrO_2-toughened ceramics to improve high-temperature creep (and further enhance low-temperature properties). Both strategies, which are at an early development stage exemplified above[35,41,44], necessitate fabrication via hot-pressing. This is a serious constraint in an already-difficult area of net-shape component fabrication for monolithic ceramics. The fabrication of CVI composites is currently applicable only to simple shapes with semi-continuous fibre reinforcement. Improvement in high-temperature fibre and interface stability, especially in oxidising atmospheres, is an additional requirement.

In conclusion it is important to emphasise the degree of sophistication which has evolved over the past decade in control of ceramic microstructure and properties beyond that of the 'as-sintered' state. In some ZrO_2-based ceramics solid-state precipitation is used in development of microstructures which utilise a martensitic transformation as a toughening mechanism. Improved high-temperature performance in liquid-phase-sintered ceramics is achieved via post-sintering heat-treatments designed to crystallise residual glass matrices and to enhance oxidation-resistance via transformation of surface microstructure. Thus the development of ceramic alloys is paralleled by the earlier development of metallic alloys in which initial chemistry and subsequent thermal treatment are dictated by stress, temperature and environment in service.

ACKNOWLEDGEMENTS:

The author wishes to thank research associates at Warwick and elsewhere who have supplied both published and unpublished Figures for this review. Financial support for research programmes at Warwick which relate to part of this review has been received from Lucas-Cookson-Syalon, Rolls-Royce, S.E.R.C. and the Wolfson-Foundation.

REFERENCES :

1. D J Green, in 'Industrial Materials Science and Engineering; ed. L E Murr, (Marcel Dekker 1983) 89.

2. R N Katz, Mat.Sci. and Engineering 71 (1985) 227.

3. S K Bhattacharyya, A Jawaid and M H Lewis, Proc.XII NAMRI Conf., Michigan Tech.Univ., (1984).

4. S K Bhattacharyya, A Jawaid and J Wallbank, Metalwork.Prod. 126 (1982) 104.

5. R C Garvie, R H Hanninck and R T Pascoe, Nature, 258 (1975) 703.

6. F F Lange, J.Mat.Sci., 17 (1982) 225.

7. K Prewo and J J Brennan, J.Mat.Sci. 17 (1982) 1201 and 2371.

8. R Naslain and F Langlais, in 'Tailoring Multiphase and Composite Ceramics' ed. Tressler and Bradt (Plenum 1985) in press.

9. M H Lewis and R J Lumby, Powder Metall. 26 (1983) 73.

10. R W Davidge in 'Micromechanisms of Plasticity and Fracture' ed. Lewis and Taplin (Parsons Press 1983) 167.

11. D B Marshall, A G Evans, B T Khuri Yakub, J W Tien and G S Kino, Proc.Roy.Soc. A385 (1983) 461.

12. M H Lewis, S Mason and A Szweda in 'Proc.Conf. on Non-Oxide Technical and Engineering Ceramics' ed. Hampshire (Elsevier 1985) in press.

13. M H Lewis and B S B Karunaratne in 'Fracture Mechanics for Ceramics, Rocks and Concrete', ed. Freiman and Fuller (ASTM STP745 1981) 13.

14. T J Chuang, J.Amer.Ceram.Soc. 65 (1982) 93.

15. B S B Karunaratne and M H Lewis, J.Mat.Sci. 15 (1980) 449 1781.

16. A G Evans, Mat.Sci. and Engineering 71 (1984) 3.

17. M H Lewis and P Barnard, J.Mat.Sci. 15 (1980) 443.

18. M H Lewis, B S B Karunaratne, J. Meredith and C Pickering, in 'Creep and Fracture of Engineering Materials and Structures', ed. Wilshire and Owen (Pineridge Press (1981) 365.

19. S Prochazka in 'Silicon Carbide-1973', eds. Marshal, Faust, Ryan, (University of S.Carolina Press 1974) 391.

20. S.Prochazka in 'Ceramics for High-Performance Applications', eds. Burke, Gorum, Katz (Brook Hill 1974) 239.

21. F Porz, G Grathwohl and F Thummler, Mat.Sci. and Engineering 71 (1985) 273.

22. T L Francis and R L Coble, J.Amer.Ceram.Soc. 51 1968) 115.

23. G Grathwohl, Th. Reetz and F Thummler, Sci.Ceram. 11 (1981) 425.

24. J L Chermant, Mat.Sci. and Engineering 71 (1985) 147.

25. G G Trantina and C A Johnson, J.Amer.Ceram.Soc. 58 (1975) 344.

26. G. Grathwohl, R Hamminger, H Iwanek and Thummler, Sci.Ceram. 12 (1984) 583.

27. K D McHenry and R E Tressler, J.Mat.Sci. 12 (1977) 1272.

28. G D Quinn and M J Slavin, Proc. 23rd ATD meeting, Dearborn, MI (1985).

29. M G Scott, J.Mat.Sci. 10 (1975) 1527.

30. M V Swain and R H J Hanninck in 'Advance in Fracture Research' 4, ed. D Francoi (Pergamon Press 1981) 1559.

31. M Ruhle, N Claussen and A H Heuer, i 'Advances in Ceramics' 1 (Amer.Ceram.Soc. 1984) 352.

32. N Claussen in 'Advances in Ceramics' 1 (Amer.Ceram.Soc. 1984) 325.

33. N Claussen and M Ruhle, in 'Advances i Ceramics 3' (Amer.Ceram.Soc. 1981) 137.

34. N Claussen, F Sigulinski and M Ruhle, i 'Advances in Ceramics 3 (Amer.Ceram.Soc 1981) 164.

35. N Claussen, Mat.Sci. and Engineering 7 (1985) 23.

36. R A Sambell, A Briggs, D C Phillips and H Bowen, J.Mat.Sci. 7 (1972) 663 and 676

37. R A Sambell, D C Phillips and D H Bowe in Proc.Int.Conf. on Carbon Fibres (Plastics and Polymers Conf.Suppl. No.6 1974) 105.

38. S Yajima, K Okamura, J Hayashi and Omori, J.Amer.Ceram.Soc. 59 (1976) 324.

39. J J Brennan in 'Tailoring Multiphase an Composite Ceramics' ed. Tressler an Bradt (Plenum 1985) in press.

40. K M Prewo in 'Tailoring Multi-phase an Composite Ceramics' ed. Tressler an Bradt (Plenum 1985) in press.

41. T N Tiegs and P F Becher, 'Tailorin Multiphase and Composite Ceramics' ed Tressler and Bradt (Plenum 1985) i press.

42. E Fitzer and J Schlichting, i 'High-Temperature Science' 13 (1980) 149

43. T Hirai, in 'Tailoring Multiphase an Composite Ceramics' ed. Tressler an Bradt (Plenum 1985) in press.

44. R Hayami, K Ueno, I Kondou, N Tamari an Y Toibana, in 'Tailoring Multiphase an Composite Ceramics' ed. Tressler an Bradt (Plenum 1985) in press.